SYNTHESIS AND CHARACTERIZATION OF SILICA GEL FROM DEALUMINATED KAOLIN INDUSTRIAL RESIDUE FOR A TARGETED APPLICATION OF DYE REMOVAL

By

Belete Asmamaw Melaku

A Thesis Submitted to

The Department of Chemical Engineering

School of Mechanical, Chemical and Material Engineering

Presented in Partial Fulfillment of the Requirement for the Degree of Master's in Chemical Engineering (Specialization in Process Engineering)

Office of Graduate Studies

Adama Science and Technology University

June, 2023

Adama, Ethiopia

Synthesis and Characterization of Silica gel from Dealuminated Kaolin Industrial Residue for a Targeted Application of Dye Removal

Belete Asmamaw Melaku

Advisors: Melaku Tesfaye (PhD)

A Thesis Submitted to

The Department of Chemical Engineering

School of Mechanical, Chemical and Material Engineering

Presented in Partial Fulfillment of the Requirement for the Degree of Master's in Chemical Engineering (Specialization in Process Engineering)

Office of Graduate Studies

Adama Science and Technology University

June, 2023

Adama, Ethiopia

Declaration

I hereby declare that this Master Thesis entitled **"Synthesis and characterization of silica gel from dealuminated kaolin industrial residue for a targeted application of dye removal"** is my original work. That is, it has not been submitted for the award of any academic degree, diploma, or certificate in any other university. All sources of materials that are used for this thesis have been duly acknowledged through citation.

Belete Asmamaw Melaku _____ _____

Candidate Signature Date

Recommendation

I, the advisor of this thesis, hereby certify that I have read the revised version of the thesis entitled **"Synthesis and characterization of silica gel from dealuminated kaolin industrial residue for a targeted application of dye removal"** prepared under our guidance by Belete Asmamaw Melaku submitted in partial fulfillment of the requirements for the degree of Mater's of Science in Chemical Engineering. Therefore, I recommend the submission of the revised version of the thesis to the department following the applicable procedures.

Melaku Tesfaye (PhD)	_____	_____
Advisor	Signature	Date

Approval Page of M.Sc. Thesis

I, the advisors of the thesis entitled **"**Synthesis and characterization of silica gel from dealuminated kaolin industrial residue for a targeted application of dye removal**''** and developed by Belete Asmamaw Melaku, hereby certify that the recommendation and suggestions made by the board of examiners are appropriately incorporated into the final version of the thesis.

Melaku Tesfaye (PhD _____ _____

Major Advisor Signature Date

I, the undersigned, members of the Board of Examiners of the thesis by Belete Asmamaw Melaku have read and evaluated the thesis entitled **"**Synthesis and characterization of silica gel from dealuminated kaolin industrial residue for a targeted application of dye removal**''** and examined the candidate during the open defense. This is, therefore, to certify that the thesis is accepted for partial fulfillment of the requirement of the degree of Master of Science in Chemical Engineering.

_____ _____ _____

Chairperson Signature Date

_____ _____ _____

Internal Examiner Signature Date

_____ _____ _____

External Examiner Signature Date

Finally, approval and acceptance of the thesis is contingent upon submission of its final Copy to the Office of Postgraduate Studies (OPGS) through the Department Graduate Council (DGC) and School Graduate Committee (SGC).

_____ _____ _____

Department Head Signature Date

_____ _____ _____

School Dean Signature Date

_____ _____ _____

Office of Postgraduate Studies, Dean Signature Date

DEDICATION

This Thesis is dedicated to in loving memory of my beloved father Asmamaw Melaku and who passed away recently. I also dedicate this research work to my beloved family Sosina Teshome, Your endless support, encouragement, appreciated sacrifice, and constant love have sustained me in success throughout my life.

AKNOWLEDGMENT

First of all, I would love to provide my immensely thanks to Almighty God for blessing me with achievements throughout my study, and for granting me with strength, power, and good health to attain my ambition. I would really like to express my genuine gratitude to my advisors Dr. Melaku Tesfaye for his continuous guidance, indispensable comments, encouragement, support and excellent supervision throughout my research work. Thank you for generously sharing your time, and for all your support to succeed this research.

I would like to extend my acknowledgment to my Family for unreserved help and useful advice throughout this study. I would like to thank Bundi Roba for his valuable guidance, and kindly support me in completing the laboratory analysis work at Adama science and technology university chemical engineering laboratory. My thanks to all Academic and Research Assistants of Chemical engineering department and Awash Melkassa chemical factory quality control staff. This thesis would not have been possible without the inspiration and support of a number of wonderful individuals. Thank you all of my friends for being part of this journey and making this thesis possible.

TABLE OF CONTENTS

LIST OF TABLES

LIST OF FIGURES

LIST OF ABREVATIONS

AAS	Atomic Absorption Spectroscopy
CCD	Central Composite Design
SSS	Sodium silicate solution
SG	Silica gel
MB	Methylene blue
DTG	Derivative Thermogravimetric
FTIR	Fourier-Transform Infrared Spectroscopy
m_{ads}	Mass of adsorbent
RSM	Response Surface Methodology
SEM	Scanning Electron Microscopy
SWR	Solid Waste Residue
TGA	Thermogravimetric analysis
XRD	X- Ray Diffraction
Abs.	Absorbance
BET	Brunauer-Emmett-Teller
AMCF	Awash melkassa chemical factory

ABSTRACT

The dealuminated kaolin residue is the tailings generated from the production process of aluminum sulphate industry and is mainly stacked in an open air at present, so how to ensure the extraction of silica gel from the stockpile is important, this *was examined for its effectiveness in removing of methylene blue dye from wastewater. Excess methylene blue dye in the human body can lead to various health problems. Therefore, it is crucial to remove methylene blue from wastewater. Physical, chemical, and biological technologies have been used for dye removal, but they have limitations regarding cost and complexity in achieving the required concentration level. The adsorption process is a preferred technologies based on its simple design, versatility, lowest cost, and reusability. This work aimed to synthesize and characterize silica gel for removing methylene blue dye from wastewater. Silica gel was synthesized by the first step was extraction sodium silicate from SWR by reacting with caustic soda for 2 hours at 80 °C with 1:10 solid liquid ratio. And the synthesis of silica gel was carried out by acidifying the silicate solution with sulfuric acid and followed by sol-gel method. AAS, XRD, FTIR, SEM, BET, and TGA were used to characterize the chemical composition, crystalline structure, specific functional groups, morphological properties, specific surface area, and thermal stability of silica gel. The BET-specific surface area of silica gel was determined to be 444.54 m2/g. Moreover, the optimization effects of adsorption parameters such as contact time, adsorbent dose, pH, and initial methylene blue dye concentration were carried out, and the results confirmed that 94.95% of MB dye was removed from synthetics and 90.61 from wastewater at an optimum time of 120 min, a 0.03 g adsorbent dose, a pH level of 7.99, and 15 mg/L of initial MB dye concentration. Furthermore, equilibrium isotherm, kinetics, and thermodynamic properties of the adsorption process were examined. The adsorption isotherm data were best fitted to the Langmuir model with a maximum adsorption capacity of 85.18 mg/g. The results of the kinetic model proved that the pseudo-second-order model provided a good description of the experimental data with a maximum R^2 of 0.999. The results of the thermodynamic parameters demonstrated that the adsorption process is spontaneous and endothermic. The removal efficiency of 62.75% of MB was found after three cycles of desorption and adsorption, indicating the wonderful reusability of the adsorbent. The results illustrate that silica gel is an excellent and promising adsorbent for removing methylene blue dye from wastewater.*

***Key words**: silica gel, Methylene blue, Adsorption, kinetics, isotherm, cationic dye*

CHAPTER ONE

1. INTRODUCTION

1.1. Background of the study

Under Chemical Industry Corporation Awash Melkassa Chemical Factory is located 105 Km South-East of the Capital Addis Ababa on the main road to Assella in the Oromia Regional State. The factory was established as Public Enterprise, by the Council of Minister Regulations No.235/1995. The Factory aimed mainly to produce & sell chemicals such as Aluminum Sulphate and other Sulphate salts, Sulphuric Acid, Oleum and now days the company Constructed a Hydrogen peroxide factory and starts the production of 50%w/w H_2O_2 chemical.

The filter cake is a waste discharged from aluminum sulphate production at Awash Melkassa Aluminum Sulfate and Sulfuric Acid Factory. Kaolin is a cheap natural material containing silica and alumina in a high percentage, however, it is inert and inactive it requires activation through the calcination process (Alamdari, 2017). In the production of aluminum sulfate from kaolin, Al_2O_3 is leached out from kaolin with H_2SO_4 in the presence of water at high temperatures and pressure. The process includes post-reaction suspension, filtration, and filtrate concentration, solidifying, and crushing. The unreacted material was separated by a filter press. It gave filtrate and filter cake. The filter cake is backwashed with hot water and dried with compressed air to remove scrap and disposed to the stockpile area of the factory. About 14,500 kg per day of the filter cake is dumped into the stockpile area. Depending on the amount of filter cake released, 5,800kg per day of silica was discharged as waste from the factory to the environment. The filter cake during the production of aluminum sulphate from kaolin mainly includes silicon dioxide; unleached kaolin, alum, and water; however, silicon dioxide has a large amount in the contents of filter cake (residue) the composition of silicon dioxide is about 65% of the residue.

The chemical compound silicon dioxide, also known as silica (from the Latin silex), is an oxide of silicon with the chemical formula SiO_2. Silica is most commonly found in nature as sand or quartz, as well as in the cell walls of diatoms. Silica is manufactured in several forms; including fused quartz, crystal, fumed silica, colloidal silica, silica gel, and aerogel (Besbes et al., 2009; Gunde, 2000).

Silica gel is an adsorbent prepared from the coagulation of a colloidal solution of silicic acid. The term silica denotes the compound silicon dioxide and encompasses its various forms including crystalline silica, vitreous silica's, and amorphous silica's. The term "Gel" merely indicates the condition of the material at one stage of its manufacture. It is a highly porous structure, characterized by uniformity of the arrangement of the pores and their sizes, the pore area of silica gel varies with method of manufacturer (Yu et al., 2014). Silica gel is a versatile material with a wide range of applications, including as an adsorbent for removing pollutants from wastewater. This study explore the procedures for synthesizing silica gel from kaolin byproduct, the factors affecting the adsorption capacity of the silica gel, and the potential applications and future prospects of the synthesized silica gel.

The sol-gel method is a simple and cost-effective approach for the synthesis of silica gel from kaolin byproduct. The sol-gel process involves the conversion of a liquid precursor into a gel, which is then dried and calcined to yield the final product (Dahliyanti et al., 2022). The sol-gel method has several advantages over conventional methods, including low energy consumption, low cost, and the ability to control the size and morphology of the synthesized particles. The synthesis of silica gel from kaolin by-product involves several procedures, including acid leaching, precipitation, and drying. The kaolin residue is first treated with acid to remove impurities and increase the silica content. The resulting slurry is then subjected to precipitation using a base such as ammonium hydroxide to form silica gel. Drying is then carried out to obtain the final product. The variables affecting the synthesis process include the concentration of the acid and base, reaction time, and temperature (Lazaar et al., 2017).

Dyes are widely used as one of the key ingredients in many industries like textile, paint, varnish, etc. These industries discharged the dye into the environment with their wastewater, and one of the major problems concerning textile wastewater is the highly colored effluent, which In addition, the main concern is that some dyes degrade into compounds that have toxic, mutagenic, and carcinogenic effects on living organisms (Gómez et al., 2014; Mousavi et al., 2017). Azo dyes can be particularly toxic upon degradation and this class of dyes is widely used in many industries such as methylene blue ($C_{16}H_{18}ClN_3S$).

The textile industry uses around 15% of the world's total dye output, and it releases its waste into the environment (Houas et al., 2001). Organic compounds used as textile dyes that are not biodegradable. Methylene blue ($C_{16}H_{18}N_3SCl$), one of the more popular dyes, has a number of benefits like being a basic dye, easy to acquire, and having a low cost. The amount of methylene blue used in the coloring process is about 5% bonded, and the other 95% is wasted as waste. As a result, the presence of dye in water systems reduces the amount of sunlight that can diffuse through water bodies, which prevents aquatic plants from photosynthesis, hinders bacterial growth, and is harmful to humans (Mousavi et al., 2017; Yuan et al., 2019).

This study demonstrates how kaolin by-product released during the production of aluminum sulphate can be used effectively in synthesizing pure and amorphous forms of silica gel through a simple procedure involving alkaline solubilization during which Aluminosilicate components are dissolved leaving behind soluble Silica precursors. The synthesized material also exhibited excellent potential for application in wastewater treatment methods due to its highly efficient adsorption capacity, environmentally friendly and cost-effective towards methylene blue dye from wastewater.

1.2. Statement of the problem

Awash melkassa chemical factory focus to use kaolin for the production of aluminum sulphate since the raw material available in country Ethiopia, the filter cake stockpile occupied a large area of the company and makes the working area dirty and unattractive. The waste contains micrometer level particles that can be inhaled at the windy day as dust rose, which affects the community's breathing system. The white powder particles of silica reflect sunlight during the day time which hurts the eye of the people living there. The filter cake (residue) is rich by silicon dioxide, which has a versatile application in different industries they uses as a raw material.

The discharge of untreated wastewater containing dyes into water bodies has become a major environmental concern due to its potential adverse effects on aquatic life and human health. Methylene blue dye is widely used in various industries such as textile, paper, and pharmaceutical industries, and its discharge into the environment can lead to serious ecological problems. The main environmental concern with dyes is their absorption and reflection of sunlight entering the water and thus causing reduction in photosynthesis (Adak et al., 2005).

Therefore, there is a need to develop an efficient and cost-effective method for the removal of methylene blue dye from wastewater. Silica gel is an interesting amorphous material with a high adsorption capacity, and is use as an adsorbent of humidity, or as important adsorbent in liquid phase. Silica gel is also chemically inert and with low toxicity, with a very high melting point (Gómez et al., 2014).

Silica gel is a well-known adsorbent used for the removal of various pollutants from wastewater due to its high surface area and porosity. However, the synthesis of silica gel from pure silica sources is expensive and not environmentally friendly. On the other hand, kaolin residue is an abundant and inexpensive byproduct of the mining industry, and its utilization for the synthesis of silica gel can provide a sustainable and cost-effective solution for wastewater treatment (Lazaar et al., 2017). Therefore, the problem addressed in this study is the development of an efficient and sustainable method for the synthesis of silica gel from kaolin byproduct and its characterization for the target application of methylene blue dye removal from wastewater. The study aims to address the challenges associated with the synthesis of silica gel from sustainable sources and to contribute to the development of an effective approach for the treatment of wastewater contaminated with methylene blue dye.

1.3. Basic research questions

1. Is it possible to convert Aluminum sulfate solid waste residue of Awash Melkassa Chemical factory into valuable products particularly adsorbent?
2. What is the maximum amount of methylene blue dye that can be removed by the synthesized silica gel?
3. What are the optimum parameters such as pH, adsorbent dose, contact time, and initial dye concentration to get higher dye removal?
4. What is the maximum number of regeneration cycles that can be achieved with the synthesized silica gel for methylene blue dye removal?

1.4. Objectives

1.4.1. General objective

The general objective of study is to synthesize and characterize of silica gel from dealuminated kaolin industrial residue for a targeted application of dye removal.

1.4.2. Specific objectives

The specific objectives of the research are:-

- ✓ To synthesize and characterize silica gel using techniques such as X-ray diffraction (XRD), Atomic absorption spectroscopy (AAS), Thermogravimetric analysis (TGA), Scanning electron microscopy (SEM), Fourier transform infrared spectroscopy (FTIR), and Brunauer-Emmett-Teller (BET).
- ✓ Investigating and statistically optimizing the methylene blue removal efficiency of silica gel at distinct operational conditions such as methylene blue initial concentration, silica gel dosage, pH of the solution, and contact time.
- ✓ Explore the adsorption kinetics, equilibrium isotherm, and thermodynamics effect using batch adsorption experimental data.
- ✓ To investigate the reusability mechanism of the used silica gel by conducting a series of regeneration experiments.
- ✓ Validating the optimum condition, it performed on actual textile dye house wastewater.

1.5. Significance of the study

Industrial waste residue, produced during the manufacturing of Aluminum sulfate (alum) from kaolin by the presence of sulfuric acid is highly acidic (pH about 3) and is considered hazardous. A large amount of solid waste residue is estimated as 5000-5500 tones/year of waste accumulated in Awash Melkassa Chemical Factory, Ethiopia. The advantage of this research was converting this byproduct to valuable products, particularly adsorbents for methylene blue adsorption from wastewater.

In this study aluminum sulfate solid waste residue, which exists in Awash Melkassa Chemical Factory, can be used as raw material to produce silica gel as an adsorbent, which has an excellent removal efficiency and adsorption capacity of methylene blue dye that can exist in aqueous solutions and wastewaters. The study provides basic information about the adsorption of methylene blue dye from wastewater. The removal of methylene blue dye by using low-cost adsorbents from industrial waste residue is found to be promising in the long term due to the adsorbent product obtained from material locally and abundantly available in Ethiopia. The other benefit of this study is replacing the expensive commercial adsorbents with easily available and low-cost adsorbents.

1.6. Scope of the study

The scope of this study includes the synthesis and characterization of silica gel from kaolin byproduct for the target application of methylene blue dye removal. The synthesis of silica gel from the solid waste residue, the solid waste residue reacts with caustic soda and followed by filtration. The obtained purified sodium silicate solution will be used to synthesize silica gel using sol-gel method by acidifying with sulfuric acid. The synthesized silica gel will be characterized using techniques such as X-ray diffraction (XRD), scanning electron microscopy (SEM), Fourier transform infrared spectroscopy (FTIR), and Brunauer-Emmett-Teller (BET) surface area analysis. The performance of the synthesized silica gel for methylene blue dye removal will be evaluated by conducting batch adsorption experiments under different conditions such as pH, contact time, initial dye concentration, and temperature. The adsorption process will be optimized by varying the parameters such as adsorbent dosage, pH, and contact time. The adsorption data will be analyzed using various isotherm and kinetic models to understand the adsorption mechanism and kinetics. The study will compare the performance of the synthesized silica gel with other adsorbents reported in literature for methylene blue dye removal. The potential application of the synthesized silica gel for methylene blue dye removal and its suitability for large-scale wastewater treatment will be tested. The study will contribute to the development of an effective and sustainable approach for the treatment of wastewater contaminated with methylene blue dye.

CHAPTER TWO

2. LITERATURE REVIEW

2.2. Silicon dioxide

Silica is the common name for materials composed of silicon dioxide (SiO_2) and occurs in crystalline and amorphous forms. Crystalline silica exists in multiple forms. Quartz and, more specifically a-quartz, is a widespread and well-known material. Upon heating, quartz is transformed into b-quartz, trydimite and cristobalite. Porosil is the family name for porous crystalline silica. Quartz exists in natural and synthetic forms, whereas all porosils are synthetic. Amorphous silica can be divided into natural specimens (e.g. diatomaceous earth, opal and silica glass) and human-made products (Il'Ves et al., 2015).

Porous silica (SiO_2) is one of the inorganic porous materials that can be easily produced from a precursor of sodium silicate (Bageru & Srivastava, 2017). The important features of this material are that it has high thermal and chemical stability, high mechanical strength, good resistance for bacteria, narrow pore size distribution, excellent shaping ability, and can be synthesized with well controlled pore size range and transparency (Besbes et al., 2019) . Porous silica is manufactured mainly by three processes, they are the thermal-phase separation, the sol-gel process and the crystallized process.

Silica dioxide also known as sand is one of the most abundant resources and is considered the most important material in the production of glass, cement and ceramics. It is composed of silicon and oxygen and free silica can be found in crystallographic forms depending on temperature and pressure. At atmospheric pressure, pure silica will crystallize into three mineral structures; quartz, trydimite and cristobalite (Submitted & Fulfillment, 2020). Sands are good example of commercial silica that is mined as unconsolidated beach deposits, cemented sandstones or quartzite. The resistance of silica materials to thermal shock, chemical attack and mechanical wear permits them to be used in refractory products such as bricks and kiln. Silica sand can be used to make a feedstock for refined silica products such as elemental silicon metal, silicon carbide, silica glass and gels (Ref et al., 2015). The SiO_2 structure is based upon a SiO_4 tetrahedron structure. Each silicon atom is bonded to four oxygen atoms and each oxygen atom in turn bonded to two silicon atoms (Ekwenna et al., 2023).

2.2. Structure and Chemical properties of silicon dioxide

Silica's molecular formula is SiO_2, so it can be thought to be a polymer of silicic acid that contains cross-linked SiO_4 units. Figure 2.1 illustrates how two silica molecules shared an oxygen atom just a tiny part of a giant SiO_2. It shows the Si - O - Si bond angle (Ravindra & Narayan, 1986). Additionally, colloidal silica particles have a density of 2.1 to 2.3 g/cm^3. In nature, silica can be found in a variety of forms, including quartz and sand. The colloidal condition of silica particles in liquid is known as colloidal silica. Silica particles will be joined together in colloidal silica in both small (1 nm) and sufficient (1 mm) sizes (Ref et al., 2015).

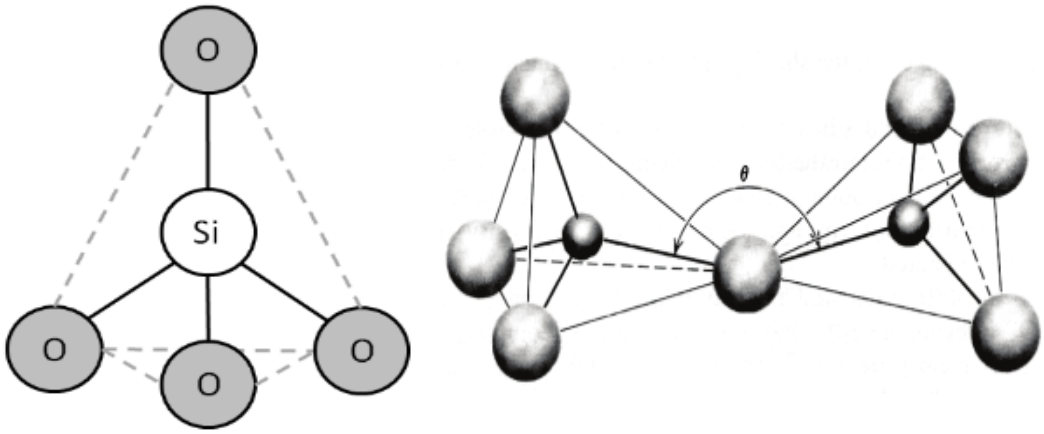

Figure 2.1: Schematic representation of adjacent SiO_4 tetrahedral with Si - O- Si bond angle, small circle, Si, large circle

All silica forms are odourless solids composed of silicon and oxygen atoms obtained as transparent to grey in its crystalline or amorphous powdered form. Silica particles get suspended in air and form non-explosive dust. Silica can be combined with oxides and other metallic elements for the formation of silicates (Submitted et al., 2020). Silica compounds are further divided into amorphous Silica (a-silica or non-crystalline Silica) and crystalline (or c-silica). Most of the silicon dioxide is extracted even from quartz mining, it can also be prepared using acid neutralization of an aqueous alkali metal - silicate solution. This kind of method is known as a wet process and forms amorphous SiO_2 grey, crystalline, or an amorphous solid. They have melting and boiling points as 1713 ºC and 2950 ºC, respectively (Ekwenna et al., 2023). The Si forms two double bonds with oxygen. Therefore, it is a very stable molecule. Table 2.1 shows the important properties of SiO_2 (Il'Ves et al., 2015).

Table 2.1: Properties of pure SiO_2

Properties	Values
Density	2.0 – 2.3 gm./cm3
Electrical conductivity	Varies widely
Breakdown field	>1E7 V/cm in thermal oxides, Can be as low as 1E6 V/cm in CVd oxides
Thermal conductivity	0.01 W/cm K
Thermal diffusivity	0.009 cm2/sec
Coefficient of thermal expansion	0.5 ppm/K
Refractive index	1.46
Dielectric constant	3.9

2.3. Silica gel

Silica gel is one of the synthetic adsorbents obtained from silica that is the most abundant and most complex material in the world. They have been used extensively as catalysts and for adsorbing organic compounds and removing heavy metals from wastewater because porous silica materials have large specific surface areas, controllable narrow pore size distribution, and high adsorption capacities (Asghar Ali et al., 2009). Silica gel generally possess the properties of higher porosity and larger surface area together with very smaller pore sizes. Silica gel is a controlled dehydrated polymeric structure made from the coagulation of a colloidal solution of silicic acid with the formula $SiO_2.nH_2O$ (Lazaar et al., 2022). It is a chemically inert, non-toxic material composed of amorphous silicon dioxide. The pore area of silica gel varies with the method of synthesis Silica gel is a type of amorphous silica, which is a form of silicon dioxide. Silica gel is a versatile and widely used material with many practical applications in industry and daily life such as desiccant and adsorbent (Besbes et al., 2009).Silica gel is a porous form of silicon dioxide (SiO2) commonly used as a desiccant to control humidity and moisture levels in a variety of applications. It is synthesized by a sol-gel process, which involves the formation of a colloidal suspension (sol) and subsequent gelation to form a solid network (gel). Preparation of the precursor solution, Hydrolysis and condensation gelation are the major steps to synthesize silica gel from silica containing precursor (Hastuti et al., 2019).

Table 2.2: Typical characteristics of silica gel (El-didamony et al., 2019)

Characteristics	Values
Range of pore radial	1-12
Total porosity	0.5-0.65
Pore volume	0.45-1cm^3/g
Specific surface area	200-800m^2/g

2.4. Methods of silica gel synthesis

There are several methods to synthesize silica gels, Tetraethylorthosilicate (TEOS) is one of the most common raw materials on silica production. Actually, sodium silicate as another kind of silica raw materials has many benefits, such as a slow grow rate, low cost, possibility of particle surface modification etc. Most commonly silica gels are manufactured by acidifying an aqueous solution of sodium silicate. The materials that 1st form is called a hydrosol, the particles of which agglomerate and results in the growth of silica polymers. The hydrosol is typically formed at low pH and if the subsequent washing steps are also conducted at relatively low pH, the final product then has high surface area (> 700 m^2/g). When hydrosol ceases to flow like a liquid (the gel time), it is termed as hydro gel (Taylor & Kushwaha, n.d.). Interaction of acid with sodium silicate solution produces orthosilicic acid which is an intermediate product of the hydrolysis. It is very unstable substance which readily condenses with itself to give a colloidal polymer of silica sol (Ingrachen-Brahmi et al., 2020).

There are several methods to synthesize silica gels these are the Stöber method and sol-gel method. However, the Stöber method has to use a high-cost alkoxide or organ metallic compound and is also only used to control the perfect particle size of colloids or pore size of mesostructured material due to high production cost (Ui et al., 2014). Therefore, in this study, a sol-gel method was demonstrated. The term "sol" is intended to encompass any suspension of fine silica particles in an aqueous media. The term "gel" is intended to encompass a three-dimensional network formed by silica particles, in either wet or dry form due to the reaction of sodium silicate and sulfuric acid.

(Lazaar et al., 2022) studied the sol-gel method obtains a high purity silica gel powder; however, the process yields a low percentage. In sol-gel mainly two types of silica sources were used to synthesize this porous silica, that is, tetraethylorthosilicate (TEOS) and sodium silicate solution (Lazaar et al., 2017). However, these raw materials are expensive, especially the TEOS is more expensive than sodium silicate due to this the cost of adsorbent silica materials increase. Therefore, substitute silica sources must be found. The solid waste residue contains a large amount of silicon oxide, which can be used as the raw material for synthesizing silica gel materials. In this study, sodium silicate is derived from solid waste residue by using sodium hydroxide (NaOH) as an extraction solvent. Sodium silicate solution was selected due to the cost of synthesizing silica.

Even though both gelation and coagulation will make silica sols lose their stability, they are different from each other. When a sol is gelling, colloidal silica particles link with each other one by one and form long chains. As a result, sol will become more viscous and finally look like soft solid materials. On the other side, coagulation somehow means that precipitation. Silica particles will link with each other and form clusters. When clusters become large enough, they will settle down. Fig 2.2 (Contractor et al., 2006) Shows the difference between a sol, gel, and precipitate of silica.

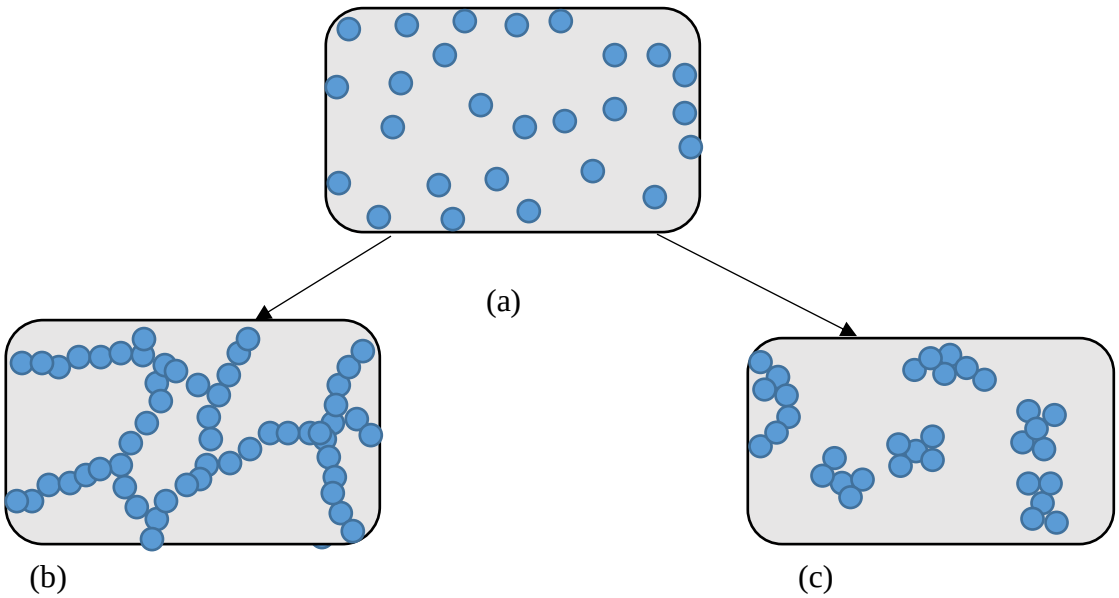

Figure 2.2: Silica gel versus precipitate: (a) sol, (b) gel, and (c) flocculation and precipitation

The silica gel can be prepared in two steps; Solution-sol-gel or sol-gel (for short) processing starts with a solution or a sol which becomes a gel. The solution can be prepared from either inorganic salts or organic compounds which then are hydrolyzed and condensed to make a sol or a gel. According to (Science, 2020) One can stop at the sol stage which refers to a dispersion of particles of colloidal dimensions in a liquid or proceed to the gel state which refers to a three-dimensionally-linked solid network with liquid filling the pores.

Initially, sodium silicate was dissolved in distilled water and a homogenous sol was prepared via the dropwise addition of acidified water to form silicic acid and a sodium salt. This is the initial hydrolysis stage in which Si–OH bonds are formed. Subsequently, a condensation step occurs via the expulsion of water to form a highly cross-linked gel network called a 'hydrogel' in which water is entrapped in the porous network (Besbes et al., 2009). These hydrogels are highly sensitive to the outside atmospheric conditions, and hence proper aging is required to strengthen the gel network. The presence of sodium ions will induce brittleness in the gel. Thus, to tackle this issue, the aged gel is washed several times with a surplus amount of water to remove the Na^+ ions. The Na_2SiO_3 : H_2O molar ratio, which reflects the silica content present in the gels, is an important factor in the preparation of sodium silicate gels. As the molar ratio increases, the SiO_2 content in the sample increases, thereby generating a strong network of Si–O–Si bonds (Minju et al., 2021). In the study done by (Rao *et al.* in 2004), for a molar ratio $> 8.86 \times 10^{-3}$, no shrinkage of the gel network was observed.

The basic steps in the production (extraction) of silica from SWR are:

1. Dissolution of silica in caustic soda as sodium silicate (Na_2SiO_3) from the SWR

$$\underset{\text{(SWR)}}{SiO_2} + \underset{\text{(Caustic Soda)}}{2NaOH} \xrightarrow{80\text{-}90^oC} \underset{\text{(Sodium silicate)}}{Na_2SiO_3} + H_2O \qquad (2.1)$$

2. Silica is precipitated from sodium silicate solution using H_2SO_4

$$\underset{\text{(Sodium Silicate)}}{Na_2SiO_3} + \underset{\text{(Sulphuric acid)}}{H_2SO_4} \xrightarrow{\text{room temp.}} \underset{\text{(Silica)}}{SiO_2} + \underset{\text{(Sodium sulphate)}}{2Na_2SO_4} + H_2O \qquad (2.2)$$

3. Filtration and drying of the final product (pure silica)

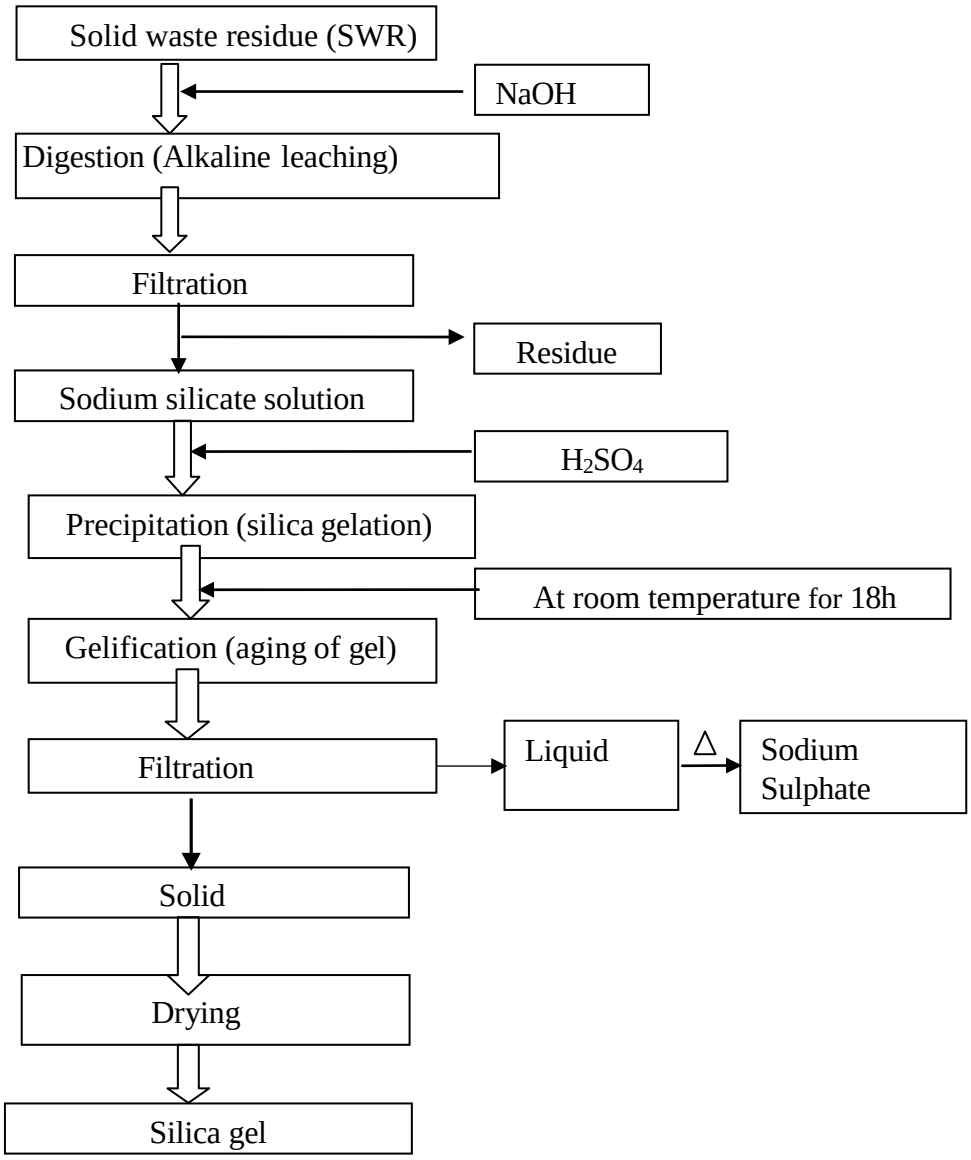

Figure 2.3: Schematic diagram of Silica gel synthesis from siliceous by product (SWR)

Extracted sodium silicate solution serves as precursors in the preparation of gels. Most commonly silica gels are manufactured by acidifying an aqueous solution of sodium silicate. According to (Lazaar et al., 2022) studies the material that first forms is called a hydrosol, the particles of which agglomerate and results in the growth of silica polymers. One can stop at the sol stage which refers to a dispersion of particles of colloidal dimensions in a liquid. The hydrosol is typically formed at low pH and if the subsequent washing steps are also conducted at relatively low pH, the final product then has a high surface area. When hydrosol ceases to flow like a liquid (the gel time), it is termed hydrogel. The process of transforming a liquid sol

into a gel state with subsequent post-treatment (washing) which have an advantage to produces a uniform structure with high purity gel obtained at room temperatures (Besbes et al., 2009a).

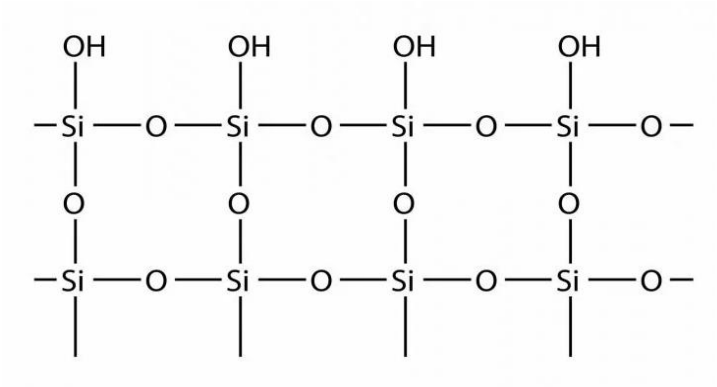

Figure 2.4: Different forms of hydroxyl group that can occur on the surface of Silica gel

Further condensation of silica sol takes place on standing which assumes the form of a gel. Silica gel is a continuous three-dimensional network of spherical particles of colloidal silica. Both siloxane (-Si-O-Si-) and silanol (-Si-OH) bonds are present in the gel structure. The pores of the gels are interconnected and filled with water from hydrolysis and condensation reactions. The silanol groups in turn may condense to form siloxane bridges (-Si-O-Si-) (Lorber et al., 2009) as shown the surface composition of silica gel fig. 2.4.

2.5. Factors affecting synthesize of silica gel

2.5.1. Raw material

The major inherent ash forming elements in kaolin residue include Ca, Si, Al, Ti, Fe, Mg, Na, K, S, and P. The composition of ash affects its behavior under high temperatures of combustion and gasification reactors, due to this raw material have an impact on the properties of silica gel product, Pore structure, Purity and yield of the end product. Since a silica gel is a structurally amorphous material, almost any silicon contain solid material can be converted into silica gel (Lailun et al., 2022). There are previous studies relating to this, silica gel with high surface area and pore volume can be produced from a large amount of silicon-containing raw materials like agricultural waste which include siliceous by-product rice husk, coal, cane bagasse, peanut shell, and other by- products due to low cost of production scraps (Chan & Wisconsin, 1989; Ui et al., 2014). In the selection of raw material for the preparation of porous silica gel, several factors are taken into consideration. The factors are: High silica (SiO_2) content, Low heavy metals content, Low density and sufficient.

According to the above factors the AMCF solid waste can be a good candidate for the synthesis of sodium silicate due to its high silica content and easy availability. In Table 2.4 the bulk chemical composition of SWR is provided showing that SiO_2 is the major constituent of the residue, comprising up to 60.48 wt %. In addition to other major oxides, SWR contains a range of potentially leachable elements Ti, Mg, Mn, Ca, K, and water (Alouani et al., 2019) the crystalline phases in solid waste residue can be categorized into three groups: 1) silicates: albite, diopside, melilite, and quartz, 2) carbonates: calcite and dolomite, and 3) iron oxides: magnetite and hematite. Overall, only 20.5wt % of the residue consist of crystalline phases, and the rest (79.5wt %) is amorphous. The presence of high amorphous content and silicate minerals makes this fraction of SWR good for the extraction of silica under alkaline conditions.

Table 2.3: Chemical Composition of AMCF solid waste (filter cake), five batch average

Compounds	**Content (wt. %)**
SiO_2	60.48
CaO	0.14
Al_2O_3	14.93
Fe_2O_3	0.15
K_2O	0.45
MgO	0.04
P_2O_5	<0.01
MnO	<0.01
TiO_2	<0.01
H2O	5.75
LOI	18.22

Source: AMCF quality control analysis

2.5.2. The Particle size of SWR

The particle size of kaolin residue has a significant effect on the production of silica gel. Smaller particle sizes lead to higher yields of silica gel, as well as a more uniform product. This is because smaller particles have a greater surface area, which allows for more efficient reaction with the silica-forming agents. Additionally, smaller particles are less likely to agglomerate, which can lead to a more free-flowing product (Northcott et al., 2007). According to (Park et al., 2012)the production of silica gel from kaolin residue was investigated using a variety of

particle sizes. The results showed that the yield of silica gel increased from 50% to 75% as the particle size decreased from 100 μm to 10 μm. Additionally, the particle size distribution of the silica gel became more uniform with smaller particle sizes.

The effects of particle size on the properties of silica gel are also significant. Smaller particle sizes lead to a more porous product, which has a greater surface area. This can lead to improved properties such as adsorption capacity, catalytic activity, and rheological behavior. The details about the effects of particle size on the production of silica gel from kaolin residue (Alouani et al., 2019):

- ✓ Yield: The yield of silica gel increases with decreasing particle size. This is because smaller particles have a greater surface area, which allows for more efficient reaction with the silica-forming agents.
- ✓ Particle size distribution: The particle size distribution of silica gel becomes more uniform with decreasing particle size. This is because smaller particles are less likely to agglomerate.
- ✓ Properties: Smaller particle sizes lead to a more porous product, which has a greater surface area. This can lead to improved properties such as adsorption capacity, catalytic activity, and rheological behavior.

2.5.3. Temperature

Temperature affects the extraction efficiency that is soluble silica content in sodium silicate solution. According (Z. Liu et al., 2014) study result shows that 80 ^{o}C is the optimum temperature to obtain the better amount of soluble silica content during the extraction process (reaction between SWR and caustic soda) (Wakene et al., 2021). When the temperature increase there is no significant difference between silica content in extracted sodium silicate solution and also when the temperature decrease 20% of the available silica was dissolved at 20 ^{o}C during the first 24 hr, it needs much time to increase dissolved silica content. Temperature affects the reaction of Sulphuric acid with sodium silicate during this reaction, the favorable temperature was found by (Alam et al., 2019), which is at room temperature is to produce a good quality product. As reported by several authors, temperature significantly affects the production yield of silica gel and also the quality of silica gel.

2.5.4. Time

Reaction time has a greater impact on the extraction of silica. From a previous study, the extraction times normally used were from (Sdiri, 2014) 1hr to 3 hour for kaolin residue and clay As time increased, the percentage of yield decreased gradually and the surface area also increased, this result is possibly due to the raw material composition, which results in the formation of silica gel. From studies of (Ingrachen-Brahmi et al., 2020) the reaction time of 30 and 45 min, no silica extraction was observed even the acid and base concentration was kept and therefore the extraction time should be above 45 min

2.5.5. Solvent concentration

(Amin, 2016) studies, the concentration of sodium hydroxide (NaOH) affects the extraction of silica. The amount of silica increases with the increase in the concentration of alkali 1M up to 3M. Above this concentration, a slight decrease in the amount of extracted silica was observed. The increase in silica with the concentration of base is attributed to the completion of stoichiometric ratio during the reaction and also the extraction of silica by less than 1M concentration of sodium hydroxide (NaOH) the amount of extracted silica decrease (Ui et al., 2014)Amorphous silica is capable of forming sufficient silanolates for the subsequent micelle formation at solid-liquid ratios greater than 0.25. The concentration of sodium silicate affects characteristics of purity, bulk density, and yield of silica gel. The concentration of Sulphuric acid has an effect during, the silica gel formation; no silica precipitate is formed on the extracted silica with 1 and 1.5 N Sulphuric acid, and above this concentration, silica precipitate started. Maximum silica precipitated is observed with 2.5 N Sulphuric acid above which slight decrease in silica. The decrease in silica above 2.5 N may be the re-dissolution of silica in a highly acidic environment (Amin, 2016).

2.5.6. Salt effect

The dehydration reaction of silicic acid will happen in the alkali solution (Alam et al., 2019) In this case, silica forms nuclei first and thus particle grows further. Therefore, increasing salt concentration means increasing sodium ion concentration, resulting in a larger particle size of produced silica. However, during the synthesis of the silica powder, the remaining Na+ in sodium silicate affects the network therefore it was removed through the sol-gel process. According to (Fleury et al., 2017) Studies in the silica sol, the Na+ ion was breaking the silica

network structures as a modifier during silica sol-gel gelation and decreasing the purity of silica powders. To remove the sodium from sodium silicate, sodium silicate was mixed with Sulphuric acid. Silica hydrogel was made by the sol-gel reaction after the sodium ions were removed by washing until the pH becomes 7 (El-didamony et al., 2019)

2.5.7. pH

The pH has a great effect on not only porosity but also the particle size of silica particles. (Ali et al., 2009) found that pH strongly affects the surface area of silica particles. Surface area decreases with an increase of pH value, i.e. the silica obtained at pH 9 had the lowest surface area (237 m^2/g), while the highest surface area (634 m^2/g) was obtained at pH 3. When pH increases from 3 to 9, as shown in the following two paths, a condensation reaction may happen during gel formation, resulting in increased particle size and porosity

$$(OH)_3Si - OH + OH \longrightarrow (OH)_3Si - O^- + H_2O \quad (2.3)$$

$$(OH)_3Si - OH + (OH)_3Si - O^- \longrightarrow (OH)_3Si - O^- Si(OH)_3 + OH \quad (2.4)$$

Where, the OH plays an important catalyst role. In the acid regime, reduced pH leads to changing of silanol bonding (Si - OH) to siloxane bonding (Si - O- Si) and gel formation is slow. As can be seen above, the OH increases the reaction of equation (2.3). In the acid solution, decreasing of OH will result in more silanol groups (Si - OH) change into siloxane linkages (Si - O- Si) so, that colloidal suspension becomes more stable. In the basic solution, the reaction will reverse so will siloxane change into silanol groups In this case; silica is composed of small particles and therefore, possesses a high surface area. In the basic regime, surface siloxane bonding tends to form silanol bonding. Siloxane linkages create negative charges and increased electrostatic repulsion between silica particles (Engineering, 2017). The charge develops silica particles to connect, so that particle size becomes larger when pH increases. Therefore, low porosity and lower surface area will be obtained in this situation. The quality of silica gel was greatly affected by changes in the pH level of the hydrosol, this may be due to the reason that pH 7 stabilized sol particles grew to gel (Hafiz et al., 2009), while the low pH level ($pH \leq 2$) of the hydrosol, the gelation can take several days, even several weeks for $pH \leq 2$, whereas, for basic solutions, the gelling is instantaneous. The gelling time is a parameter that depends on pH and metasilicate solution concentration (Ali et al., 2009).

2.5.8. Mixing rate

Preparation of silica gels as affected by mixing rate and it was observed in previous studies that the product quality, purity, and gel size were changed by changing the stirring rate. (Ali et al., 2009) Studies show that the addition of HCl was slowed down in sodium silicate solution, the reaction was completed in18-20 min, and slow constant stirring was done to promote gel formation.

2.6. Dyes

It is estimated that more than 700,000 tons of dye material are generated each year, made up of more than 100,000 commercially accessible dyes. William Henry Perkin made the accidental discovery of mauveine, the first contemporary synthetic organic color, in London in 1856. Actually, neither this dye nor the other ones that were generated were the first synthetic dyes to be created in a lab. Picric acid, which was created in 1845 by nitrating phenol, was the first synthetic organic colours (Ziarani et al., 2018). According to the color theory put forward by dye scientist Otto N. Witt in 1875, a compound's color results from the presence of specific groupings of atoms or groups known as chromophores. A chromogen-chromophore with an auxochrome is typically used in the synthesis of dyes to create a chemical structure that is colored. When combined with the chromogen, the chromophore group, also known as the "color giver," serves as the foundation for the chemical classification of dyes. The azo (-N=N-), carbonyl (-C=O), and nitro ($-NO_2$) groups are the three most significant chromophores. The maximum absorption of the chemical is significantly altered by the presence of auxochromes, which also provide a bonding affinity (Benkhaya et al., 2020).

2.6.1. Classifications of dyes

There are two methods used to classify dyes, either according to their chemical structure (particularly considering the chromophoric structure present in the dye molecule) or according to how it is applied to the substrate. The first method is adopted by practicing dye chemists and includes azo, Anthraquinone, etc. dyes. The latter method is adopted by the colour index (Oros et al., 2004).

❖ Chemical structure method

The most appropriate way to classify dyes is by chemical structure which has many advantages as follows (Benkhaya et al., 2020): 1) It easily identifies dyes as relating to a group which has characteristic properties, for example azo dyes (strong, low cost) and anthraquinone dyes (weak, expensive). 2) There are a manageable number of chemical groups. The dye molecules are categorized using this method according to structurally related groupings. For instance, the most significant class of dyes are azo dyes, which include at least one azo group (-N=N-) connected to two radicals, at least one of which may or may not be aromatic. The carbonyl functions (-C=O) are found in the next-most significant dye class. Synthetic dyes come in a wide range of structural configurations, including cationic, nonionic, anionic, dispersion, azo, diazo, anthroquinone-based, and metal complex dyes.

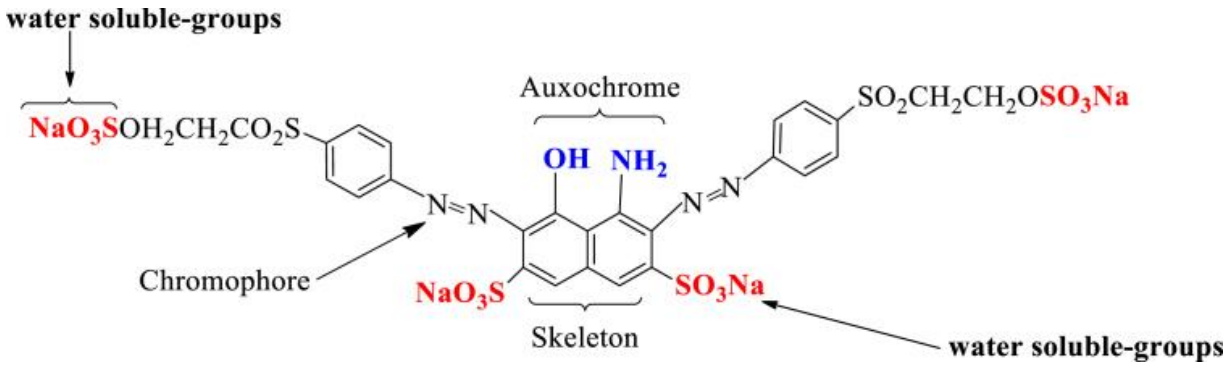

Figure 2.5: Chemical structure of azo dye (Reactive dye)

Azo dyes are the class of commercial organic dyes most studied due to their wide usage (they represent 70% of the dyes used in the textile industry and are also widely used in the food, cosmetic, and pharmaceutical industries) and their high toxicity (Vaiano & De Marco, 2023). They contain two nitrogen atoms linked by a double bond and two functional groups, R and R'. The chemical structure of an azo dye is represented by a backbone, the auxochrome groups, the chromophoric groups, and the solubilizing groups (Rauf et al., 2011). As schematically represented in Figure 1, they can be further classified into acid, basic, sulfur, reactive, disperse, and vat dyes.

- Usage or application method

Dyes are classified based on their method of application and their parent structure. Based on the method of application, dyes can be classified into two types: Acid dyes and Basic dyes[12]. Acid dyes are azo dyes and are characterized by the salts of sulphonic or carboxylic acids. These are usually applied to wool, silk and nylon and have no affinity for cotton. Basic dyes contain Amino group in unsubstituted (-NH2) or Substituted form (-NR2) as chromophore (colour bearing group) or auxochrome (colour enhancing group) (Benkhaya et al., 2022).
The color index's main strategy is to categorize dyes according to how they are used or applied because polyester and cotton make up the majority of textile fibers (Vaiano & De Marco, 2023).

The exact substrate being colored and the specified fastness attributes define the type of dyestuff to be employed. Due to their large range of color hues, high wet fastness profiles, ease of application, dazzling colors, and low energy requirements, reactive dyes are widely used for textile dyeing (Ziarani et al., 2018).

Basic dyes are called so since they are salts of organic bases. They are also known as cationic dyes because of the presence of positive charge in the dye molecules under dyeing conditions. During dye application, the negatively charged acrylic fiber attracts the positively charged dye cations for ionic bonding (Khan et al., 2004). Due to high attraction between the oppositely charged fiber and dye molecules, there is risk of unlevel dyeing because of high rate of dyeing. This risk may be reduced by careful control of dyeing temperature and used of suitable retarding agents. The basic dyestuffs are well known for their intense hues and brilliant shades, unrivalled by any other class of dyes. Basic dye has excellent light fastness because of their resistance to destructive effect of ultraviolet radiations in sunlight. Their washing fastness is also quite good, which may be attributed to hydrophobic nature of the acrylic fiber and good substantively of the dye for the fiber. The basic dyestuff are most commonly used for dyeing polyacryonitrile or acrylic materials. Basic dye is also used for dyeing wool and silk fibers (Rahman & Foisal, 2016).

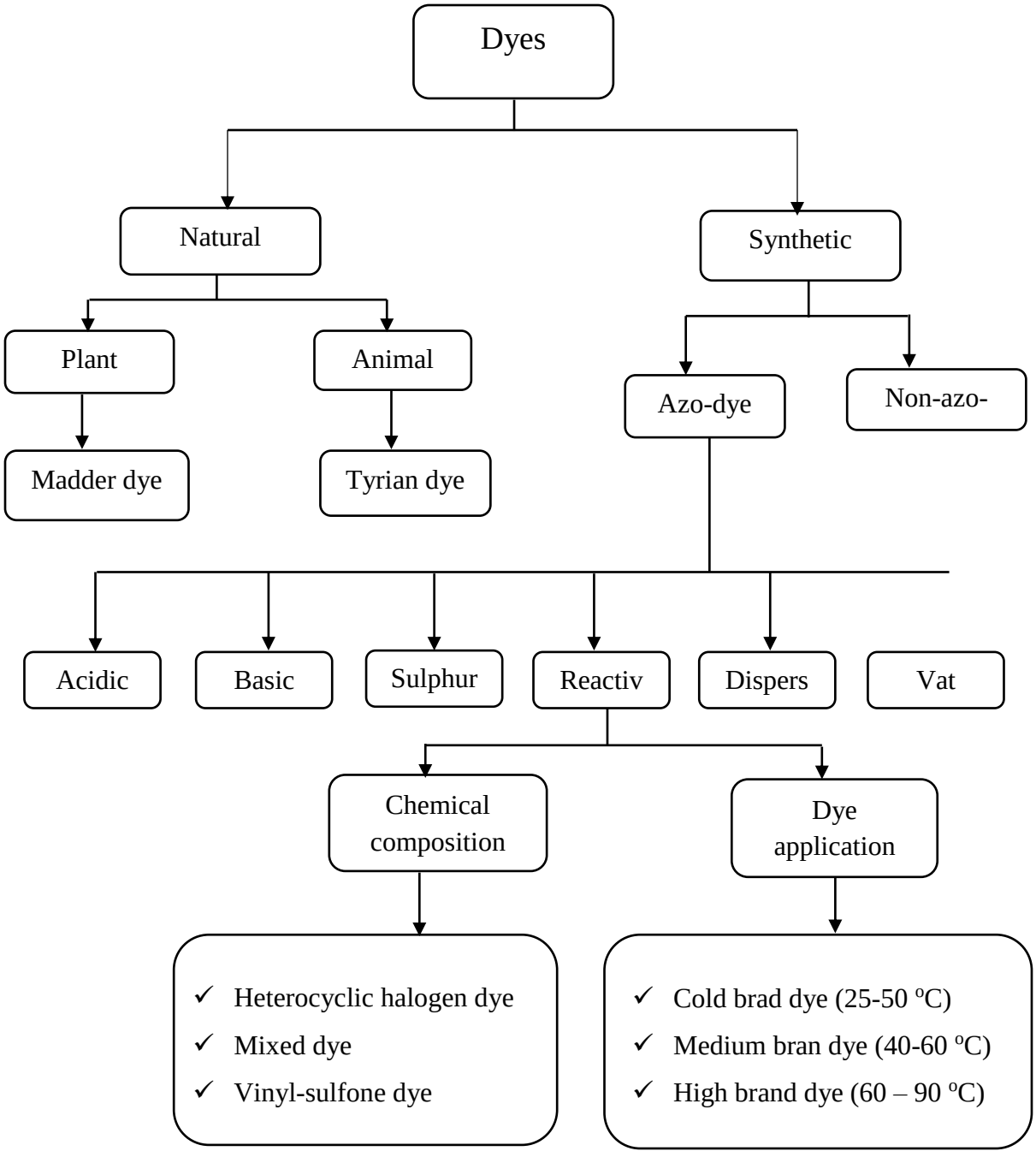

Figure 2.6: classifications of dyes

2.6.2. Toxicity of dyes

Basic dyes are very visible even at very low concentrations and have intense color (Benkhaya et al., 2022). The drawbacks are displayed in Table 2.4 by dye class.

Table 2.4: Disadvantages of different dye class

Dye class	Disadvantages
Basic dye	It has high brilliance and intensity of colors and is highly visible even in a low Concentration.
Azo groups	Their reductive cleavage of azo linkages is responsible for the formation of toxic amines in the effluent.
Anthraquinone-based Dyes	It is most resistant to degradation due to their fused aromatic ring structure and thus remains colored for a longer time in wastewater.

2.7. Methylene blue

Methylene blue is a synthetic dye that is commonly used in the textile, printing, and paper industries as a colorant. It is a cationic dye that has a deep blue color and is water-soluble. (Mubarak et al., 2015).

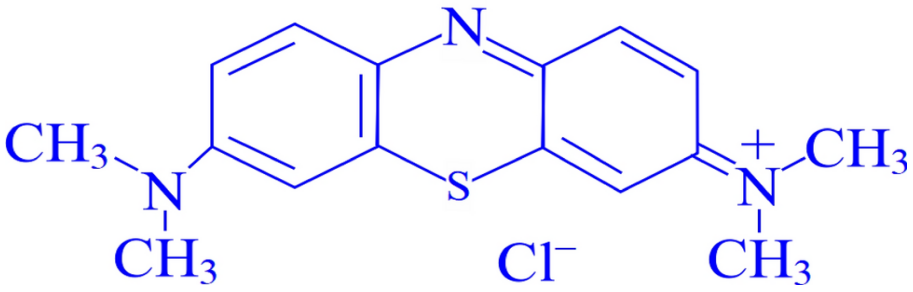

Figure 2.7: Molecular structure of methylene blue

The structure of both forms is represented in Figure 2.7 the colour of MB depends on its chromophoric and auxochrome groups. The chromophore group of MB is the N–S conjugated system on the central aromatic heterocycle, while the auxochrome group is N-containing groups with lone pair electrons on the benzene ring (Sarkar Phyllis et al., 2022) . The absorption spectra of the MB reveal the most intense absorption peak at around 664 nm associated with an MB monomer, with a shoulder peak at about 612 nm attributed to MB dimer.

Table 2.5: Chemical and physical properties of MB dye

Chemical and physical properties	Values
Melting Temperature	$180^{o}C$
Boiling Temperature	No data
Solubility in water	35.5 g/L
PH value	3(10 g/L H_2O)
Molecular weight	319.09 g/mol
Color	Dark blue-green in oxidized form, colorless in reduced form (leucomethylene blue)
Chemical formula	$C_{16}H_{18}ClN_3S$

The discharge of wastewater containing methylene blue into water bodies has become a major environmental concern due to its potential adverse effects on aquatic life and human health(Jia et al., 2016). Methylene blue is toxic to aquatic organisms and can cause skin irritation and other health problems in humans (Sdiri, 2014).

Table 2.6: Dose related toxicity of MB dye

Animal studies	Toxic doses (mg/Kg)	Toxic Manifestation
Rat	5-50	Neuronal apoptosis, reduced MAC isoflurane
Dog	10-20	Hypotension, decreased SVR, renal blood flow, pulmonary hypertension
Human studies	Toxic doses (mg/Kg)	
	2-4	Hemolytic anemia, skin desquamation in infants
	7	Nausea, vomiting, abdominal pain, chest pain, fever, hemolysis
	7.5	Hyperpyrexia, confusion
	20	Hypotension
	80	Bluish discoloration of skin (similar to cyanosis)

Furthermore, the presence of methylene blue in water bodies can reduce the penetration of light into water, affecting photosynthesis and the growth of aquatic plants. Methylene blue toxify has occurred at a wide range of dose. Dose-related toxicity of MB summarized in table 2.6 (Jodeh, S., Amarah, J., Radi, S., Hamed, O., Warad, I., Salghi, R., ... & Alkowni, 2015)

2.8. Dyes Impact on environment

Any industrial activities causes pollution in one form or the other so is the textile industry. Wastewater is the most environmentally damaging, and the wastewater from textile plants is classified as the most polluting of all the industrial sectors, considering the volume generated as well as its composition. The dyestuff lost through the processes of the textile poses a major problem for wastewater treatment (Mousavi et al., 2022)

Through the dyeing process, depending on the class of the dye, its loss in wastewaters could vary from 2% for basic dyes to as high as 50% for reactive dyes, leading to severe contamination of surface and ground waters. Color is the first wastewater contaminant to be recognized, since a very small amount of dye concentration in water (<1ppm) are highly visible that affects aesthetic merit, transparency and water-gas solubility (Jia et al., 2016).

Many dyes are also highly toxic to the ecosystem and mutagens, meaning they can have acute to chronic effects upon organisms, depending on exposure time and dye concentration. For example, dye effluent has been connected to growth reduction, metabolic stress and death in fish, and growth and productivity in plants. Contamination therefore limits downstream human water use such as recreation, drinking, fishing and irrigation (Bery et al., 2022). Therefore, wastewater containing residual dyes need to be treated before discharging to the receiving environment to keep the environment eco-friendly and sustainable.

2.9. Environmental legislation

With respect to legislation, there is as yet no international consensus concerning discharging textile effluent, including dyes, and there is no official document listing the different effluent limit values applied in different countries. Many developed countries, such as the United States of America, Canada, Australia and the nations of the EU enforce environmental legislation, which establishes limits. Countries, such as Thailand, have copied the US system, whereas others, such as Turkey and Morocco, have copied the EU model. In other nations, including

India, Pakistan and Malaysia, the effluent contamination limits are recommended, but not mandatory. In the majority of developing countries like Ethiopia, dye limitations are not specified as separate from that of groupings such as 'total dissolved solid' concentration (Hessel et al., 2007).

2.10. Treatment of wastewater containing dyes

The classification methods of dyes are introduced according to the chemical structure and application or usage methods. The most common methods for wastewater treatment are described and special attention has been given to adsorption processes for the treatment of wastewater containing dye. Pollution by organic chemicals including that by dyes is one of the most serious environmental problems facing life on earth. There are several sources of water pollution by dyes and pigments, such as leather tanning, paper, rubber, food technology and the textile industry. These dyes have a variety of complex organic compounds and toxic substances with unknown environmental behavior such as aromatic amines (C_6H_5-NH_2), which are suspected to have carcinogenic effect, phenyl (C_6H_5-CH_2) and naphthyl (NO_2-OH). The resistance of these organic compounds to decomposition due to the complex chemical structure of synthetic pigments in dyes results in a difficult to treat wastewater which is also resistant to degradation by biological methods. Many researchers have studied different methods to remove dyes from wastewater including chemical, physicochemical and biological processes such as, adsorption, chemical precipitation, electrochemical oxidation, chemical oxidation, and aerobic and anaerobic biological processes (Samsami et al., 2020). Several reported methods for removal of dye pollutants from wastewater are summarized in Table 2.7.

There are various treatment technologies that can be roughly categorized into three types: biological, physical, and chemical methods. Bear in mind that any dye depletion technique has its own merits and demerits; therefore, a combinatorial treatment method can be advantageous. Moreover, the role of nanotechnology in the dye degradation or removal process has been marked as a promising technique in comparison to existing processes. This chapter aims to compose various information about dye, dye effluent, and existing treatment technologies for wastewater.

2.10.1. Biological Method

Biological treatment is relatively economical methods compared to other physical and chemical processes. Biodegradation methods such as fungal decolonization, microbial degradation, adsorption by (living or dead) microbial biomass and bioremediation systems are commonly applied to the treatment of industrial wastewater because many microorganisms such as bacteria, yeasts, algae's and fungi are able to accumulate and degrade different pollutants (Ledakowicz & Pazdzior, 2021). However, their application is often restricted because of technical constraint. According to (Samsami et al., 2020) biological treatment requires a large land area and is constrained by sensitivity toward diurnal variation as well as toxicity of some chemicals, and less flexibility in design and operation. Further, biological treatment is incapable of obtaining satisfactory dye removal with current conventional biodegradation processes. Moreover, although many organic molecules are degraded, many others are recalcitrant due to their complex chemical structure and synthetic organic origin

2.10.2. Chemical Methods

Chemical methods include coagulation or flocculation combined with flotation and filtration, precipitation–flocculation, electroflotation, electrokinetic coagulation, conventional oxidation methods by oxidizing agents (ozone), irradiation or electrochemical processes. These chemical methods are often expensive, and although dyes are removed, accumulation of concentrated sludge creates a disposal problem. There is also the possibility that a secondary pollution problem will arise because of excessive chemical use (Kathing & Saini, 2022).

2.10.3. Physical method

Different physical methods are also widely used, such as membrane – filtration processes (nano filtration, reverse osmosis) and adsorption techniques. The major disadvantages of the membrane processes are: (i) a limited lifetime before membrane fouling occurs and (ii) cost of periodic replacement which need to be included in any analysis of their economic viability (Ledakowicz & Pazdzior, 2021). Adsorption is one of the most popular methods for the removal of pollutants from wastewater since proper design of the adsorption process will produce a high-quality treated effluent. This process provides an attractive alternative for the treatment of contaminated waters, especially if the sorbent is inexpensive and does not require an additional pretreatment step before its application (Samsami et al., 2020).

Table 2.7: Principal existing and emerging processes for dyes removal

Dye removal method		Advantages	Disadvantages
Conventional treatment process	Coagulant flocculants	Simple, economically feasible	High sludge production, handling and disposal problems
	Biodegradation	Economically attractive, publicly acceptable treatment	Slow process, necessary to create an optimal favorable environment, maintenance and nutrition requirement
	Adsorption on silica gel	The most effective adsorbent, great, capacity, produce a high-quality treated effluent	Ineffective against disperse and vat dye, the regeneration is expensive and result in loss of the adsorbent, non-destructive process
Establish recovery process	Membrane separation	Remove all dye types, produce a high-quality treated effluent	High pressure, expensive, incapable of treating large volumes
	Ion-exchange	No loss of sorbent on regeneration, effective	Economic constraints, not effective for disperse dye
	Oxidation	Rapid and efficient process	High energy cost, chemical required
	Advanced oxidation process	No sludge production, little or no consumption of chemicals, efficiency for recalcitrant dyes	Economically unfeasible, formation of by- products, technical constraints
Emerging removal processes	Selective Bio adsorbents	Economically attractive, regeneration is necessary high selectivity	Requires chemical modification, nondestructive process
	Biomass	Not efficiency and selectivity, no toxic effect on microorganism	depends on some external factors (pH, salts)

Generally, all the dye removal methods have their own advantages and disadvantages as reviewed in Table 2.8. There is no obvious stand out method; all have both advantages and disadvantages (Kathing & Saini, 2022). This work examines the potential for the adsorption process to overcome for textile dye removal from wastewater

2.11. Adsorption

Adsorption is a surface phenomenon in which it is characterized by chemical species (adsorbate) from its vapor or liquid solution phase onto or near the surface of solid (adsorbent). The presence of excess surface occurs when the attractive energy of a substance with the solid surface that is adhesive work is higher than that of cohesive energy of the substance. Adsorption is the mass transfer operation of solute (adsorbate) exists in a fluid phase to the surface of solid phase (adsorbent) due to the existent of high molecular interaction between them. It is a process of the interface in which a film of adsorbates is created on the surface of the adsorbents of material. Thus, it is the result of surface energy (Dąbrowski, 2001). Adsorption is commonly employed as a polishing step to remove organic and inorganic contaminants in water and wastewater treatment. The surface area or active sites, the lack of selectivity, and the adsorption kinetics usually limit the efficiency of conventional adsorbents. Adsorption is a term used to describe the metal or organic substances in solution attached to a solid adsorbent at low, medium, and high coverage. Adsorption as a separation process is widely applied in our manufacturing economy and daily life. The adsorption process takes advantage of the ability of a particular solid to preferentially concentrate a particular substance in a solution (gas or liquid) on the surface. Therefore, the required purpose of purification or separation can be achieved by contacting the fluid with such a solid (Kecili & Hussain, 2018).

Adsorption can be categorized into physical adsorption (physisorption) and chemical adsorption (chemisorption) in nature. Physical adsorption has relatively weak intermolecular forces. It does not allow the sharing or transfer of electrons. Hence always maintains as individuality of interacting species. Even though the process is slow due to the occurrence of diffusion of molecules, the interactions are fully reversible which enables desorption to occur at a similar temperature (Kecili & Hussain, 2018). Not only the adsorbed molecules are free to move and cover the entire surface, but also have low heat in the case of physical adsorption.

The main characteristic of chemical adsorption is the large interaction potential, which leads to a high heat of adsorption close to the value of the chemical bond. This fact, combined with other spectroscopy, electron spin resonance, and susceptibility measurements, confirms that chemical adsorption involves the transfer of electrons and the formation of true chemical bonds between the adsorbate and the solid surface. Because chemisorption involves chemical bonding, it often occurs at high temperatures and is generally, related to the activation energy. Furthermore, the adsorbed molecules are located in specific locations and therefore cannot freely migrate to the surface. Table 2.9 Comparison of physical and chemical adsorption. Generally, adsorption can occur at any interface. That is either gas-solid interface or liquid-solid interface (Dąbrowski, 2001).

Table 2.8: The difference between chemical and Physical Adsorption

Parameters	**Chemical Adsorption**	**Physical Adsorption**
Force of Attraction	Strong attraction forces or chemical bond such as ionic bonds	Weak inter particle bond as van der waal forces
Temperature	Higher heat of adsorption	Low heat of adsorption
Electron transfer	electron transfer leading to bond formation between sorbate and surface	Not involve electron transfer, although polarization of sorbate may occur.
Adsorption layer	Monolayer only	Monolayer or multilayer
Kinetics Adsorption	Activated, may be slow and irreversible	Rapid, non- activated and fully reversible
Adsorption sites	Site specific, adsorbed molecule are fixed at specific sites	Not site specific, the adsorbed molecules are free to cover the entire surface

The most literature studies showed that adsorption process could considered an efficient treatment method for the removal of emerging compounds from water. It allows reaching good removal percentage. In addition, a process does not imply by-products formation, which could be more toxic than parent compounds. It is obvious that adsorption process encompassed in an integrated treatment system, which involves many factors, such as available space for the construction of treatment facilities, waste disposal constraints, desired finished water quality,

and capital and operating costs. All these factors imply the achievement of the optimal operating conditions for low-cost high efficiencies (Mousavi et al., 2017).

2.12. Mechanisms of adsorption

The molecules diffuse into the bulk through the extreme planes of the laminar layer around the solid particles to the turbulent flow as result of the concentration gradient given by the four diffusion mechanisms that tends to be natural. The first is the diffusion of molecular-scale adsorbed water into the liquid film that surrounds the adsorbent molecules in bulk. The second film diffusion is the diffusion of adsorbed water on the surface sites of the adsorbent molecules in a liquid film. On the third, a pore diffusion of intraparticle diffusion of adsorbed water in the interstices of the adsorbent. Lastly, the adsorption of adsorbed water on the inner surface of the adsorbent (Kecili & Hussain, 2018).

In the context of adsorption, the main challenge is to select the most promising types of adsorbents, mainly in terms of low cost, high capacity (often expressed as q_{max} values) high adsorption rates, high selectivity, and fast kinetic adsorption mechanisms(s), especially adsorbents/adsorbates Interactions that occur at interfaces. This is an important topic because the adsorption mechanisms involved in the collection of contaminants are what dictate the design of desorption strategies (e.g., the recovery of certain contaminants, such as "precious" metal ions, is also an important parameter for the economics of the process (Ahmad et al., 2022). The basic principle of adsorption: The preferred concentration of seeds on the surface of the adsorbed solid operates in two different processes (S. Liu et al., 2015)

2.13. Applications of adsorption

Today, the capacity of various types of adsorbents is increasing, and the recent interest in biotechnology and green technology has greatly expanded the use of adsorption in many fields. Here is a partial list of adsorption applications for liquid-phase adsorption (Wang et al., 2022).

- ✓ Decoloring, drying, or degumming of petroleum products
- ✓ Removing of dissolved organic species from water supplies
- ✓ Removing odor, taste, and color from water supplies
- ✓ Advanced treatment of waste water (domestic and industrial)
- ✓ Decoloring of crude sugar syrup and vegetable oils

- ✓ Recovery and concentration of proteins, pharmaceuticals, and bio-compounds from dilute suspensions
- ✓ Bulk separation of paraffin and isoparaffins

  For gas-phase adsorption
- ▪ Recovering organic solvent vapors and Dehydration of gases
- ▪ Removing toxic agents and odor for personal protection
- ▪ Air separation and separating normal paraffins from isoparaffin aromatics
- ▪ CO2 capture for addressing climate change

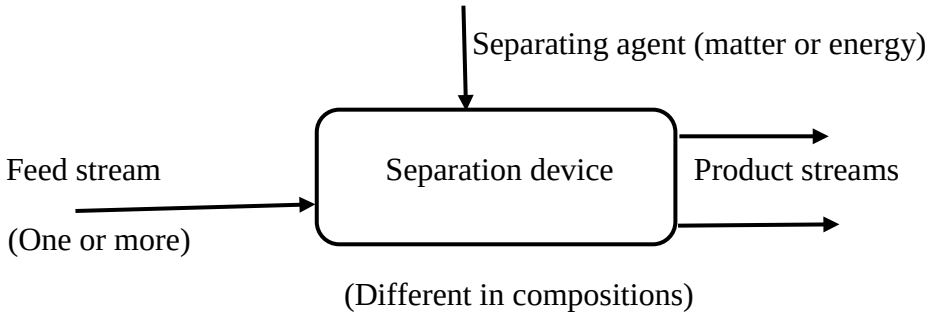

Figure 2.8: A general representation of the separation process

The adsorption separation method is an attractive process that can be easily applied to wastewater treatment and has efficiency and flexibility. Compared to other treatments, it looks better than other treatments. Several factors that affect adsorption efficiency, such as adsorbent type, contaminant concentration, adsorbent particle size, pH, contact time, and temperature, are very important in this process.

2.14. Factor affecting Adsorption

The effect of different process parameters such as pH, Initial methylene blue concentration, contact time, and adsorbent dose strongly study and the optimum conditions determined in various studies found.

2.14.1. Effect of pH

The adsorption ability of the surface and the type of surface-active centers are indicate by the significant factor that is the point of zero charge (pHpzc). The pH at which the surface charge is zero called the point of zero charge (pzc) and typically used to quantify or define the electro kinetic properties of a surface. The value of pH is use to describe pzc only for systems in which

H+/OH− are the potential determining ions (Yuan et al., 2019). Many researchers studied the point of zero charge (pHpzc) of various adsorbents prepared from agricultural solid wastes; in order to understand the adsorption mechanism. Due to the presence of functional group such as OH− group, cationic dye adsorption is favored at pH > pHpzc, whereas, anionic dye adsorption is favored at pH < pHpzc where the surface becomes positively charged (Khan et al., 2004). They observed that, the effect of pH on the removal of methylene blue in the presence of activated carbon. When initial pH of the dye solution is increase from 4 to 11 values, the percentage removal also increased from lower to higher. The increasing trend of removal of the methylene blue with increasing pH is dependent on the nature of the adsorbent. At lower pH, the percentage of the removal of methylene blue decrease and interestingly, at higher pH, the trend of the removal was increased. As the electrostatic attraction between the cationic dye and activated carbon is strengthen along with PH increasing, the highest adsorption amount obtained around PH ~10 under testing conditions conversely (Mousavi et al., 2022).

2.14.2. Effect of contact time

Researcher state that, the percentage dye removal increases rapidly with time up to 60 min and thereafter the adsorption rate is decrease gradually. This indicates that higher the contact time between dye and adsorbent, higher is the removal efficiency until the equilibrium time is reach Similar result obtain by (Iakovleva, 2020) Effect of time in adsorption system is necessary to develop cost effective procedure. Removal time significantly depend to AC surface properties such as pore size, pore volume and surface. In wastewater treatment procedure, decreasing the removal time is necessary. This goal can be achieved using high amount of small size adsorbent or modification of adsorbent surface. The adsorption of MB onto AC was studied in various contact time to determine the adequate adsorption equilibrium time (Dąbrowski, 2001; Kecili & Hussain, 2018).The rapid uptake and quick establishment of equilibrium show the efficiency of particular adsorbent in terms of usage in wastewater treatment. The initial adsorption rate is rapid because of high available surface area and vacant site of AC and then gradually increase with raising the time and reach equilibrium contact time (Park et al., 2012).

2.14.3. Effect of adsorbent dose

The amount, size and pore volume of adsorbent significantly influence the capacity of adsorption toward various molecules. The vacant site and pore size of adsorbent limit the rate

and amount of migration of dye molecule to the adsorbent surface. AC reaction sites depend to the amount of adsorbents (Science, 2020). The removal efficiency increased sharply with increasing amount of activated carbon up to fixed amount of activated carbon then removal efficiency decrease beyond the fixed carbon dosage. Then removal efficiencies not changed significantly with increasing amount of adsorbent (Adak et al., 2005). Removal of methylene blue from wastewater using activated carbon prepared from rice husk. That is adsorption efficiency increased due to the increased number of adsorption sites.

2.14.4. Initial methylene blue concentration

Removal efficiency is greatly depended on the initial concentration of solution of adsorbate. The removal efficiency is decreased with increasing of initial concentrations, although the amount of total methylene blue accumulation increased. The total accumulation of methylene blue increased with increasing initial concentration is probably due to more contact of adsorbent sites with methylene blue. At low concentration, most of methylene blue in the sample, solution might contact with active sites of adsorbent and when the concentration is increased all methylene blue species will not be available to contact with the active surface due to active sites already filled up (Jia et al., 2016). Studies show that, the effect of initial dye concentration on the adsorption of methylene blue (MB) by pine leaves and they noticed that as the initial dye concentration increased from10 to 90mg/l the percentage of dye removal decreased from 96.5 to 40.9%. On increasing the initial dye concentration from 10 to 90 mg/l after 240 min (Mousavi et al., 2017). Dye adsorptions onto grape processing waste silica gel showing the maximum monolayer adsorption capacity of 142 mg/g for methylene blue (Ingrachen-Brahmi et al., 2020). This may attributed to the fact that ZnCl2 selectively extracted H and O away from the GW rather than ACs. Hence, this causes eventually to an increase in the surface area and porosity ().

2.14.5. Surface area of adsorbent

The extent of adsorption is generally considered to be proportional to the specific surface area. Specific surface area is that proportion of the total surface area which is available for adsorption. The more finely divided and more porous adsorbents would be expected to yield more adsorption per unit weight of adsorbent. The surface can be characterized either as external when it involves bulges or cavities with width greater than depth or internal when it involves pores and cavities that have depth greater than width (Hu & Xu, 2019).

2.14.6. Effect of Particle size

The smaller particle size reduces the restriction of internal diffusion and mass transfer and allows the adsorbate inside the adsorbent to penetrate (i.e., the equilibrium can be more easily achieved and almost full adsorption capacity can be achieved (Lyu et al., 2021). According to (Suresh Kumar et al., 2019) studied, the removal efficiency of silica gel through three different particle sizes of (45, 125, and 250 μm, 500 μm). It is observed that the maximum adsorption efficiency is achieved with a particle size of 45 micrometers. This is because most of the inner surface of these particles can be used for adsorption

2.15. Adsorption isotherm

Isotherm refers to the relationship between the equilibrium adsorbate concentrations in the liquid-phase and the equilibrium adsorption amount on the solid-phase at a certain temperature. Sorption equilibria deliver fundamental physicochemical data for assessing the relevance of sorption processes as a unit operation. Sorption equilibrium is normally described by an isotherm equation whose parameters express the surface properties and affinity of the sorbent, at a constant temperature and pH. Therefore an accurate mathematical description of the equilibrium isotherm, preferably based on a correct sorption mechanism, is essential to the effective design of sorption systems (Rosly et al., 2021). We can model the equilibrium adsorption data by the isotherms, and investigate the adsorption information, such as the adsorption mechanisms, the maximum adsorption capacity, as well as the properties of adsorbents by the isotherms (Lazaar et al., 2022). According to the paper, studied by (Koner et al., 2011) adsorption isotherm can be described as a curve that explains the phenomenon governing the retention (release) or mobility of a substance to a solid at constant temperature and pH in an aqueous porous medium or aquatic environment. Adsorption isotherm gives an idea about relation between the adsorbate and the extent of adsorbate adsorbed on the surface of adsorbent at fixed temperature. The adsorption equilibrium has continuously been clarified by the isotherm equations such that their parameters demonstrate the surface characteristics and affinity of the adsorbent toward the adsorbate (Vaiano & De Marco, 2023). Equilibrium state of two phase's composing the adsorption system. The two popular isotherms are Langmuir and Freundlich isotherms which have been used to explain the equilibrium of an adsorption system (Bery et al., 2022; Lonappan et al., 2016).

2.16. Adsorption kinetics

Adsorption kinetics reflects the evolution of the adsorption process as a function of time. This is an important parameter to consider when choosing an adsorbent. Fast adsorption is recommended for treatment methods that use adsorption as a purification process. Several models have been developed that describe the diffusion of solutes on the surface of particles and within pores (such as film distribution models, intra-particle diffusion models, out-of-particle diffusion models, and pore diffusion models). In the case of nitrates removal, simplified models such as pseudo-first-order kinetics and pseudo secondary kinetics were common (Koner et al., 2011)

The adsorption dynamic is one of the foremost imperative issues for understanding both the mechanisms of adsorption and the evaluation of persuasive factors on the reaction rate. Kinetics explains solute take-up rates additionally characterize the residence time of the adsorbate at the solid-liquid interface. Kinetic modeling was used to investigate the adsorption mechanism and potential velocity control processes (Ahmad et al., 2022)

2.17. Adsorption Thermodynamics

Another important factor characterizing adsorption is the enthalpy of adsorption. During adsorption, the residual forces on the surface always decrease. In other words, the surface energy, which appears as heat, is reduced. Therefore, adsorption is always an exothermic process. That is, the enthalpy of adsorption (ΔH) is always negative. When a gas or liquid is adsorbed, the freedom of movement of its molecules is limited. This corresponds to reduce in entropy of the adsorbed molecule after adsorption. That is, ΔS is negative. Thus, not only the entropy of the adsorption system but also the lowering of the enthalpy is included. For the process to be spontaneous, the thermodynamic requirement is that ΔG, must be added at a constant temperature and pressure, i.e. the Gibbs energy decreases (Jia et al., 2016).

According to the equation,$\Delta G = \Delta H - T\Delta S$ if ΔH has a sufficiently high negative value - ΔG can be negative because TΔS is positive. Therefore, the spontaneous adsorption process is a combination of these two factors is added ΔG. As adsorption proceeds, ΔH becomes increasingly negative, eventually ΔH becomes equal to TΔS, and ΔG becomes zero generally, these parameters indicate whether the adsorption process is spontaneous as well as it also

indicates whether it is exothermic or endothermic. The standard enthalpy changes (ΔH^o) in the adsorption process are: (i) Positive values indicate that the process is endothermic in nature. (ii) Negative values indicate that the process is heat generating in nature and that the amount of heat given when the metal ions on the adsorbent surface bind are released. This can be obtained with an adsorption rate (Cads) vs. temperature (T) plot. The adsorption rate increases as the temperature rises. This shows the endothermic process and the reverse phenomenon of fits. When the value of (ΔS^o) becomes positive.

2.18. Adsorbent Regeneration

Regeneration is a very important aspect of adsorption from an economic and environmental point of view. The disposal of adsorbents is one of the problems associated with the adsorption methods. The regeneration can reduce the need for new adsorbents and additionally reduce the trouble of disposal of used adsorbents. Numerous regeneration methods were used with different degrees of success. The recovery of many solutes became viable with the aid of using solvent washing (Momina et al., 2019). The problem of dyes loaded adsorbent is also challenging because the continuous accumulation of pollutants on the adsorbents gradually reduces the overall adsorption efficiency of the adsorbent and also affects the environment due to leaching of adsorbate (Dahliyanti et al., 2022). Regeneration of adsorbents is important, using a proper technique helps in improving adsorption efficiency by removing pollutants, improves the overall cost of treatment process, reduces the generated waste and tackles the disposal problem. According to literature reviews, the prevalent and widely used regeneration techniques for silica gel based adsorbents are chemical, thermal, supercritical extraction, photocatalytic and biological techniques This study is based on the regeneration of silica gel using solvent washing with portions of 6N HCl then washed with deionized water, and left to dry at room temperature for two days (Radoor et al., 2020).

CHAPTER THREE

3. MATERIAL AND METHODS

3.1. Materials

The main raw material that was used to generate silica gel during the experimental work was aluminum sulphate solid waste residue from Awash Melkassa chemical factory, which is located in the central part of the Ethiopian Rift Valley, is utilizing to synthesize silica gel. Analytical grade chemicals such as Methylene blue solution (chemical formula, C16H18N3ClS and molecular weight of 319.5, Sulphuric Acid (98%, Merck) with (sp. gr. 1.84) and, NaOH, HCl and distilled water. The diluted solution of HCl and NaOH used to adjust the pH.

3.2. Equipment and apparatus

Equipment that were used for experimental work includes; electronic balance, magnetic stirrer, ball mill, Autoclave, conical flask, beaker, funnel, water dispenser, measuring cylinder, magnetic stirrer, beaker, filter paper, burette, various mesh size, oven dryer, different size of conical, Micro Pipette, Erlenmeyer and round bottom flasks, measuring cylinder , Vacuum filtration Pump (MZ-2C NT, Germany), mortar and pestle, UV-Vis Spectrophotometer (SP-UV 300, china), pH meter (Auto deluxe,-LT-10, Indian), Mechanical Shaker (Edmund Buhler SM-30C, Poland), FTIR (Nicolet IS50, Germany), BET (Horiba SA- 4000E Series), SEM (JCM -6000 Plus), TGA (DTG-60H), XRD (XRD-7000s) AAS (spectr AA-20plus). The experimental work Preparation of the raw material and Production of silica gel was done at Chemical Engineering Laboratory, ASTU and Awash Melkassa chemical factory, AMCF.

3.3. Methods

3.3.1. Raw material preparation

The dealuminated solid waste residue was collect from the factory solid waste damping area the collected from different piles samples were mixed together to make sure homogeneity. The SWR was washed sufficiently with distilled water several times until the filtrate became neutral; this result indicates the complete removal of heavy metals from SWR, Afterward, and the sample was crushes, ground, and sieve through 80 –120 µm and then dry in an oven at 105 ^{o}C for overnight.

3.3.2. Extraction of sodium silicate from solid waste residue

By adjusting the reaction time while stirring slowly and utilizing a magnetic stirrer to dissolve silica, it was possible to study the silica extraction from the SWR. Awash Melkassa Chemical Factory's fresh aluminum sulfate solid waste residue was dried overnight at 105 ^{o}C in the oven. The Solid to liquid ratio of 1:10 was used. Based on this 100 g of powder dried Aluminum sulphate filter cake was mixed within 4M NaOH (1000 ml) at 80 ^{o}C; stirred using heated magnetic stirrer and let reacted for 2 hr. followed by cooling. This solution was vacuum filtered to separate into the filter cake residue and the filtrate, the clear filtrate solution contains the sodium silicate solution (SSS), which was used to obtain silica gel.

3.3.3. Synthesis of the silica gels

The synthesis of silica gels involves three steps: hydrolysis, condensation, and drying. To begin the hydrolysis, 2.5N H_2SO_4 solution was gradually added to sodium silicate solution until the pH of the solution reached 3. It was added and forcefully stirred with minimal splashing 120 RPM), the RPM was raised to 250 and gradually increase to 300 over a period of several (18 to 20) minutes in a sealed container at room temperature. The reaction was carried out at room temperature. To encourage gel formation and enhance the surface area of silica gel, The sol was then quenched in a prepared hot acidified and basic water medium for 3 hours to solidify the silicic acid sol into the more stable polysilicic acid gel provides the multiple functions of; Speeding up the gel, Diluting the salt present in the sol thereby requiring less washing and Having the gel form into discrete individual agglomerates which allowed for the migration.

The gel then Aged for 18 hour at room temperature The sodium sulphate formed during the reaction will be removed by washing the hydro gel by hot acidified water until the pH become 7 which indicates the complete removal of sodium and sulphate ions. The resultant gel slurry was then vacuum filtered by using filter paper to rid the excess salt. The washing of the hydro gel is necessary in order to get good quality product and optimum yield. Drying was carried out in order to remove the adhered water from the gel. The prepared of silica gels will be placed in an oven at 110^{o}C then left it for overnight stay. The heating time will be prolonged till constant weight was obtained. On drying, the product automatically disintegrated into transparent crystals of various sizes depending on the experimental conditions, afterwards the dried gel was milled. Synthesis of the silica gels from the SWR experimental setup was shown in fig 3.1.

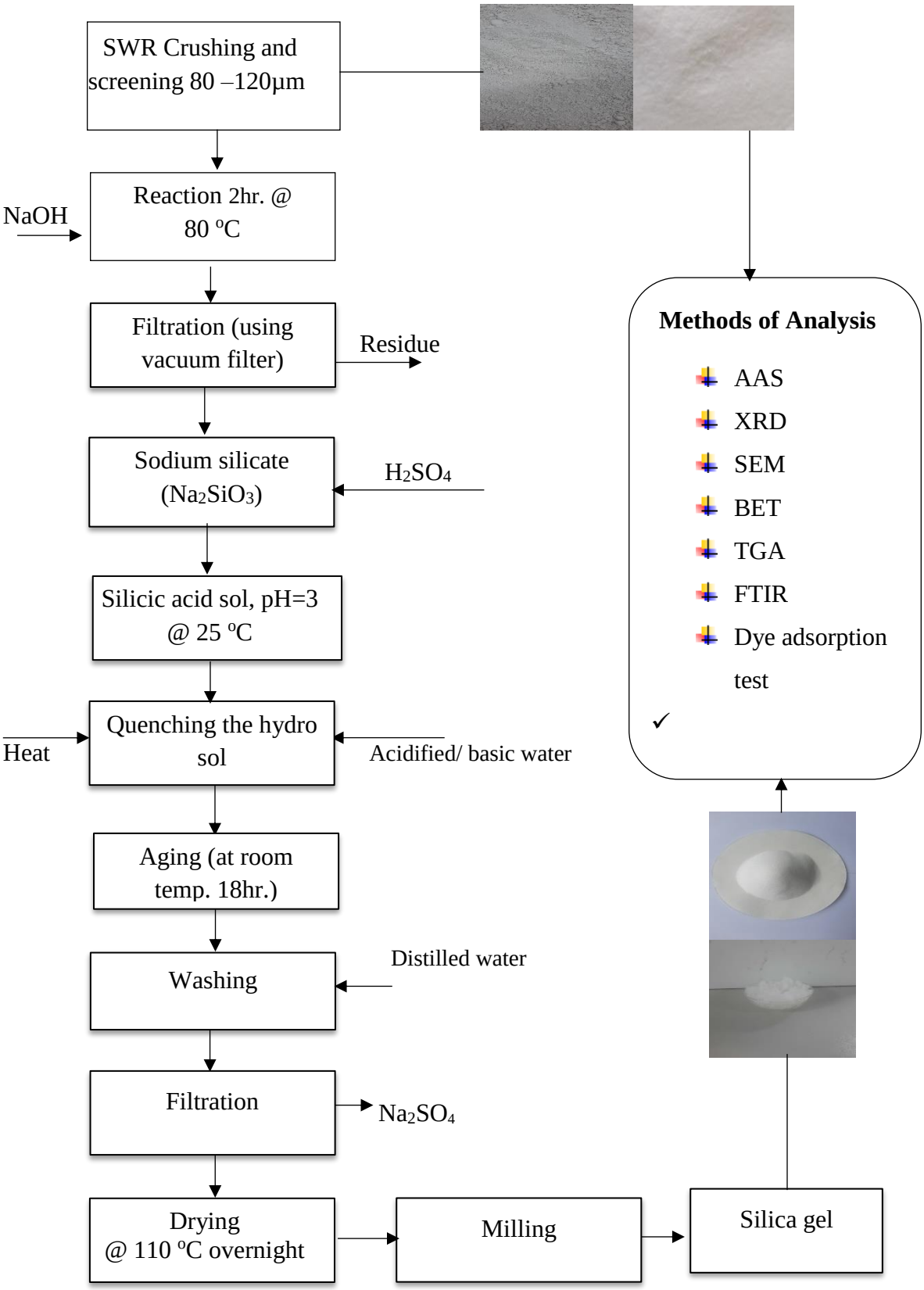

Figure 3.1: Scheme of experimental

3.4. Material Characterization

3.4.1. Absorption Spectroscopy

To determine the chemical compositions of solid waste residue of Awash Melkassa chemical factory and produced silica gel, Complete Silicate Analysis using analytical methods of Lithium Metaborate fusion ($LiBO_2$ Fusion), HF attack, Gravimetric, Colorimetric and Atomic Absorption Spectroscopy (AAS) were conducted. The analysis performed at Addis Ababa Ethiopian Geological survey.

3.4.2. X-ray Diffraction (XRD)

X-ray diffraction (XRD) is one of the most considerably used techniques for characterization. Commonly, XRD gives information regarding the crystalline structure, nature of the phase, lattice parameters, and crystalline grain size. In this study the analysis of SWR of aluminum sulphate plant, silica gel before and after adsorption were subjected to XRD machine model shimadzu XRD-7000s x-ray diffractometer using cu-kα radiation. The measurement condition for each test includes voltage = 40.0 (kV), current = 30.0 (mA) and scan range from 10.00 to 80.00 with 0.02 step size. The average particles size are calculated by using Scherrer equation.

$$D = \frac{K.\lambda}{\beta \mathrm{Cos}\theta} \tag{3.1}$$

Where, D is crystalline size, K = (0.9) is a Scherrer constant, λ is the wavelength of the x-ray, θ is Bragg angle of corresponding diffraction peak and β is full width at half maximum (FWHM)

$$n\lambda = 2dsin\theta \tag{3.2}$$

Where n (an integer) is the "order" of reflection, λ is the wavelength of the incident X-rays, d is the interplanar spacing of the crystal and θ is the angle of incidence.

3.4.3. Fourier Transform Infrared Spectrometry (FTIR)

The functional group of silica gel and solid waste residue of aluminum sulphate plant were detected using Nicolet IS50, Germany type. The FTIR spectrum from 4000-400 cm^{-1} in resolution 4 cm^{-1} recorded. Sample for the FTIR analysis were prepared by weighting the amounts of sample, 1 gm, and Potassium Bromide (KBr) powder, 100 gm into an agate mortar. The FTIR pattern is plotted within the FTIR machine by generating the transmittance peaks (%)

as the Y-axis versus wavenumber (cm^{-1}) as the X-axis.

3.4.4. Brunauer-Emmett-Teller (BET)

The Brunauer-Emmett-Teller (BET) method is commonly applied to calculate the specific surface area based on nitrogen adsorption isotherm measurements at 77 K. In this study the specific surface area of the silica gel were carried out using Horiba Instruments, Horiba SA-4000E Series surface area analyzer at 300 ^{o}C degassing temperature for 1 hr. and 22 minutes in the presence of nitrogen gas.

3.4.5. Thermal gravimetric analysis (TGA)

Thermal gravimetric analysis (TGA) analysis was performed using (DTG-60H, TGA) analyzer. The Nitrogen gas used as carrier gas and the heating rate was set at 20 ^{o}C/min to determine the thermal stability of 10 mg of the solid waste residue of aluminum sulphate plant and silica gel. The temperature was adjusted between 20 ℃ to 800 ℃ and the decomposition of sample weight (%) against temperature (℃) was recorded. This analysis resulted two types of curve, TGA curve and derivative Thermogravimetric (DTG) curve.

3.4.6. Scanning electron microscope (SEM)

A concentrated electron beam is used to scan a sample's surface in a scanning electron microscope (SEM), which creates images of the sample. The sample's surface topography and chemical composition are revealed by the signals that are created as a result of the electrons' interactions with the sample's atoms. In this investigation, a SEM analyzer of type JCM-6000PLUS Bench Top SEM, manufactured by JEOL in Japan, was used to compare the morphology of silica gel before and after the adsorption of methylene blue dye. The analysis process includes mounting a 30 mg sample on a metal stub with sticky carbon tape to improve conductivity. The clip securely holds the sample, and it does not block any of the areas you want to photograph. The specimen must be electrically grounded to the sample holder to minimize specimen charging. Specimen exchange, evacuation, and automatic adjustment of image carried out to photographing and finally the image saved.

3.5. Preparation of methylene blue solutions

About 1 g of methylene blue was taken in a 1000 mL volumetric flask and diluted up to the

mark by addition of deionized water. Different concentration; 2,4, 6 ,8,10,12,14,were prepared in order to plot the calibration curve and 5, 10, 15, 20, 25, and 30 mg/L were prepared for adsorption, equilibrium isotherm and kinetics study by dilution

3.6. Calibration curve for methylene blue

The concentration of MB was analyzed by UV-visible Spectrophotometer (SP UV-300). The calibration curve of absorbance against methylene blue concentration was obtain by using standard MB solutions. The calibration curves shows the Beers law obeyed in concentration range of (2-14mg/l). Working methylene blue solution was prepared by diluting the stock methylene blue solution. The Concentrations of methylene blue in solutions were estimated by measuring absorbance at maximum wavelength of the dye λ max = 664 nm by UV spectrophotometer (SP UV-300) and examined the calibration curve of absorbance versus methylene blue concentration.

3.7. Adsorption experiment

The maximum absorbance (λmax = 664 nm) as determined from the plot was used for measuring the absorbance of residual concentration of MB. The pH of solutions was adjusted using roughly concentrations of 0.1M HCl and 0.1M NaOH. By conducting batch mode experimental studies the efficiency of the adsorbent was evaluated. The adsorption behavior of the new surface with MB dye was studied. The effects of pH, temperature, dose of adsorbent, concentration of MB solution and the contact time on the adsorption of MB dye were studied. The adsorption capacity was investigated using kinetics and pH effects. Equilibrium Isotherm studies were done by varying the following parameters: initial concentration of MB dye solution, time, pH and adsorbent dose on the uptake of dye from the solution. At the end of time intervals, adsorbent was removed by mechanical shaker at 200 rpm and supernatant was analyzed by UV-visible spectrophotometer (SP UV -300) for the residual concentration of MB, at 664 nm wavelength. The percentage removal dye is defined as the ratio of difference in dye concentration before and after adsorption ($Ci - Cf$) to the initial concentration of dye in the aqueous solution (Ci) and was calculated according to the equation 3.8.

3.8. Design of Experiment

3.8.1. Response surface method (RSM)

RSM typically involves the following steps:

1. **Design of experiments:** A series of experiments were designed to study the effect of the different factors such as pH of solution, contact time, adsorbent dose, and MB concentration on the response.
2. **Data analysis:** The data from the experiments are analyzed using statistical methods to identify the important factors and their interactions.
3. **Modeling:** A mathematical model is developed to describe the relationship between the factors and the response.
4. **Optimization:** The model is used to optimize the response by finding the best combination of factors.

3.8.2. Central Composite Design (CCD)

CCD is a type of experimental design that is used to study the interaction effect between multiple factors. CCD typically involves the following steps:

1. Select the factors: The first step is to select the factors that are thought to affect the response.
2. Choose the levels: The levels of the factors are chosen based on the range of values that they can take.
3. Design the experiments: The experiments are designed using a CCD software package.
4. Run the experiments: The experiments are run and the data is collected.
5. Analyze the data: The data is analyzed using statistical methods to identify the important factors and their interactions.
6. Model the response: A mathematical model is developed to describe the relationship between the factors and the response.

Alpha (α) value can be defined as the calculated distance of each individual axial point (star point) from the center in the center composite design. If Alpha (α) is less than 1, which indicates the axial point must be a cube, and if it is greater than 1, it indicates it is outside the cube. In central composite design, each factor has five levels, i.e., Extreme high or otherwise called a star point, higher point, center point, low point, and finally, extreme low star point. The

independent factor was coded at five levels: −α, −1, 0, +1 and +α where, α (minimum) 1 (low), 0 (center), +1 (height) and +α (maximum) obtained from a preliminary experiment.

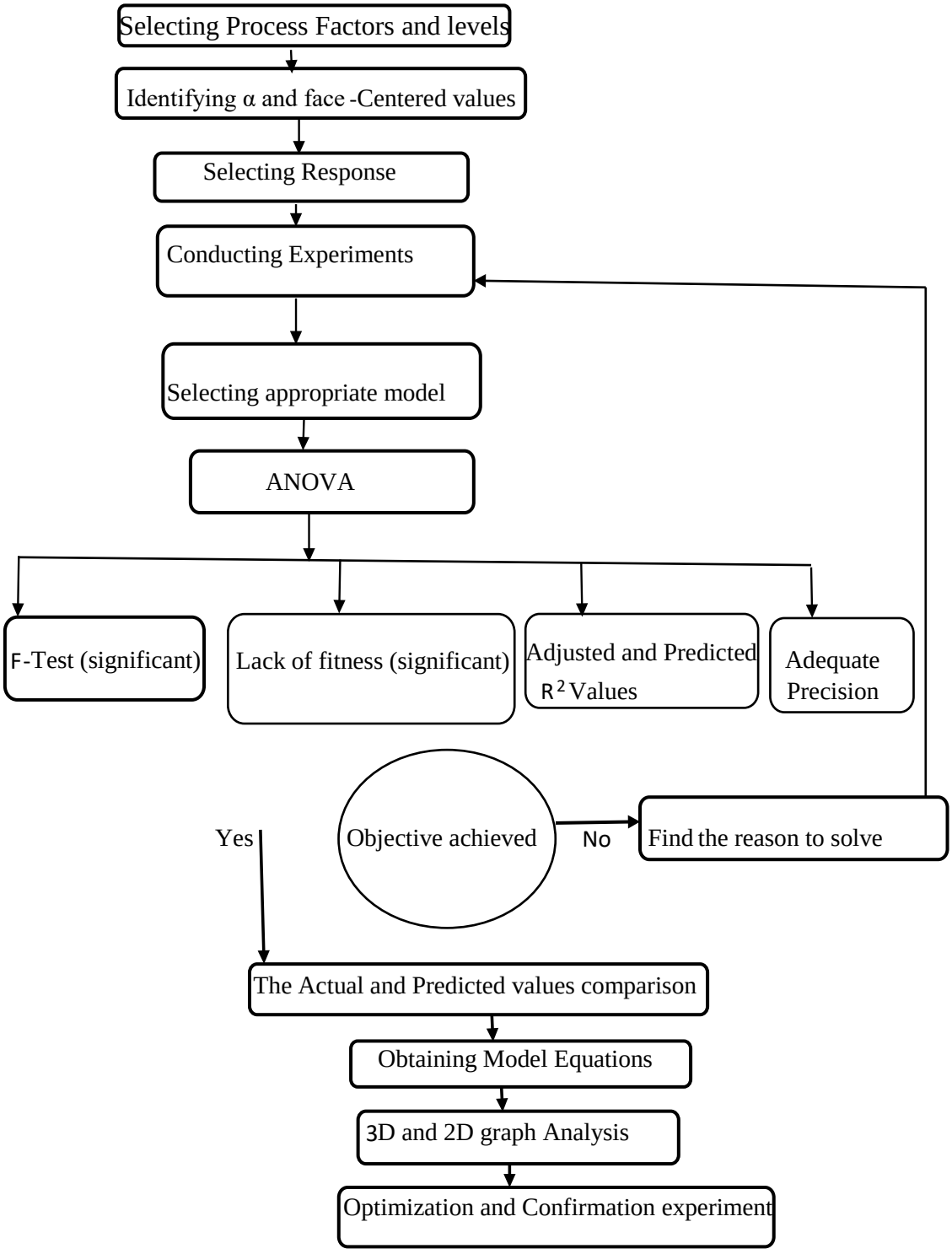

Figure 3.2: Central Composite Design Analysis flow chart for optimization process

To determine the local axial point, it is necessary to identify the alpha value in the CCD model, Depending on the alpha vale design can face cantered, rotatable, and orthogonal. To perform optimization in process the fundamental tasks are screening, identifying the significant and important factors. The variable range and level are given in Table 3.1 in coded units resulting from RSM studies. The design was composed of 2k factorial points augmented by 2^k axial points and a center point where k is the number of variables. Thus, 30 experiments (2^k +2k + 6 = 30) were performed.

Table 3.1: Experimental ranges and levels of the independent variables

Independent Variables	Units	- α	-1	0	+1	+ α
pH		3	5	7	9	11
Contact time	min	30	60	90	120	150
Adsorbent Dose	g	0.01	0.02	0.03	0.04	0.05
MB. Concentration	mg/L	5	10	15	20	25

The relation between the coded and actual values of a factor

$$\alpha = (2^k)^{1/4} \tag{3.3}$$

$$-\alpha = X_{min} \; and + \alpha = X_{max} \tag{3.4}$$

Where, Xmin and Xmax represent the minimum and maximum level of factor.

$$-1 = \frac{(\alpha - 1)Xmax + (\alpha + 1)Xmax}{2\alpha} \tag{3.5}$$

$$-1 = \frac{(\alpha - 1)Xmax + (\alpha + 1)Xmax}{2\alpha} \tag{3.6}$$

$$+1 = \frac{(\alpha - 1)Xmax + (\alpha + 1)Xmax}{2\alpha} \tag{3.7}$$

The methylene blue dye removal efficiency (Re, %) the ratio of difference in methylene blue concentration before and after adsorption calculated according the following formula given below:

$$R_e = \frac{C_0 - C_e}{C_0} \times 100 \tag{3.8}$$

$$R_t = \frac{C_0 - C_t}{C_0} \times 100 \quad (3.9)$$

Dye adsorption Capacity at equilibrium (Qe) will calculated as:

$$Q_e = \frac{(C_0 - C_e)V}{m} \quad (3.10)$$

Where C_0 is the initial MB concentration (mg/L), Ct MB concentration at given time t and Ce is the equilibrium concentration of MB (mg/L). V is the volume of working solution (L), and m is the dosage in (g)

The regression analysis was performed to estimate the response functions as a second order polynomial as shown below

$$y = \beta_0 + \sum_{i=1}^{4} \beta_i x_i + \sum_{i=1}^{4} \beta_{ii} x^2 + \sum_{i=l}^{3} \sum_{j=1+1}^{4} \beta ij\ xij + \varepsilon \quad (3.11)$$

Where y is percentage of MB dye removed; Xi and Xj are the i^{th} and j^{th} coded independent variables; and β_0, Bi, Bii, and Bij denote the intercept, linear, quadratic, and interaction effect regression coefficients, respectively.

$$y = \beta 0 + \beta 1A + \beta 2B + \beta 3C + \beta 4D + \beta 11A2 + \beta 22B2 + \beta 33C2 + \beta 44D2 + \beta 12AB + \beta 13AC + \beta 14AD + \beta 23BC + \beta 24BD + \beta 34CD \quad (3.12)$$

A, B, C, D are linear effects, A^2, B^2, C^2, D^2 are squared effects, AB, AC, AD, BC,BD, CD are interaction effects and Y is the predicted response. β_0 is constant coefficient, β_1,β_2,β_3,β_4 are linear coefficients, β_{11},β_{22},β_{33},β_{44} are squared coefficients, and β_{12},β_{13},β_{14},β_{23},β_{24},β_{34} are interactive coefficients, respectively. Design expert version 11, was used for regression analysis of the data obtained as well as to estimate the coefficient of the regression equation. The equations were validated by the statistical test called ANOVA. The significance of each term in the equation is to estimate the goodness of fit in each case. Response surface used to determine the individual, square and interactive effects of test variable on percentage removal of methylene dye.

3.9. Adsorption kinetics

3.9.1. Pseudo-first order kinetics

Lagergren presented a first-order rate equation to describe the kinetic process of liquid–solid phase adsorption that is expressed:

$$\frac{dq_t}{dt} = K_1(qe - qt) \quad (3.13)$$

Where q_e (mg/g) and q_t (mg/g) are the amounts of dye adsorbed on the adsorbent at equilibrium and at any time t, respectively, and k_1 (min^{-1}) is the rate constant of the first-order adsorption. After integration and applying boundary conditions $q_t = 0$ at t = 0 and $q_t = q_t$ at time = t, the integrated form:

$$\ln(q_e - q_t) = lnq_e - K_1 t \quad (3.14)$$

The value of k_1 and q_e can be obtained from the slope and intercept of the linear plot of ln (qe − qt) versus t, respectively

3.9.2. Pseudo-second order kinetics

The pseudo-second-order kinetic model can be expressed as the following equation

$$\frac{dq_t}{dt} = K_2(qe - qt)^2$$

Where K_2 (g/mg min) is the rate constant of the second-order equation; qe (mg/g) is the maximum adsorption capacity; and qt (mg/g) is the amount of adsorbate adsorbed at time t (min). After integration:

$$\frac{1}{q_t} = \frac{1}{k_2 {q_e}^2} + \frac{t}{q_e} \quad (3.15)$$

The value of q_e and k_2 will be obtained from the slope and intercept of the linear plot of t/qt versus t, respectively. The value of q_e and k_2 can be obtained from the slope and intercept of the linear plot of t/qt versus t, respectively.

3.9.3. Intraparticle diffusion

According to the intra-particle diffusion model, the plot of qt versus the square root of time ($t^{0.5}$) should be linear if the intra-particle diffusion is involved inside the adsorption process.

Moreover, if these lines pass through the origin when the intra-particle diffusion is the race-controlling step, and two or more slopes could occur in a multi-step adsorption process (Ingrachen-Brahmi et al., 2020). Intraparticle diffusion model based on the theory proposed by Weber and Morris was used to determine whether particle diffusion was rate-limiting step or not during adsorption of dye (methylene blue) onto silica gel. The mathematical equation for intraparticle diffusion model is given in Equation below

$$q_t = K_p t^{0.5} + C \quad (3.16)$$

Where qt is the amount of dye adsorbed (mg/g) at a given time t (min) and k_p (mg/g $min^{1/2}$) is the intraparticle diffusion rate constant and C is intercept. The kp and C value were obtained from plotting of qt versus $t^{0.5}$.

3.10. Adsorption isotherm

Adsorption isotherm is a curve describing the phenomenon governing the retention (release) or mobility of a substance from the aqueous porous media or aquatic environments to a solid phase at a constant temperature and pH (Chowdhury et al., 2020) .

3.10.1. Langmuir isotherm

A Langmuir isotherm model was originally used to describe dye adsorption on monolayer homogeneous solid surface. The assumption for this model includes identical adsorption sites could be used to predict adsorbate–adsorbent interaction at liquid–solid interface.

$$q_e = q_{max} \frac{K_l C_e}{1 + K_l C_e} \quad (3.17)$$

$$\frac{C_e}{q_e} = \frac{1}{q_{max} K_l} + \frac{C_e}{q_{max}} \quad (3.18)$$

$$\frac{1}{q_e} = \frac{1}{q_{max} K_l} . \frac{1}{C_e} + \frac{1}{q_{max}} \quad (3.19)$$

Where, qe is the amount adsorbed (mg/g), C_e is the equilibrium concentration of adsorbate (mg/L), while q_{max} and K_L are constants related to adsorption capacity and energy of adsorption, respectively. The dimensionless constant, commonly known as separation factor (R_L) defined by Webber and Chakkravorti, is presented in in equation below:

$$R_L = \frac{1}{K_L C_0} \quad (3.20)$$

Where, K_L (L/mg) refers to the Langmuir constant and C_0 is the adsorbate initial dye concentration (mg/L). The computed R_L value suggests the adsorption nature to be either unfavorable ($R_L > 1$), linear ($R_L = 1$), favorable ($0 < R_L < 1$) or irreversible ($R_L = 0$).

3.10.2. Freundlich isotherm

The Freundlich isotherm is empirical equations, which use to describe non-ideal adsorption on heterogeneous surfaces and multilayer adsorption; Freundlich isotherm summarized according to equation 3.22.

$$q_e = K_f C_e^{1/n} \tag{3.21}$$

$$\ln q_e = \ln K_f (\frac{1}{n}) \ln C_e \tag{3.22}$$

Where Ce is the equilibrium concentration (mg/L), kf, and n are Freundlich isotherm constants related to adsorption capacity and adsorption intensity, respectively. The magnitude of the exponent, 1/n, gives an indication of the favorability of adsorption. Values of n > 1 represent favorable adsorption condition. Values of K_f and n are calculated from the intercept and slope of the plot.

3.10.3. Temkin isotherm

Temkin isotherm model can relate the effects of indirect adsorbent/adsorbate interactions on the adsorption process; it is also assumed that the heat of adsorption of all molecules in the layer decreases linearly as a result of increase surface coverage (Başar, 2006)). This isotherm consists of a aspect that explicitly takes into consideration of adsorbent–adsorbate interactions through ignoring the extremely low and huge value of concentrations, the model assumes that heat of adsorption (function of temperature) of all molecules within the layer would decrease linearly instead of logarithmic with coverage (A.O, 2012). The linear form of Temkin isotherm model is given by the following equations. The adsorption parameters (A_T and B) were determined from the slope and intercept of the qe versus ln Ce plot based on the linearized equation as presented in 3.23.

$$q_e = \frac{R_T}{b} \ln(A_T C_e) \tag{3.24}$$

$$q_e = \frac{R_T}{b_T} \ln(A_T) + \frac{R_T}{b_T} \ln(C_e) \tag{3.25}$$

$$q_e = B \ln A_T + B \ln C_e \quad (3.26)$$

$$B = \frac{R_T}{b_T} \quad (3.27)$$

Where A_T = Temkin isotherm equilibrium binding constant (L/g) b_T = Temkin isotherm constant R= Universal gas constant (8.314J/mol.K) T = Temperature 298 K B = Constant related to heat of adsorption (J/mol).

3.11. Adsorption thermodynamics

The thermodynamic reputation of the adsorption operation is important to study when the adsorption operation is favorable or unfavorable. This adsorption behavior can occur using thermodynamic factors involving the Gibbs free energy difference (ΔG), the enthalpy difference (ΔH), and the entropy change (ΔS). The units for ΔG and ΔH are joules, and the unit for ΔS is joules per kilogram. Gibbs free energy indicates the spontaneous character of the adsorption (ΔG < 0 for the spontaneous process), while enthalpy values determines the endothermic or exothermic nature of the process (ΔH< 0 is exothermic while ΔH > 0 is endothermic). Positive values of ΔS indicate increased randomness at solid-liquid interphase during the sorption processes, hence increased adsorption performance (Sharma et al., 2021). The following equation is the main equation and that can be used to connect the between the adsorption factors.

$$\Delta G = \Delta H - T\Delta S \quad (3.28)$$

T assigned to the absolute temperature in Kelvin.

The difference in Gibbs free energy can be also determined by the equation:

$$\Delta G = -RT\ln K_d \quad (3.29)$$

When; R assigned to the universal gas constant that equals 8.314 J/mol.K. Kd assigned to the thermodynamic equilibrium constant that equals (qe/Ce) with a unit of mol or (L/g). The combination of the last two equations will give this equation:

$$\ln K_d = \frac{\Delta S}{R} - \frac{\Delta H}{RT} \quad (3.30)$$

The plot of lnKd versus (1/T) will give a straight line with (-ΔH/R) as a slope and (ΔS/R) as an intercept. The resulting graph is known as Van't Hoff plot.

$$K_d = \frac{q_e}{C_e} \tag{3.31}$$

These parameters can be obtained from experiments at various temperatures using the equations prior to the ΔH^o and ΔS^o values are determined from the slope and intercept of a linear plot of (lnKd) versus (1/T).

3.12. Desorption experiment

Regeneration is very important aspect of the adsorption from economy and environmental point of view. The regeneration can reduce the need of new adsorbent and reduce the problem of disposal of used adsorbent. Various regeneration methods use with different degrees of success. These methods includes solvent washing, thermal, chemical and electrochemical regeneration. (Radoor et al., 2020). The recovery of the dye from the silica gel was carried out at 25 ^oC. The adsorbent was collected by filtration, washed with portions of 6N HCl then washed with deionized water, and left to dry at room temperature for two days. The adsorption capacity of the regenerated Silica gel was tested good conditions and compared to the first use. A 0.03 g of the regenerated adsorbent was added to a 100 mL of 15 ppm MB dye solution at pH 7.99. The comparison of the uptake capacity of the recycled adsorbent showed an excellent adsorption ability and has a good stability and can be reused many times without decreasing its extraction percentage.

CHAPTER FOUR

4. RESULT DISCUSSION

4.1. Characterizations of materials

4.1.1. Atomic Absorption spectroscopy

According to the analyses shown in Table 4.1, the mass ratio of SiO_2/Al_2O_3 is 4.05. The ratio indicating there is a significant amount of free silica (quartz) present in SWR. The dehydroxylation of the sample and removal of its organic constituents is attributed to the solid waste residue's 17.99% loss-on-ignition (LOI). By oxidizing clay at a high temperature in a muffle furnace and measuring the weight loss, a method known as loss on ignition (LOI) is frequently used to assess the volatile matter content of clay. This test is performed to determine how much moisture or contaminants escape from the sample when it is burned in the circumstances outlined in each specific monograph (Alouani et al., 2019; Battas et al., 2019).

Table 4.1: Complete Silicate Analysis in (%) of elements determined for SWR (5 batch average) and silica GEL

Components	SWR (%)	SG (%)
SiO_2	60.47	86.40
Al_2O_3	14.93	<0.01
Fe_2O_3	0.09	<0.01
CaO	0.18	0.18
MgO	0.09	0.28
Na_2O	0.17	0.74
K_2O	0.42	<0.01
MnO	< 0.01	< 0.01
P_2O_5	<0.01	0.09
TiO_2	< 0.01	<0.01
H_2O	5.96	8.25
LOI	17.99	5.29

Where, LOI indicates Loss on Ignition

The AAS result analysis provides information on the weight percentage of oxides present in the

silica gel sample the silica gel contains significant amounts of silicon, oxygen, H_2O and LOI. The AAS test also indicates the presence of trace amounts of other chemical elements such as aluminum, iron, calcium, magnesium, and sodium oxides in the silica gel. As shown in table 4.2 the percentage of silicon dioxide in the silica gel sample is found to be the highest at approximately 86.4%. The percentage of aluminum is comparatively lower, at around 1%. The results of the analysis can provide information on the concentration of trace elements present in the sample, which can be used to ensure the quality and purity of the material. LOI stands for Loss on Ignition, and it is a measure of the amount of water and other volatile materials that are lost when a sample is heated to a high temperature. The LOI result of 5.29 and 8.25 H_2O indicates the amount of water present in the sample. LOI can affect the accuracy of the analysis because it can cause the sample to weigh less than it actually does. This is because the water and other volatile materials that are lost during heating will have a lower mass than the solid components of the sample (Patel, 2017).

4.1.2. XRD Result analysis

Figure 4.1 demonstrates the X-ray diffraction spectra of Awash Melkassa chemical factory, silica gel before and after Adsorption. As shown from figure 4.1 silica was found with the highest peak in a major constituent. The sharp peak at 2θ from 20 – 40 degrees indicates the presence of amorphous phase of SiO_2. According to (Sdiri, 2014) studied that acid leaching of kaolin results in an amorphous phase due to the disintegration of the layered structure of the kaolin by acid. In addition to the diffraction peak of the amorphous phase of silica, the crystal phase also appeared in the x-ray diffraction pattern of residue silica. The other broad peak at 2θ of 15.18 and, 21.01, 25.39, 26.6, 27.47, 30.66, 33.72, 34.15 indicate the presence of crystalline silica and other types of clay minerals such as magnesium, calcium, iron, and aluminum silicate according to X'pert high scholar. The well-defined diffraction at 2-Theta values of 12.4^o and 62.5^o corresponds to kaolinite. Moreover, the peaks corresponds to the 2θ values of 27.5 and 41.6 are typical characteristics of kaolinite. The band at $2\theta = 25^o$ indicates the presence of crystal silica component in solid waste residue.

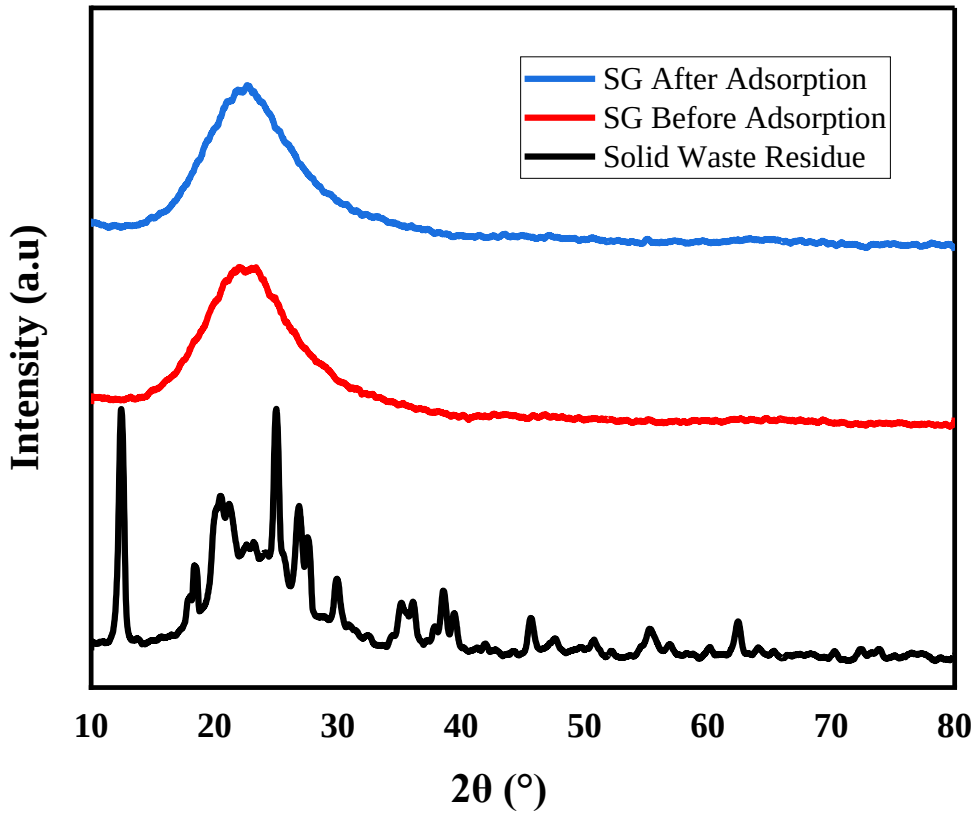

Figure 4.1: The X-ray diffraction patterns of SWR, silica gel before and after adsorption

X-ray diffraction (XRD) analysis that performed to investigate the structural properties of silica gel before and after methylene blue (MB) removal. The XRD results from silica gel samples are displayed in Figure 4.1, showing the signal varied between 2θ = 10° to 80°. This means that the X-rays were scattered by the atoms in the silica gel over a wide range of angles. The broad distribution with reflection (peak appearance) at about 2θ = 21°- 25° indicating that the materials are highly amorphous and consist of SiO_2 (Ibrahem, 2013; Lazaar et al., 2022). There are no additional peaks being observed for all samples. This result indicated the absence of impurities in the gel network after the deionized water washing that removed most of the Na_2SO_4 formed during the gelation reaction.

This indicates that the gel network is free of impurities, the impurities would have caused additional peaks to appear in the XRD spectrum. The absence of impurities in the gel network is attributed to the deionized water washing that removed most of the Na_2SO_4 formed during

the gelation reaction. Na_2SO_4 is an impurity that can be present in silica gel samples. It is removed by washing the silica gel with deionized water.

4.1.3. FT-IR result analysis

The main functional group responsible for the methylene blue adsorption process on to the SWR and silica gel adsorbent before and after adsorption was quantitatively analyzed using FTIR spectroscopy. The degree of change in the particular peaks is shown by quantitative and qualitative analysis shift or an increase or reduction in the sharpness of the peaks of that characteristic spectrum and its comparison with any other corresponding spectrum (Jamwal et al., 2021). These variances ultimately aid in estimating how much a certain functional group is involved in the adsorption process (Bayu et al., 2023). The accompanying Figure 4.2 shows the individual FTIR spectra of the SWR, loaded and unloaded adsorbents for methylene blue in the region of 4000 to 400 cm^{-1}.

The broad peak around 3438 cm^{-1} of Awash Melkassa Aluminum sulphate solid waste residue represents hydroxyl stretching vibration (Al-OH or Si-OH) (Huang et al., 2011). The broadband at 3530 cm^{-1} shown from the solid waste residue was as a result of –OH stretching that exists in the inner hydroxyl group between the tetrahedral and octahedral sheets. As (Angerasa et al., 2021) studied, the stretching frequencies of OH groups are mainly controlled by the strength of H bonding and by the nature of the neighboring cations. H_2O stretching was also found at 1650 cm^{-1}. The smaller peak around 574 cm^{-1} corresponds to Si-O-Al bending vibration that demonstrates the aluminum sulphate solid residue contains silicon dioxide and aluminum oxide. The peak around 986 cm^{-1} are corresponding to Si-O-Si stretching, which is the same result, found by (Huang et al., 2011). On the other side, the sharp peak located at 458 cm^{-1} illustrates Si-O deformation.

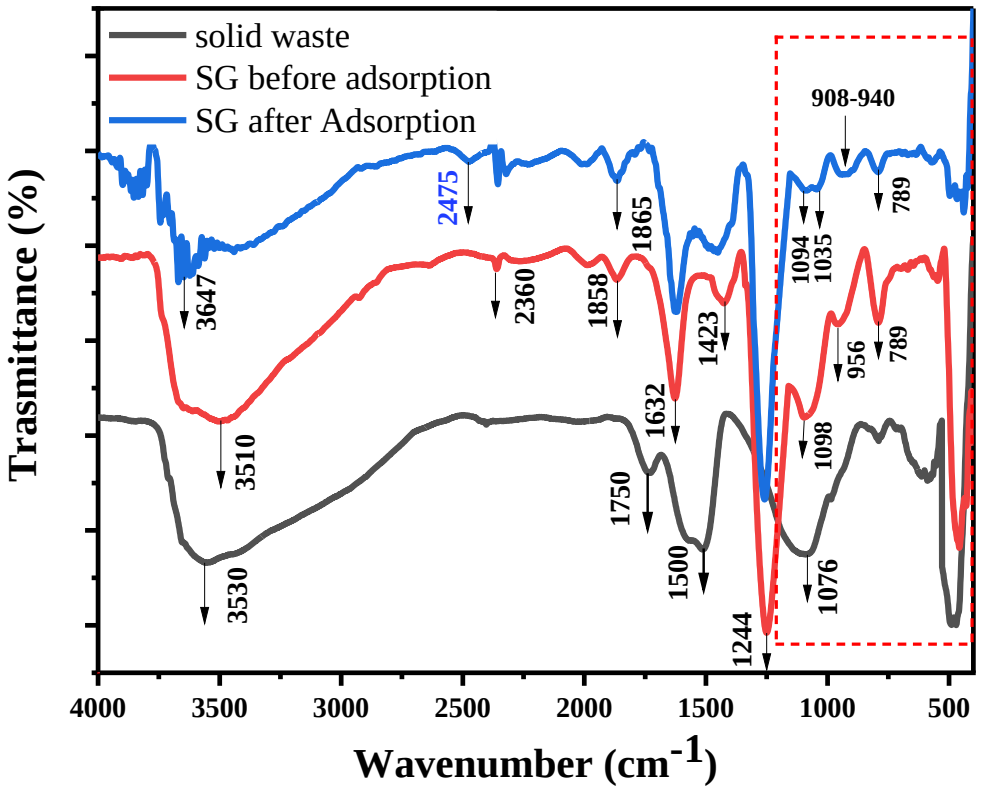

Figure 4.2: FTIR spectra of solid waste residue, Silica gel before and after adsorption

The FTIR (Fourier transform infrared spectrometer) spectra of Silica gel, both before and after MB dye adsorption, are shown in Figure 4.2. FT-IR result peaks analysis of methylene dye adsorption using silica gel involves identifying any shifts or changes in the absorption peaks and relating them to the chemical interactions between the dye and the silica gel surface. The spectra show the major chemical groups present in the prepared silica gel. The broad band at 3510 cm^{-1} is due to the stretching vibration of the OH bond from the silanol group (Si-OH) resulting from the absorbed water molecules on the silica surface of silica gel (Beagan, 2021). The band at 1168-1287 cm^{-1} is due to asymmetric stretching vibration of the siloxane bonds (Si-O-Si) while the band at 944-1082 cm^{-1} is assigned to Si-O-Si symmetric bond stretching vibration The band at 460 cm^{-1} is associated with network O-Si-O bending vibration modes. The FTIR peak after adsorption the Broad peaks in the range of 3200-3700 cm^{-1} are due to O-H and N-H stretches on 2475 cm^{-1}. An increase in intensity of these broad peaks after adsorption may indicate hydrogen bonding interactions between the silanol groups (Si-OH) of silica gel and the

adsorbed methylene blue molecules. As (Ingrachen-Brahmi et al., 2020) studied Shifts in the positions of peaks, especially to higher wavenumbers, may indicate weakening of bonds and charge transfer during adsorption. Appearance of Si-O-C hump peaks around 908-940 cm^{-1} specifically at 1035 and 1094 cm^{-1} after adsorption may indicate chemisorption of methylene blue on silica gel. Additionally the band 1098 and 956 cm^{-1} has shifted in the IR spectrum of silica gel after adsorption of MB dye. The shift in the wavenumber corresponds to the variation of the functional groups energy, this indicates the existence of bond process of MB on the surface of silica gel powder.

4.1.4. Brunauer–Emmett–Teller (BET) silica gel analysis result

The specific surface area of silica gel were determined using the Brunauer-Emmett-Teller (BET). The specific surface area of silica gel was found to be 444.54 m^2/g, as observed from table 4.4. The observations in BET were further confirmed by the pore size and the pore volume of the silica gel. The material prepared presents a pore volume of 12.99 cm^3/g, with a pore diameter of 44.87Å. These results confirm the mesoporous character of the synthesized silica gels (pore diameter under of 50Å).

Table 4.2: Surface area, pore volume and average pore radius of silica gel

BET Analysis		
Surface area (m^2/g)	Pore volume (cm3/g)	Average pore radius (A°)
444.54	12.99	44.87

The BET result shows the surface area of silica gel 444.54 m^2/g at the pH 3 hydrosol, As (Asghar Ali et al., 2009; Besbes et al., 2009) studied the pure silica gel which prepared from sodium silicate and sulfuric acid, the surface area of silica gel is 200-800 m^2/g the and water contents of about 6 %, is hydrophilic,. Therefore surface area of produced silica gel results confirm the good quality adsorbent character.

4.1.5. Scanning Electron Microscopy (SEM) result analysis

Scanning Electron Microscopy (SEM) is a powerful analytical technique that allows for the visualization of the surface and morphology of materials with high resolution. When applied to the analysis of silica gel before and after adsorption of methylene blue, SEM can provide important insights into the structural changes that occur as a result of the adsorption process. In the case of methylene blue removal using silica gel, SEM can be used to study the interaction between the dye and the adsorbent. As shown in Figure 4.3 the vacant pores of silica gel was observed before adsorption with pore diameter 500 µm.

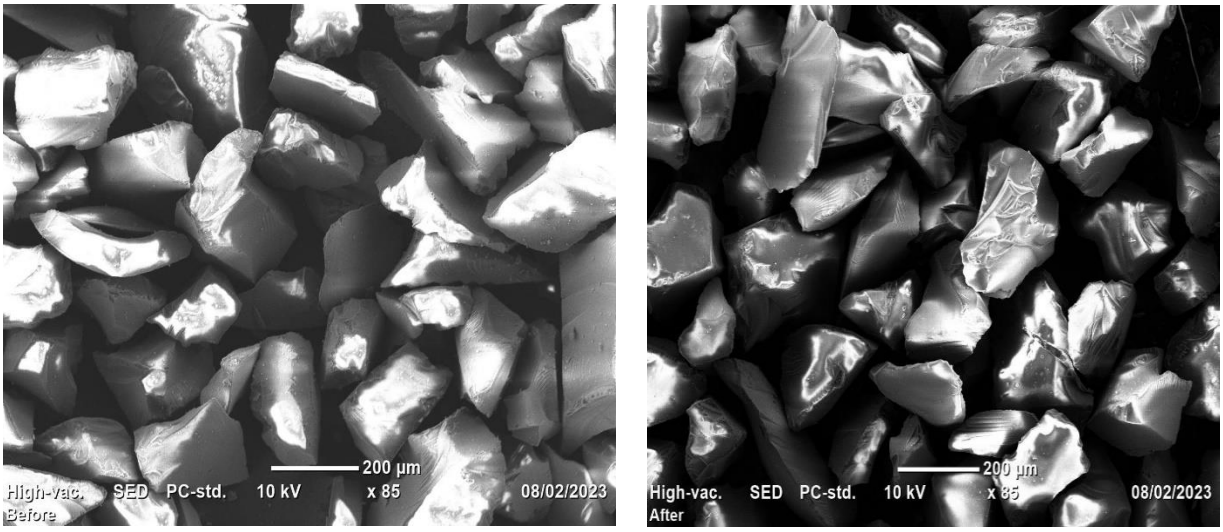

(a) (b)

Figure 4.3: SEM images of a) silica gel before adsorption b) after adsorption

The SEM images of the silica gel before the adsorption experiment showed a smooth surface with no visible features. This indicates that the silica gel was clean and free of contaminants. The SEM images of the silica gel after the adsorption experiment showed that the surface was covered with small, dark spots. These dark spots were identified as methylene blue molecules. This indicates that the methylene blue molecules had been adsorbed onto the surface of the silica gel. Moreover, The SEM images also showed that the adsorption of methylene blue caused the surface of the silica gel to become roughened. This is because the dye molecules impeded the flow of electrons to the surface of the silica gel, which created a shadow effect. The presence of the methylene blue molecules on the surface of the silica gel can be attributed to the interaction between the negative charges on the methylene blue molecules and the positive charges on the silica gel surface electrostatic interaction might take place between the charged ions.

4.1.6. TGA analysis of Awash Melkassa chemical Factory SWR and Silica gel

4.1.6.1. TGA analysis of Awash Melkassa chemical Factory SWR

Awash Melkassa residue silica was subjected to thermogravimetric analysis (DTA-TG) to obtain the weight loss profile against the temperature gradient. Which in illustrates Figure 4.4. The first 11.74 % mass loss in the TGA curve and endothermic peak in the DTA curve at 96.6 ^{o}C is due to the release of physically adsorbed water on the surface silica. The second mass loss in the TGA curve of 9.91% and the endothermic peak in the DTA curve at 623 ^{o}C was attributed to the release of structural water and organic matter. The third mass loss of the TGA curve is 9.01%, and there is an endothermic peak at 764.9 ^{o}C can be attributed to endothermic dehydroxylation (or alternatively, dehydration) to produce disordered metakaolin ($Al_2Si_2O_7$) and due to the removal of residual aluminum sulfate presented in the by-product. The remaining amount of residual silica which accounts for 69% of the total mass shows high thermal stability within the temperature range of 800 ^{o}C to 1000 ^{o}C.

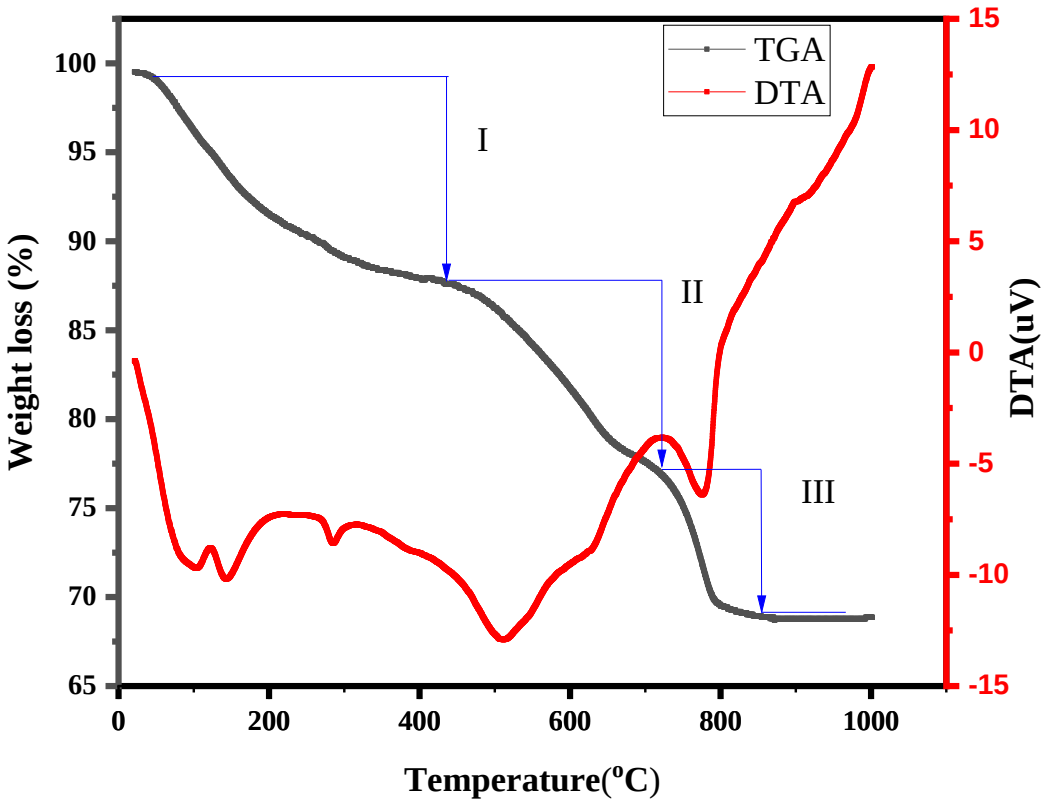

Figure 4.4: Thermogravimetric Analysis of Aluminum sulphate Solid waste Residue

4.1.6.2. Thermogravimetric analysis (TGA) analysis of silica gel

Thermogravimetric analysis (TGA) was adopted in this study for the determination of the concentration of silanol group (-OH) on the surface of porous silica samples. The non-isothermal heating by TGA on the silica gel samples was programmed from room temperature to the final temperature of 800 °C. Figure 4.5 shows the drop of sample weight from 120 °C to almost a constant value at 800 °C, for silica gel samples prepared at pH 3. The temperature-dependent behavior of the weight loss was similar in all cases. It appeared that there was weight loss regions of the TGA curves showed the abrupt decrease of the sample weight for temperatures lower than 120 °C, and this was attributed to the removal of physically adsorbed water from the silica surface and also displayed a gradual decrease of the sample weight which was the result of slow condensation of the existing silanol groups.

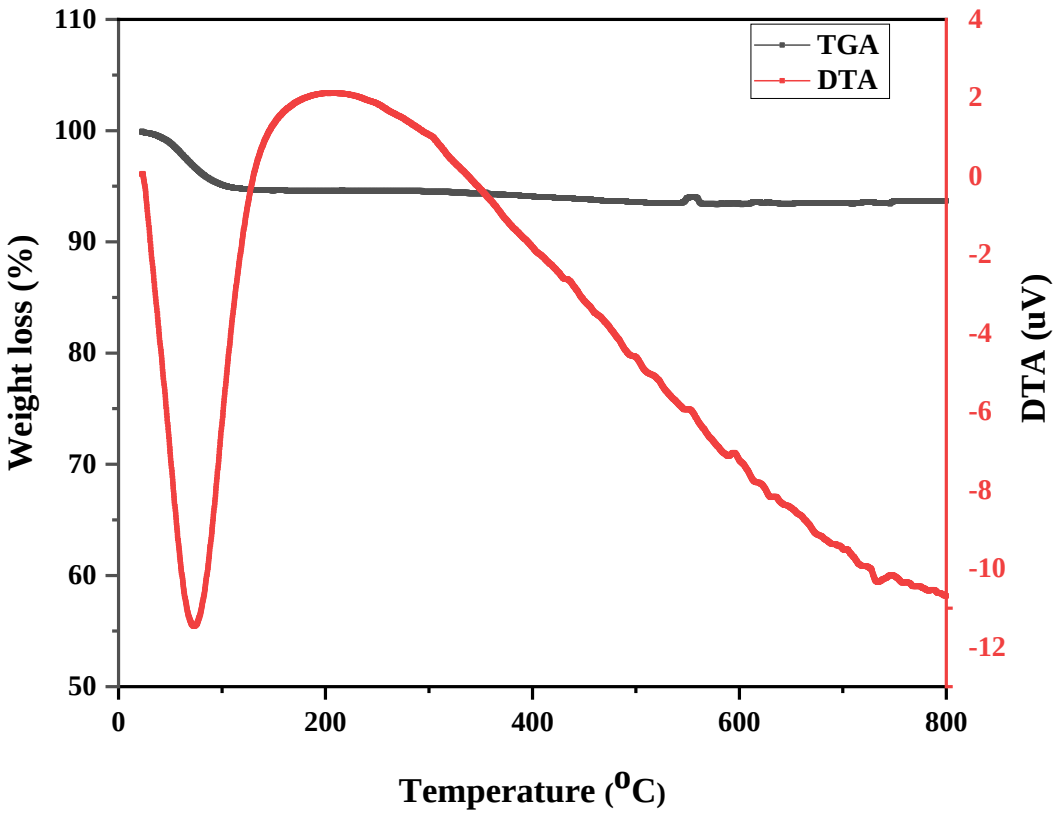

Figure 4.5: Thermogravimetric Analysis of silica gel

4.2. Design of experiment analysis result

Table 4.3: Experimental runs for MB adsorption

Run	pH	Contact time (min)	Adsorbent Dose (g/100ml)	C_o (mg/L)	C_e (mg/L)	R_e (%) Actual	R_e (%) Predicted
1	7	90	0.03	15	1.144	92.37	92.09
2	5	60	0.04	20	2.72	86.41	85.99
3	7	90	0.03	15	1.19	92.06	92.09
4	9	120	0.04	10	0.56	94.44	94.16
5	7	90	0.03	15	1.35	91.03	92.09
6	7	90	0.03	15	1.19	92.07	92.09
7	11	90	0.03	15	1.62	89.21	88.94
8	5	60	0.04	10	1.02	89.81	90.32
9	5	120	0.04	10	0.55	94.47	94.97
10	9	120	0.04	20	1.50	92.48	92.25
11	9	120	0.02	10	0.50	94.96	95.62
12	9	60	0.02	10	1.16	88.35	88.23
13	9	60	0.02	20	3.29	83.56	83.31
14	7	90	0.01	15	2.37	84.19	84.57
15	7	150	0.03	15	0.66	95.61	96.12
16	7	90	0.03	25	4.69	81.25	81.77
17	7	90	0.03	15	1.12	92.52	92.09
18	7	30	0.03	15	2.05	86.31	85.45
19	9	60	0.04	20	1.89	90.52	91.15
20	7	90	0.03	5	0.34	93.25	92.38
21	7	90	0.03	15	1.13	92.55	92.09
22	5	60	0.02	10	1.97	80.24	80.71
23	3	90	0.03	15	3.22	78.52	78.44
24	5	60	0.02	20	5.67	71.62	72.00
25	5	120	0.02	20	3.83	80.83	80.21
26	9	60	0.04	10	0.92	90.83	91.70
27	7	90	0.05	15	0.48	96.82	97.09
28	5	120	0.04	20	2.19	89.05	89.27
29	5	120	0.02	10	0.92	90.81	90.28
30	9	120	0.02	20	2.05	89.73	89.33

Where, Co= initial MB concentration, Ce = equilibrium concentration of dye after adsorption, Re = Removal efficiency of methylene blue, and Qe = Adsorption capacity. The adsorption performed using silica gel different factors: Time, PH, (MB) Concentration and adsorbent dose with constant particle size 500 µm, mechanical shaker speed of 200 rpm and 298k temperature.

4.2.1. Analysis of variance (ANOVA)

The analysis of variance (ANOVA) was used to determine the adequacy of the model. Table presents the results of the quadratic response surface model fitting in the form of ANOVA. According to (Mousavi et al., 2022), ANOVA divides the complete variation of the results into two variations: one associated with the model and the other with experimental errors so as to determine whether the variation from the model is significant or not. This is calculated by evaluating the F-value expressed as the square-to-residual error ratio of the mean model. If the calculated F-value is found to be greater than that of the tabulated F-value, then the model is a strong experimental data predictor (Pamukoglu et al., 2022).

Table: 4.4: Analysis of variance influence of the factors studied on dye Removal

Source	**sum of Squares**	**DOF**	**Mean Square**	**F-value**	**p-value**	
Model	989.93	14	70.71	131.12	< 0.0001	significant
A	165.43	1	165.43	306.76	< 0.0001	
B	170.83	1	170.83	316.77	< 0.0001	
C	235.44	1	235.44	436.59	< 0.0001	
D-	169.12	1	169.12	313.61	< 0.0001	
AB	4.76	1	4.76	8.83	0.0095	
AC	37.73	1	37.73	69.97	< 0.0001	
AD	14.31	1	14.31	26.53	0.0001	
BC	24.23	1	24.23	44.93	< 0.0001	
BD	1.87	1	1.87	3.47	0.0823	
CD	19.21	1	19.21	35.62	< 0.0001	
A^2	121.02	1	121.02	224.41	< 0.0001	
B^2	2.93	1	2.93	5.43	0.0341	
C^2	2.73	1	2.73	5.06	0.0399	
D^2	43.15	1	43.15	80.02	< 0.0001	
Residual	8.09	15	0.5393			
Lack of Fit	6.48	10	0.6484	2.02	0.2267	not significant
Pure Error	1.61	5	0.3211			
Cor Total	998.02	29				

A = pH, B = Contact Time, C = Adsorbent Dose, D = Initial methylene blue Concentration

From the ANOVA (Analysis of Variance) Table, results the higher F-Value and the lower P-value (<0.0001) indicates significance for the regression model. As the result demonstrates the model, the F-value of 131.12 implies it is significant. There is only a 0.01% chance that an F-value this large could happen due to noise. The p-value less than 0.05 implies that the model is statistically significant. They are extremely indispensable to understand the interaction among the independent variables. The result showed that pH (Factor A), Contact Time (Factor A), Adsorbent dose (Factor C), initial dye concentration (Factor D), and are the major important variables in the adsorption process with P-value < 0.0001. Based on the value both the adsorbent dose and initial dye concentration are the best important factor. From the second polynomial model, A^2 and B^2 are significant models with P-values for both models < 0.0001. In the case of interaction effects, AB (pH and contact time), AC (pH and Adsorbent dose), AD (pH and initial dye concentration), BC (contact time and Adsorbent dose), CD (initial dye concentration) are significant model terms for nitrate removal. Where there p-values are 0.0095, < 0.0001, 0.0001, < 0.0001, and < 0.0001 respectively. The Lack of Fit F-value of 2.02 implies the Lack of Fit is not significant relative to the pure error. There is a 22.67% chance that a Lack of Fit F-value this large could occur due to noise. Non-significant lack of fit is good.

The model equations from the ANOVA result can be used to relatively comparing the removal efficiency of dye (MB) within factors and levels. The equation in terms of coded factors can be used to make predictions about the dye removal efficiency for the given levels of each factor. The coded equation is useful for identifying the relative impact of the factors by comparing the factor coefficients. The highest coefficients from the equation indicates the most influence factor that affect the adsorption process of dye removal. In other side, the equation in terms of actual factors can be used to make predictions about the Removal efficiency of dye for given levels of each factors. The levels should be specified in the original units for each factor. This equation should not be used to determine the relative impact of each factor because the coefficients are scaled to accommodate the units of each factor and the intercept is not at the center of the design space.

Final Equation in Terms of Coded Factors

$$\text{Removal Efficiency} = 92.09 + 2.63A + 2.67B + 3.13C - 2.65D - 0.5456\,AB - 1.54AC + 0.9456AD - 1.23BC - 0.3419\,BD + 1.10\,CD - 2.10A^2 - 0.3268\,B^2 - 0.3155C^2 - 1.25\,D^2$$

Final Equation in Terms of Actual Factors

Removal Efficiency $= +14.45008 + 10.36797\text{pH} + 0.375191\text{Time} + 1080.48958\text{Dose} - 0.139979\text{MB. Concentration} - 0.009094\ \text{pH} * \text{Time} - 76.78125\text{pH} * \text{Dose} + 0.094563\text{pH} * \text{MB. Concentration} - 4.10208\ \text{Time} * \text{Dose} + 0.094563\text{pH} * \text{MB. Concentration} - 4.10208\ \text{Time} * \text{Dose} - 0.002279\text{Time} * \text{MB. Concentration} + 21.91250\text{Dose} * \text{MB. Concentration} - 0.525130\text{pH}^2 - 0.000363\text{Time}^2 - 3155.20833\text{Dose}^2 - 0.050171\ \text{MB. Concentration}^2$

4.2.2. Model Adequacy

The regression model was found to be significant with the correlation coefficients of determination of R-Squared, adjusted R-Squared, and predicted R-Squared having a value 0.9919, 0.9843, and 0.9603 respectively as shown from Table 4.5. The goodness fitness of the model was measured by a coefficient of determination R^2, which measured how well the real experimental data points have been approximated together with the regression model. As the result in a Table 4.5, expressed the value of $R^2 = 0.9919$ indicates the better fit of experimental data to that of predicted one. The value of larger Regression coefficient (R^2) approach to 1 illustrates, the validity of model in which it implies an acceptable agreement among the actual and predicted data. It implies 99.19% of the experimental variable studied attributed for the removal of dye. The Predicted R^2 of 0.9843 is in reasonable agreement with the Adjusted R^2 of 0.9603; i.e. the difference is less than 0.2. Therefore, this demonstrates that the measured data very well fitted with a quadratic model of the predicted value. Adeq Precision measures the signal-to-noise ratio. A ratio greater than 4 is desirable. The ratio of 48.3191 indicates an adequate signal. This model can be used to navigate the design space.

Table 4.5: The model adequacy measures

Stad. Dev.	**1.29**	**0.7344**	**R^2**	**0.9718**	**0.9919**
mean	85.25	88.89	Adjusted R^2	0.9455	0.9843
C.V%	1.52	0.8261	Predicted R^2	0.9000	0.9603
Press	89.10	39.66	Adeq Precision	24.6858	48.3191

The figure 4.6 indicates the relationship of Actual and predicted value, which can be introduced from the regression model equations of a Design Expert chart based on predicted and actual percent dye removal. The straight line shows the predicted values and the

small rectangles represent the actual experimental values. The straight line is very close to the actual values and has a correlation coefficient R^2 equal to 0.99919, which confirms the accuracy of the model. The result confirmed that all the actual and predicted values are close to the line of perfect fit. Both of them showed the good agreement between them.

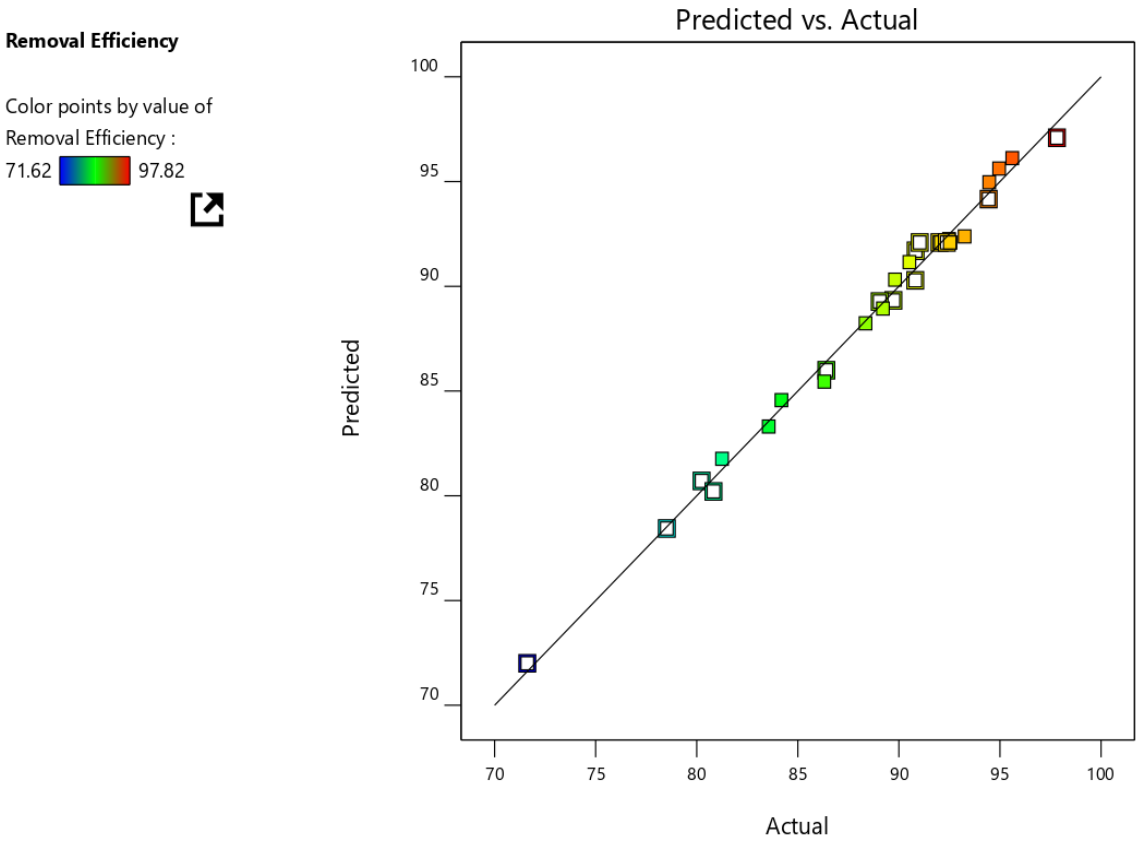

Figure 4.6: Predicted vs Actual value MB removal adsorption plot

4.2.3. Optimization of the response

Optimization was carried out after observing all the effects of color removal. The objective is to maximize removal efficiency. In order to find the optimum value of each independent variables, four statistical metrics such as the larger regression coefficient (R^2), smaller lack of fit F-value, lower p-value and higher sum squares have been used. The response optimization was used to identify the combination of independent variables particularly, Contact time, PH, initial dye concentration, and adsorbent dose within the response of dye removal efficiency. The goal of the process was to obtain high dye removal efficiency.

Table 4.6: Optimization constraints for removal efficiency of MB dye

Name	Goal	Lower Limit	Upper Limit
pH	In range	5	9
Contact time (min)	In range	60	120
MB Conc. (mg/L)	Is target 15mg/L	10	20
Silica dosage (g)	is target = 0.03	0.02	0.04
MB removal (%)	maximize	71.62	97.82

Therefore it has been set as maximum while the process parameters such as time and pH have been set as "within the range", while adsorbent dose and target at 0.03 g and 15mg/L then response surface method was used to optimize the process versus process parameters. According to the result obtained from optimizer Design-Expert version 12 software the maximum optimum removal efficiency of MB was achieved 94.95 % by using 7.99 pH, 120 min contact time, 15 mg/L of initial MB dye concentration, and 0.03 g adsorbent dose.

4.2.4. Response surface plot interaction effects

The effect of the interactions between the four independent input and output variables and their interactions on the dependent variables can be seen using three-dimensional (3D) response surface plots. As observed from Figure 4.13 - 4.18 it indicates the Plots of three-dimensional response surfaces of function of two variables with response and the remaining variables at the central level of the other variables. The effect of the interactions between the four independent input and output variables and their interactions on the dependent variables can be seen using three-dimensional (3D) response surface plots. As observed from Figure 4.13- 4.18 it indicates the Plots of three-dimensional response surfaces of function of two variables with response and the remaining variables at the central level of the other variables.

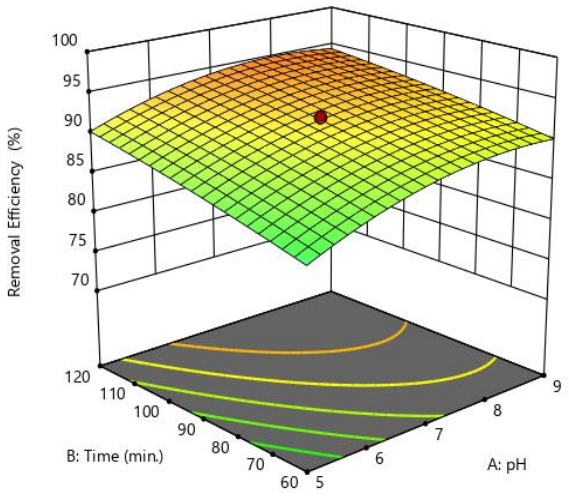

Figure 4.7: 3D interaction effect of pH and contact time on MB removal efficiency.

Figure 4.7 Shows the pH of a solution is an important factor affecting the adsorption capacities of adsorbents, especially those containing functional groups like amino groups, which can be easily protonated or deprotonated to form different surface charges in solutions at different pH lower adsorption of Methylene blue at low pH is probably due to the presence of H+ ions competing with the cations groups on the MB dye for adsorption sites, there by inhibiting the adsorption of dye according to (Boumediene et al., 2018; Han et al., 2006). In addition, the basic dye will become protonated in the acidic medium and the positive charge density would be located more on the dye molecules at low pH results the lower also reported (Atay, 2018).

As observed from the Figure 4. 13 at the lower pH value the initial concentration increase as the removal efficiency of dye decrease. In the other case, at lower initial dye concentration as pH was increased the removal efficiency also increased. After that, the removal efficiency slightly decreases. As (Jodeh et al., 2015) reported decrease in dye removal after certain pH could be due to stronger competition of hydroxide ions. The influence of pH on anion exchange reaction was occurred because of the competition among the hydroxyl ions and anions. When pH increases, the negatively charged surface takes place and the adsorption capacities for MB increase. The protonated variable of the silica gel surface which commonly affect the electrical properties of the adsorbent and therefore pH of solution had a basic influence on the adsorption of dye. The result also demonstrate that as the time increases the dye removal efficiency also increases. After 2 hrs. The time reaches maximum value for adsorption process. After that, the percentage of dye removal decreases due to saturation of free adsorbents sites as well as because

of an adsorbate releases from the adsorbent. Initially the faster rate may be due to availability of uncovered surface area of the adsorbents. However, as passage of time, the portion of the active sites of the adsorbents may be blocked and the rates becomes slower and reaches equilibrium when the surface becomes almost saturated.

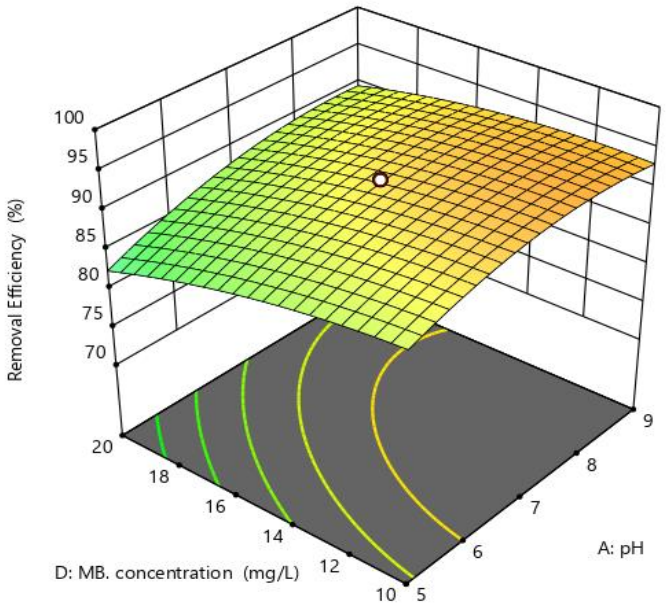

Figure 4.8: RSM plot of 3D interaction effect of pH and MB concentration

The Figure 4.8 indicates the 3D interaction of pH and initial methylene blue concentration on dye removal efficiency at constant adsorbent dose and contact time. As the graph demonstrated, as both the initial MB concentration and pH increases the dye removal efficiency also increases. The rises of initial dye concentration leads to increments in the removal of methylene blue from the solution due to the occurrences of large vacant places in the adsorbents. At the initial dye concentration of 15 mg/L, the removal efficiency reached maximum value of 89%. After that, the removal efficiency of the dye removal starting declined because of the vacant sites occupied by the methylene blue dye.

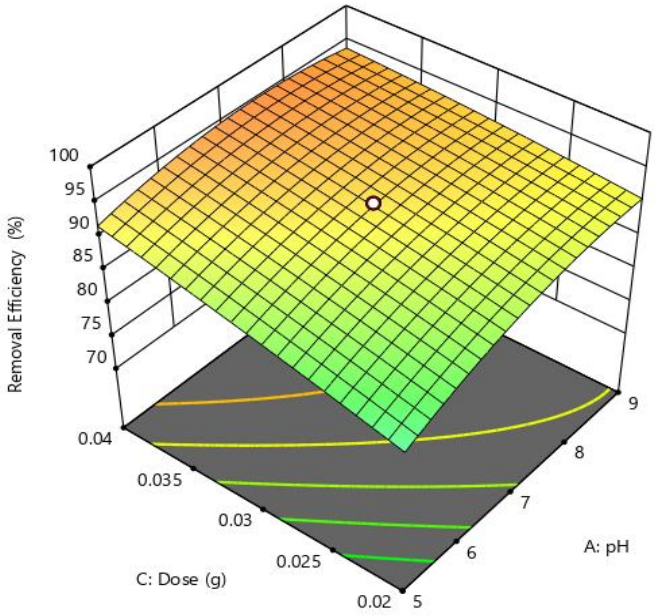

Figure 4.9: 3D interaction effect of pH and dose on dye removal efficiency

Figure 4.9 explained the 3D interaction effects of Adsorbent dose and pH on dye removal efficiency while both time and initial MB dye concentration remains constant. The sorption process was carried out on the molecules and surfaces of the SG adsorbents. Therefore, the adsorbent amount had a meaningful effect on the dye removal efficiency. The adsorbent dose has a direct and indirect effect on the process and costs like the other parameters. As it can be observed from the graph as adsorbent dose of SG increases, the dye removal efficiency also increases in the model. It is commonly understood that the presence of larger surface area and exist of more active sites of the SG adsorbent increase as larger adsorbent dose used in the sorption process. However, at higher concentrations of sorbate, the equilibrium uptake did not increase considerably with the rise within the SG adsorbent. One more reason is also the particle interaction like aggregation, which ends from a high adsorbent dose. Such aggregation would cause a decrease within the total surface area of the adsorbent and a rise in diffusional path length.

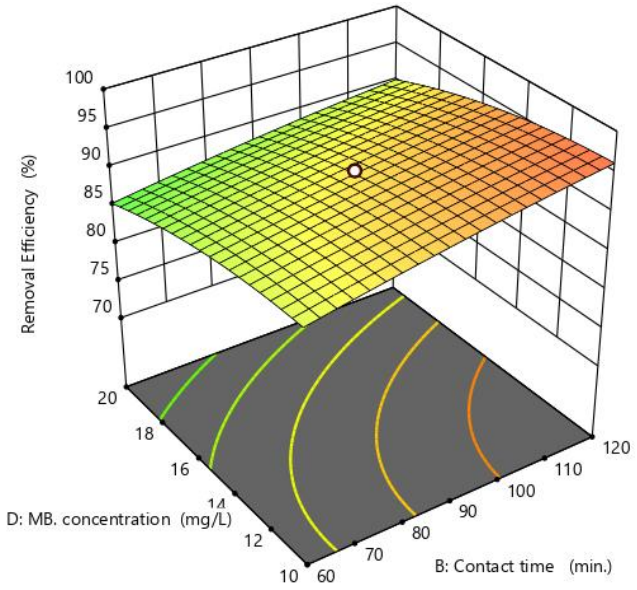

Figure 4. 10: 3D interaction effect of contact time and initial dye concentration

Figure 4.10 depicts the interaction effects of contact time and initial dye concentration on dye removal at fixed adsorbent dose and pH of solution. Initially as time increase, the removal efficiency of dye also increases. As the contact time increase after one hour, the removal efficiency dye decreases.

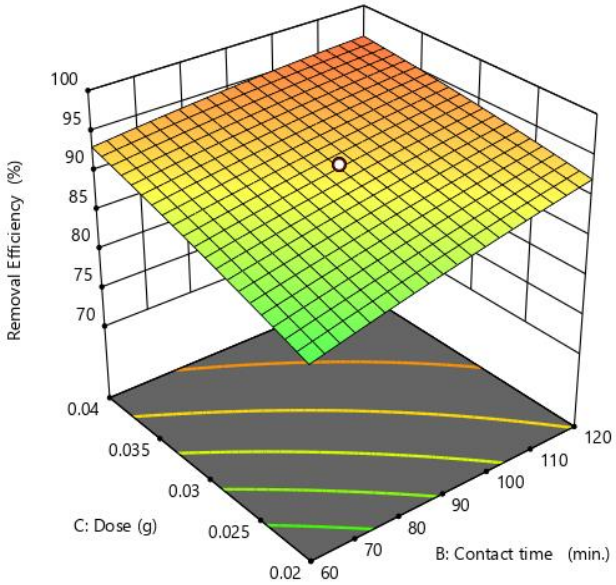

Figure 4. 11: 3D interaction effect of Adsorbent dose and time on dye removal

Figure 4.11 illustrates 3D interaction effect of Adsorbent dose and contact time on dye removal efficiency at constant pH and initial MB dye concentration. As the adsorbent dose increases,

there was an increment of dye removal efficiency. Also, the percentage of dye removal increase with increasing contact time at any initial dye concentration. The adsorbent has reached the maximum adsorption capacity within or before two hour. In the other words, the surface coverage of the adsorbent was already saturated with dye in less than two hour. Therefore, it can be concluded that the percentage of dye removal was highly dependent on the initial dye concentration, pH and weight of adsorbent and on contact time.

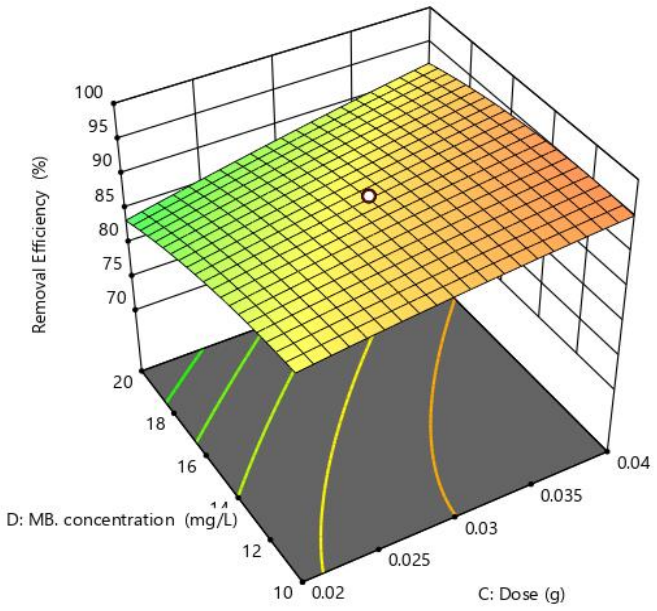

Figure 4.12: 3D interaction effect of adsorbent dose and initial dye concentration

The Figure 4.12 showed the interaction between initial dye concentration and adsorbent dose. As it demonstrated increasing initial dye concentration, the percentage removal of dye removal increased in proportional manner. The process happened due to higher concentration gradient that performed as driving force to conquer the mass transfer between the bulk solution of MB and adsorbent surfaces of SG. The adsorbent dose have no more effect on dye removal at lower value of initial MB concentration. As the initial dye concentration increased, the percentage of dye removal also increased as result of adsorbent dose increased. Therefore, adsorbent dose was the main independent variable that affects the adsorption of MB dye from the solution. The presence of high amount adsorbent dose in the adsorption process leads to increase in total available surface area, and site of (Boumediene et al., 2018).

4.3. Equilibrium isotherm

Adsorption system can be designed with the aid of adsorption isotherms typically referred to as equilibrium isotherms, which constitute the amount of solute adsorbed per unit weight of sorbent. These isotherms use equilibrium concentration of sorbent at a fixed temperature. To remove the methylene blue from the solution, a particular design is optimized in order to generate proper correlations for experimental data, which is referred to as adsorption isotherm (Igwegbe et al., 2019).

4.3.1. Adsorption isotherm

The interaction of adsorbate with adsorbent can be identified by studying isotherm, which is a critical to optimizing and designing the desired adsorption system (Yusuff et al., 2018). The equilibrium concentration of methylene blue dye at constant optimized parameters of 120 min, 0.03g/100mL of SG dose and, 7.99 pH at a room temperature were carried out. The adsorption of isotherm data for MB dye was analyzed by applying three commonly used isotherms, Langmuir, Freundlich and Temkin Isotherms.

4.3.1.1. Langmuir isotherm

Their correlation coefficients and constant parameters of adsorption of dye by SG were obtained from the slop and intercept of the graph for each equations of the isotherms. The adsorption isotherm determines the difference between the amounts of sorption and the solute concentration at equilibrium. The adsorption isotherm of methylene blue dye using SG was investigated. The concentration of dye in their respective equilibrium phase at room temperature was studied to obtain maximum adsorption capacity of SG for dye removal.

Table 4.7: Isotherm data for the removal of Methylene blue dye silica gel

C_o(mg/L)	C_e(mg/L)	log(Ce)	$1/C_e$	q_e (mg/g)	$1/q_e$	$\log(q_e)$	C_e/q_e
10	1.010	0.004	0.990	29.966	0.033	1.476	0.034
15	1.922	0.284	0.520	43.593	0.023	1.639	0.044
20	3.802	0.580	0.263	53.993	0.018	1.7323	0.070
25	5.710	0.756	0.175	64.300	0.015	1.808	0.088
30	9.358	0.971	0.107	68.806	0.014	1.837	0.136

The maximum adsorption capacity (q_{max}) can be determined from the intercept of Langmuir plots of $1/C_e$ vs $1/q_e$. The maximum adsorption capacity (q_{max}) and energy of adsorption (K_L) from Langmuir isotherm model were to be determined 85.178 mg/g and 0.467 L/mg respectively. The values of correlation factor (R^2) gained for Langmuir isotherm equals to 0.99656. The result obtained from Langmuir model indicates that the value of separation factor ($R_{L)}$ for all initial dye concentrations were greater than 0 and less than 1, which implies that the Langmuir isotherm is favorable. The values of R_L for initial dye concentration of 10, 15, 20, 25 and 30 mg/L were listed as 0.176, 0.125, 0.097, 0.078, and 0.067 respectively.

Table 4.8: Isotherm parameters for the Methylene blue dye silica gel

Isotherm	**parameters**	**Value**
Langmuir	q_{max} (mg/g)	85.178
	K_L (L/mg)	0.467
	R^2	0.996
Freundlich	n	2.874
	1/n	0.3479
	k_f (mg/g)$(1/mg)^{1/n}$	29.786
	R^2	0.9502
Temkin	B (J/mole)	139.289
	b_T	17.787
	A_T (L/mg)	5.519
	R^2	0.984

Table 4.9: The values of R_L at various initial dye concentrations

C_o (mg/L)	R_L
10	0.176
15	0.125
20	0.097
25	0.078
30	0.067

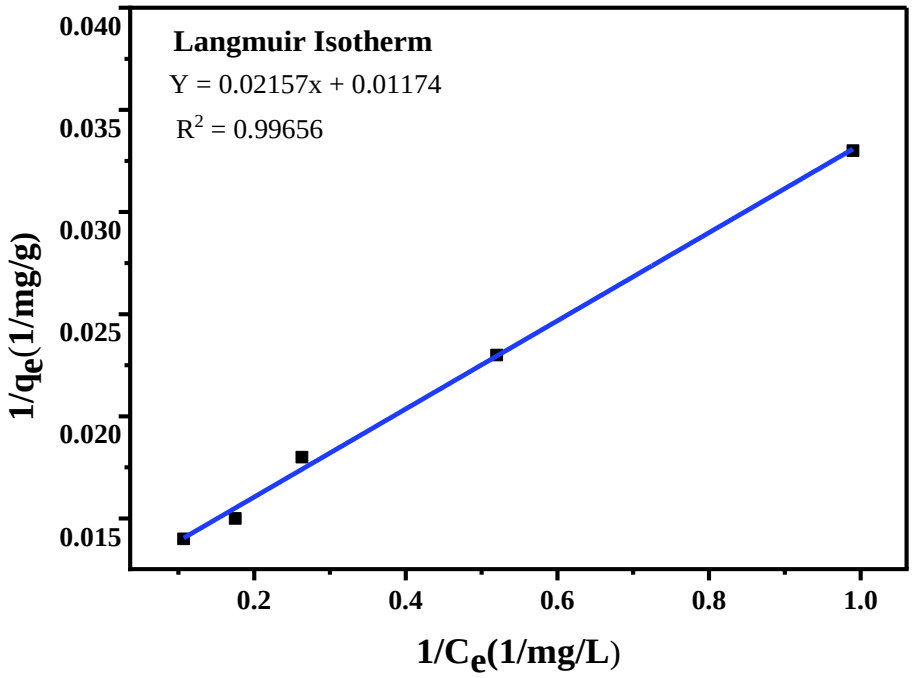

Figure 4. 19: Langmuir isotherm for methylene blue adsorption by silica gel

4.3.1.2. Freundlich isotherm for methylene blue removal by silica gel

Freundlich isotherm is an empirical equation that can be employed to describe the heterogeneous systems. The linear form of the Freundlich isotherm model from Equation 3.22 was used to investigate the multi-layer adsorption of dye on the surface of the adsorbents. The magnitude of the exponent 1/n indicates the favorability of the adsorption. 1/n is a heterogeneous factor, which is related to adsorption intensity or surface heterogeneity. The value of 1/n < 1which equals to 0.347 indicates normal adsorption (Gómez et al., 2014). In order to reach a favorable adsorption process, the value of n should be in the range of 1 to 10. Therefore, as Table 4.8 depicts the value of n was 2.874, which confirmed favorable adsorption. From the Freundlich isotherm model the values of constant parameters such as K_f and n were determined by linear regression plot of log (q_e) and log (C_e). From the Langmuir isotherm model analyzed showed the equilibrium isotherm data fit to the experimental data which implies that adsorbed dye forms a monolayer surface coverage on the silica gel and the chemisorption adsorption mechanism takes place. The values of correlation factor (R^2) gained for Freundlich isotherm equals to 0.9502.

The Langmuir and Freundlich adsorption isotherms relative parameters were calculated from their respective slope and intercept of the linear plots. High correlation coefficients ($R^2 \geq 0.9502$) indicated that both the Langmuir and Freundlich models were acceptably fit the experimental data in this study.

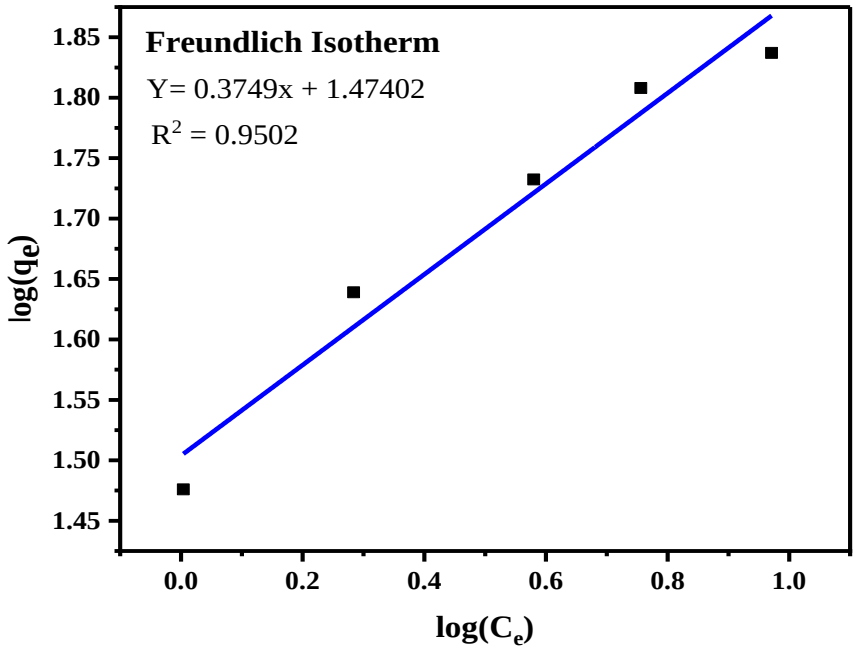

Figure 4.13: Freundlich Isotherm for MB adsorption by silica gel

The result obtained from adsorption equilibrium isotherm confirmed that the fitting the equilibrium data to both Langmuir and Freundlich isotherm models suggest that the presence of heterogeneous and homogenous adsorption surfaces on the adsorbent involved during the adsorption of MB dye. By comparing the values of correlation factor (R^2), the Langmuir models better suitable fits to with the equilibrium adsorption which gives a larger R^2 equals to 0.996 and maximum adsorption capacity of 85.178 mg/g for MB adsorption.

4.3.1.3. Temkin isotherm

The Temkin isotherm data shows that the R^2 value is 0.984, which indicates a good fit of the experimental data to the Temkin isotherm model. This suggests that the adsorption of methylene blue by silica gel follows the Temkin isotherm, and the heat of adsorption decreases linearly

with coverage. The Temkin constant B of 139.289 J/mole indicates the average heat of adsorption per mole of adsorbate on the surface of the adsorbent. A higher value of B indicates a stronger interaction between the adsorbate and the adsorbent surface. In this case, the high value of B suggests a strong interaction between methylene blue and the silica gel surface. The b_T value of 17.787 represents the strength of the interaction between the adsorbate and the adsorbent. A_T higher b_T value indicates a stronger interaction between the adsorbate and the adsorbent. The equilibrium constant of adsorption A_T of 5.519 L/mg indicates the extent to which the adsorbate is adsorbed on the surface of the adsorbent. A higher value of AT indicates a greater extent of adsorption. In this case, the high value of AT suggests that methylene blue is strongly adsorbed on the silica gel surface.

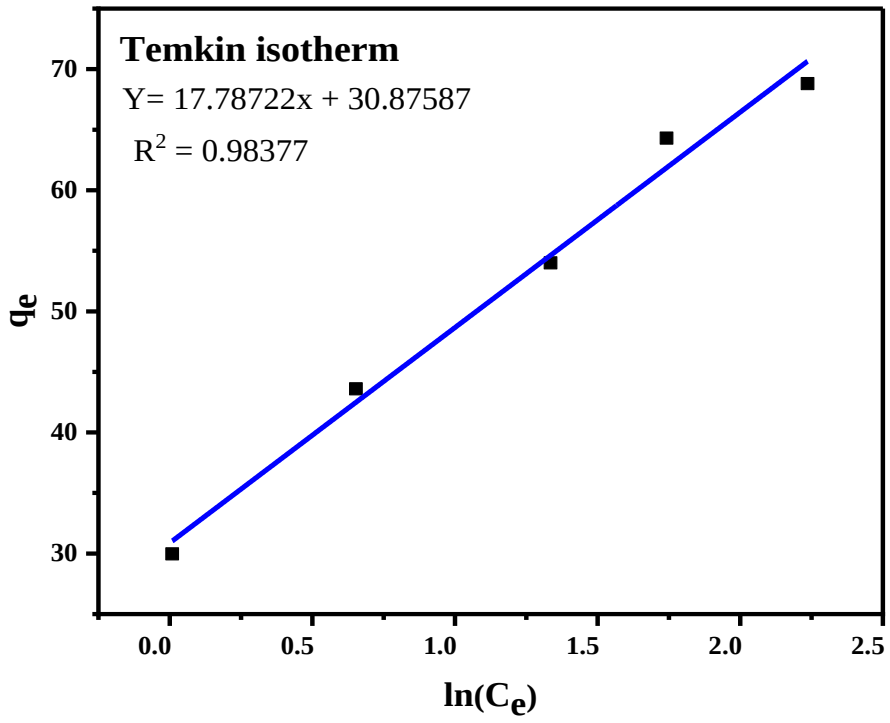

Figure 4. 14: Temkin isotherm model for MB sorption

4.4. Adsorption kinetics

Kinetic experiment were investigated to examine the rate of MB dye adsorption on silica gel adsorbent and the time required to reach equilibrium. The purpose of studying equilibrium kinetic is to identify the adsorbent retention time and provide information about the specified

time to reach the maximum capacity of adsorption and the controlling mechanism in the process that includes mass transfer or chemical reactions (Koner et al., 2011). In this study Pseudo-first-order, Pseudo-second-order and Intraparticle diffusion kinetic models were analyzed to obtain the best kinetic models for dye removal. The kinetics study time dependence of dye were investigated from 30 to 210 min at constant room temperature,15 mg/L initial MB dye concentration, pH = 7.99, adsorbent dose = 0.03g/100mL.

Comparing the correlation coefficients of three kinetic models, it definitely revealed that the pseudo-second-order model best fit the adsorption kinetic of MB dye onto silica gel and the adsorption processes were chemisorption. As shown in the Figure 4.16 the Pseudo-second-order rate model show the best agreement with the experimental results, which implies that the whole process was controlled by chemical adsorption is the rate limiting steps of the process. Pseudo-second-order kinetic model predicts that adsorption behavior involves valance forces through sharing of electrons among dye and the SG. In addition, the experimental adsorption capacity was in agreement with that of calculated adsorption capacity, which proved the model adopted is reasonable. The value of kinetic parameters were summarized in table 4.10

Table 4.10 Kinetics model parameters for Pseudo-first-order, Pseudo-second-order, and Intraparticle Diffusion

Kinetics	**parameters**	**Value**
Pseudo-First Order	q_e (mg/g)	21.727
	K_1	-0.043
	R^2	0.958
Pseudo-Second Order	q_e (mg/g)	50.125
	q_e^2	2512.5
	K_2	0.006
	R^2	0.999
Intraparticle Diffusion	K_p	0.895
	R^2	0.947
	C	39.756

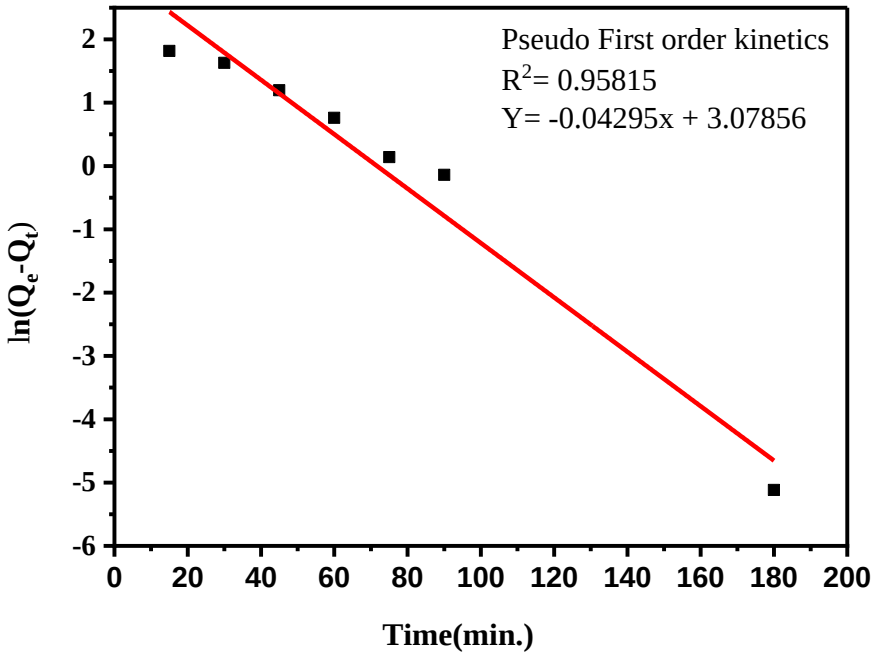

Figure 4.15. Pseudo first order for sorption of MB dye

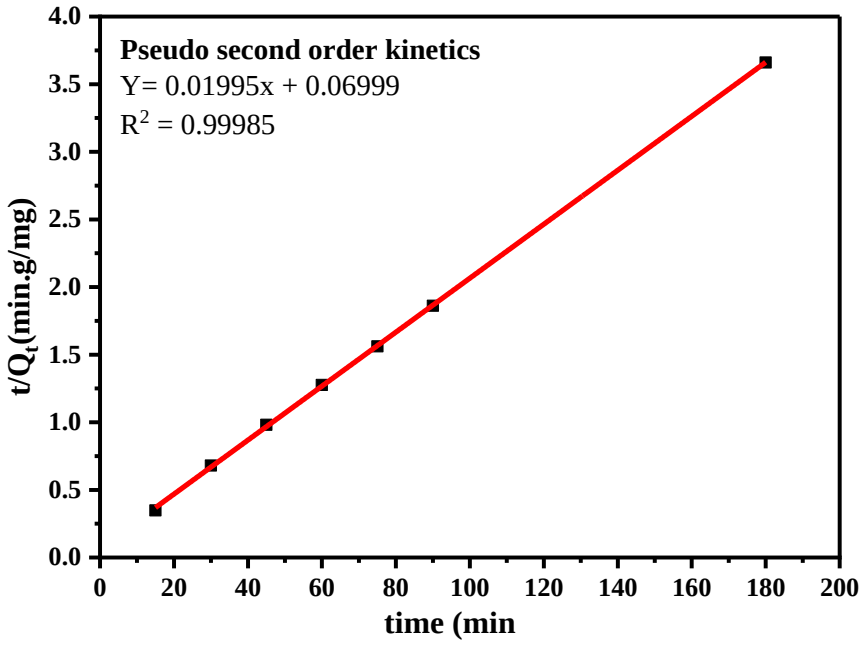

Figure 4. 16: Pseudo second order for sorption of MB dye

The intraparticle diffusion model can be describe the rate of adsorption process depends on

the speed at which adsorbate diffuses towards adsorbent. The result analyzed from the adsorption equilibrium data of intraparticle diffusion model the graph $t^{0.5}$ versus q_t was linear which demonstrates that the intra-particle diffusion was involved inside the adsorption process. In the other case, the model expresses that intraparticle diffusion is not the only rate-determining step due to the graph $t^{0.5}$ versus q_t did not pass through the origin as observed from Figure 4.17. This shows that intraparticle diffusion became not the only rate-limiting step within the adsorption of dye. Consequently, other mass transfer processes like film diffusion and bulk diffusion could be there in determining the mass transfer mechanism of MB dye from the bulk solution to the silica gel adsorbent surface. The diffusion process may affect the dye adsorption process on silica gel as result of the porous structure of the adsorbent and the attractive effect of MB dye.

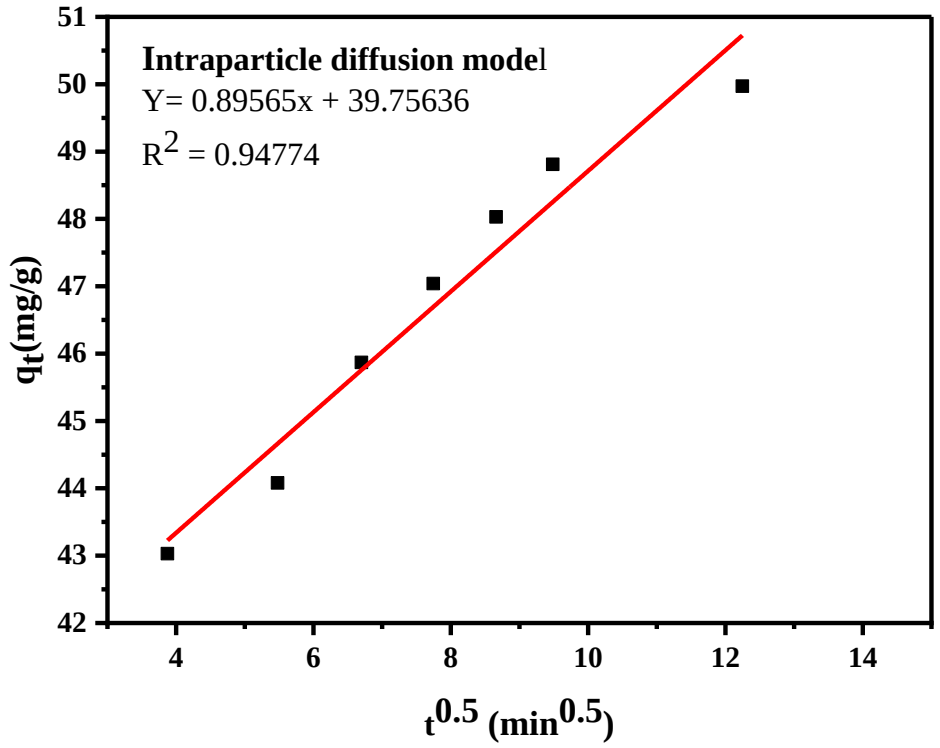

Figure 4.17: Intraparticle diffusion model for MB sorption by silica gel

4.5. Thermodynamic study

The thermodynamics parameters determined for dye adsorption on silica gel at various three temperature of 298 K, 303 K and 313 K respectively. As it summarized in Table 4.13, the values of Gibbs free change energy (ΔG^o) are found to be negative for adsorption of dye on silica gel. The particular values ΔG^o to be found includes -7.643, -7.998 and -8.899 which confirms that the spontaneous and feasibility of adsorption process as result of negative values of Gibbs free energy changes at all temperatures. As temperature increases, the magnitude of ΔG^o also more negative for dye adsorption, which implies that more spontaneity of the adsorption takes place at higher temperature. Higher temperature makes the adsorption easier due to higher driving force of adsorption.

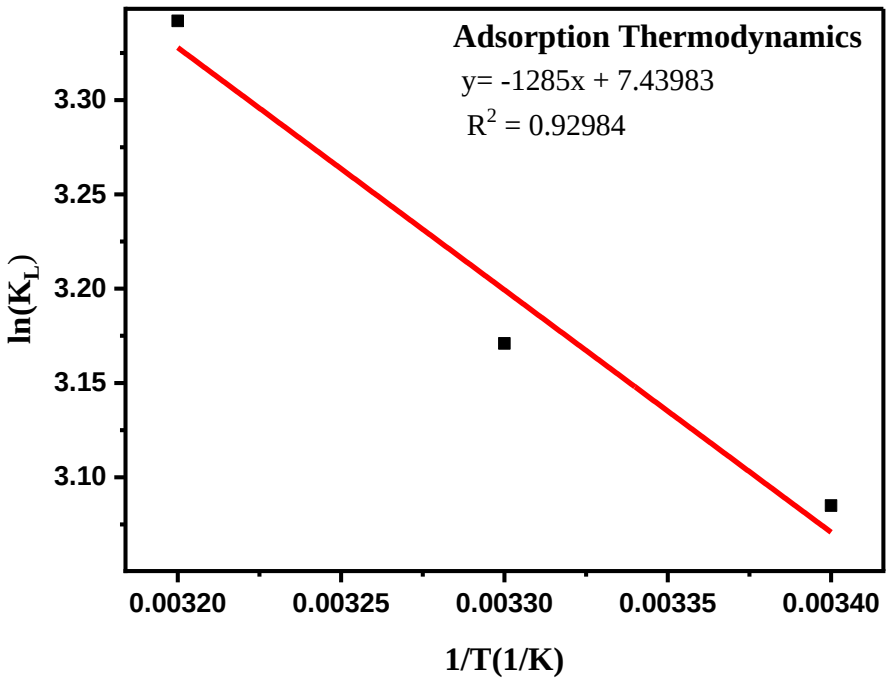

Figure 4.18: Adsorption thermodynamics of MB dye by silica gel

Similar results were found by (Huang et al., 2011) The positive value of change in enthalpy ΔH^o (10.683 KJ/mol) confirms the endothermic nature of sorption process and indicates the adsorption of dye become more favorable at higher temperature. In the other case the positive values of ΔS^o (61.855 J/molK) demonstrates that the process is entropy driven and the randomness between solid-solution interface increases throughout adsorption process. The

report studied by (Ingrachen-Brahmi et al., 2020) found similar result. Increase in randomness of dye on silica gel was as result of number of desorbed water molecules is larger than that of adsorbed MB dye and the adsorption of MB controlled by positive entropy change (Radoor et al., 2020). In addition, the presence of disorder state in the adsorption process is due to the combination of dye with a particle sites to form stable structures.

4.11: Thermodynamic parameters of MB adsorption on silica gel

Adsorbent	qe (mg/g)	Temp. (K)	K_L	ΔG^o (KJ mol^{-1})	ΔH^o (KJ mol^{-1})	ΔS^o (J mol^{-1} K^{-1})	R^2
Silica gel	43.593	298	21.884	-7.643	10.683	61.855	0.929
	44.193	303	25.354	-7.998			
	44.727	313	28.272	-8.899			

4.6. Adsorption on textile waste water

Textile wastewater from dye section were collected from TMA Textile Company and the following waste water characterization before and after adsorption were done in the laboratory.

Table 4.12: Characteristic of effluent from Textile industry

Sample no.	pH solution	MB con. (mg/l)	Removal Efficiency
1	7.7	13.25	91.26
2	7.2	15.80	89.75
3	7.4	14.35	90.82
Average	**7.43**	**14.14**	**90.61**

The color of the wastewater are extremely higher than the free discharge limit. Especially the color, even the low concentration wastewater is highly colored but the discharge regulation says wastewater to be discharged should be colorless. Generally the result of the characterization shows that dye house wastewaters are hazardous and have to be treated before discharge. Therefore due to this the dye section textile wastewater was treated by produced silica gel to observe the optimum condition effects on waste water. The methylene blue MB of the raw wastewater generated from companies dye section was 14.14 mg/L. Results from adsorption

gave a 90.61% reduction in MB levels. However, the resulting MB values were still less than the limits of effluent discharge of 1.33 mg/L.

4.7. Regeneration study

To assess the durability of this adsorbent, regeneration, and reuse studies were carried out for the adsorption of dye over three consecutive adsorption-desorption cycles. A solution of 6M of HCl was chosen as the eluent in the desorption process. High reusability of adsorbent is very indispensable for any adsorbent, which significantly increase the economic value of the adsorption process. To proceed regeneration study 0.03 g of adsorbent dose, 7.99 of pH, 15 mg/L of initial MB dye concentration at 120 min. with removal efficiency of 94.95 % were used to regenerate silica gel. As shown in bar graph figure 4.26, the removal efficiency of the first cycle was 87.53% while the second cycle resulted 79.44%. At the third and fourth cycle, the removal efficiency of nitrate ion were 62.75% respectively. This value ensures that the prepared adsorbent could be reused different times without any loss of adsorption ability. Therefore, silica gel is a promising adsorbent for removal of MB dye from wastewater.

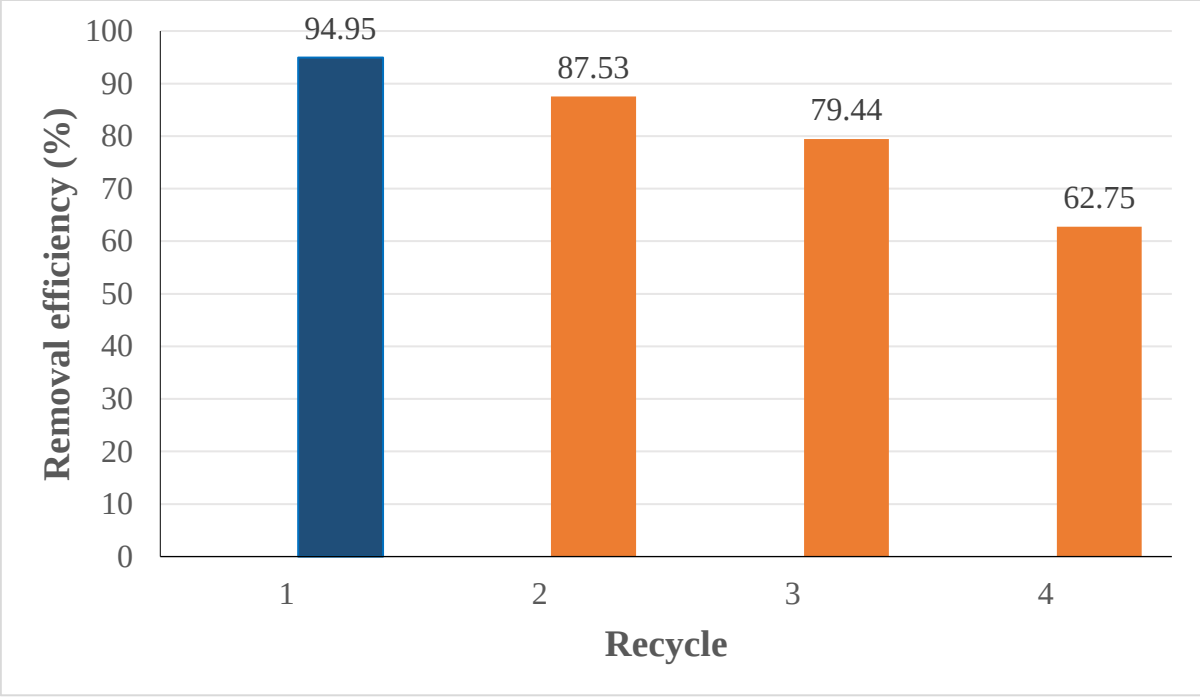

Figure 4.19: Reusability performance of silica gel

CHAPTER FIVE

5. CONCLUSION AND RECOMMENDATION

5.2. Conclusion

This research work focuses on the synthesis and characterization of silica gel adsorbent from Aluminum Sulphate solid waste residue from Awash Melkassa Chemical Factory as a raw material and silicate source to remove the MB dye from wastewater. The XRD, FTIR, and SEM results confirmed that dye was successfully adsorbed by silica gel. The FTIR 3200-3700 cm^{-1} and at 2475 cm^{-1}, O-H and N-H stretches, hump peaks at 1035 and 1094 cm^{-1} S=O stretching vibration of MB and the peak at 908 -940 cm^{-1} C-H bending vibration of MB after adsorption confirmed dye adsorption by the silica gel adsorbent. The XRD diffraction peak at 2θ of 20^o and 30^o illustrated amorphous silica gel was prepared and the impurities were removed successfully. The SEM image of the silica gel surface appears rougher due to the presence of MB. The specific surface of silica gel obtained from BET analysis was 444.54 m^2/g.

The Response Surface Method (RSM) was adopted to explore the model equation for dye removal efficiency. The central composite design was selected to study the effect of variation in pH, dye concentration, contact time, and adsorbent dose. The validation of the model using ANOVA analysis verified that the quadratic model selected is accurate, and statistically significant with a p-value less than 0.05. The optimum removal efficiency of 94.95% was obtained at pH = 7.99, Co = 15 mg/L, t = 120 min, and dose = 0.03 g. The result shows that the interaction effect of those parameters had a significant effect on the adsorption process. The Langmuir isotherm model was in better agreement with the experimental data, with a maximum adsorption capacity and correlation coefficient (R^2) of 85.178 mg/g, and 0.9993, respectively. This suggests that the adsorption process followed monolayer adsorption onto the surface of a finite number of identical adsorption sites. Dye adsorption kinetics was explained properly through the pseudo-second-order kinetics model (R^2 = 0.999), which indicated that chemical adsorption became the controlling mechanism of the adsorption process. In addition, the thermodynamic parameters recommended that the dye removal be spontaneous and endothermic in nature.

Batch experimental studies for real wastewater by selecting TAM textile, which locates Akaki Kality MB dye sources. The results investigated showed that 90.61% of MB dye was removed from wastewater, but the removal efficiency was lower than optimum efficiency. This may be due to the competing surface areas of silica gel and other waste. An adsorption regeneration study of silica gel was investigated using 6N HCl as an eluent, which is the most prominent desorption agent. The adsorption- desorption of three cycles was carried out successfully. According to this study, the results indicate that the adsorbent is determined to be the most promising and effective for the removal of MB dye from aqueous solutions and wastewater.

5.2. Recommendations

If some further research work is carried out to explore the potential of this Awash Melkassa chemical factory solid waste residue, recommended studies are listed below:

- It is recommended to perform an economic feasibility study to establish industry scale production of silica gel from SWR.
- It is recommended to study the effect of wastewater other components because it may contain a more diverse range of contaminants, including organic matter, suspended solids, and microorganisms. The presence of these contaminants can interfere with the removal of methylene blue and require additional treatment steps to achieve effective removal.
- Investigation on the application of the adsorbent to remove multiple dyes from Synthetic and actual wastewater.
- It is recommended that you study the effects of adsorption parameters such as particle size, temperature, and agitation speed.
- It is important to study desorption agent that is effective in removing the adsorbed contaminants from the adsorbent, while also minimizing its environmental impact. Some factors to consider when selecting a desorption agent include its biodegradability, toxicity, and potential for reuse or recycling

Reference

A.O, D. (2012). Langmuir, Freundlich, Temkin and Dubinin–Radushkevich Isotherms Studies of Equilibrium Sorption of Zn 2+ Unto Phosphoric Acid Modified Rice Husk. *IOSR Journal of Applied Chemistry*, *3*(1), 38–45. https://doi.org/10.9790/5736-0313845

Adak, A., Bandyopadhyay, M., & Pal, A. (2005). Adsorption of anionic surfactant on alumina and reuse of the surfactant-modified alumina for the removal of crystal violet from aquatic environment. *Journal of Environmental Science and Health - Part A Toxic/Hazardous Substances and Environmental Engineering*, *40*(1), 167–182. https://doi.org/10.1081/ESE-200038392

Ahmad, A., Jamil, S. N. A. M., Choong, T. S. Y., Abdullah, A. H., Faujan, N. H., Adeyi, A. A., Daik, R., & Othman, N. (2022). Removal of Cationic Dyes by Iron Modified Silica/Polyurethane Composite: Kinetic, Isotherm and Thermodynamic Analyses, and Regeneration via Advanced Oxidation Process. *Polymers*, *14*(24). https://doi.org/10.3390/polym14245416

Alam, Q., Hendrix, Y., Thijs, L., Lazaro, A., Schollbach, K., & Brouwers, H. J. H. (2019). Novel low temperature synthesis of sodium silicate and ordered mesoporous silica from incineration bottom ash. *Journal of Cleaner Production*, *211*, 874–883. https://doi.org/10.1016/j.jclepro.2018.11.173

Alamdari, H. (2017). Aluminium production process: Challenges and opportunities. *Metals*, *7*(4), 5–7. https://doi.org/10.3390/met7040133

Ali, H. A., Chughtai, A., & Sattar, A. (2009). *Synthesis of quality silica gel ; Optimization of parameters Silica Sol Silica Gel*. *23*.

Alouani, M. El, Alehyen, S., Achouri, M. El, & Taibi, M. (2019). *Preparation , Characterization , and Application of Metakaolin-Based Geopolymer for Removal of Methylene Blue from Aqueous Solution*. *2019*.

Amin, N. (2016). AC SC. *Journal of Cleaner Production*. https://doi.org/10.1016/j.jclepro.2016.01.042

Angerasa, F. T., Kalifa, M. A., Jembere, A. L., & Genet, M. B. (2021). Spent kaolin filter cake as an effective adsorbent for the removal of Hexavalent Chromium [Cr (VI)] from aqueous solution: Comparative study of wastewater treatment methods. *South African Journal of Chemical Engineering*, *38*(April), 90–103. https://doi.org/10.1016/j.sajce.2021.09.001

Asghar Ali, H., Chughtai, A., & Sattar, A. (2009). Synthesis of quality silica gel; Optimization of parameters. *Journal of Faculty of Engineering & Technology*, *23*, xx–xx.

Atay, U. A. (2018). Removal of methylene blue by using biosolid. *Global NEST Journal*, *8*(2), 113–120. https://doi.org/10.30955/gnj.000351

Bageru, A. B., & Srivastava, V. C. (2017). Preparation and characterisation of biosilica from teff (eragrostis tef) straw by thermal method. *Materials Letters*, *206*, 13–17. https://doi.org/10.1016/j.matlet.2017.06.100

Başar, C. A. (2006). Applicability of the various adsorption models of three dyes adsorption onto activated carbon prepared waste apricot. *Journal of Hazardous Materials*, *135*(1–3), 232–241. https://doi.org/10.1016/j.jhazmat.2005.11.055

Battas, A., El Gaidoumi, A., Ksakas, A., & Kherbeche, A. (2019). Adsorption study for the removal of nitrate from water using local clay. *Scientific World Journal*, *2019*. https://doi.org/10.1155/2019/9529618

Bayu, A., Nandiyanto, D., Ragadhita, R., & Fiandini, M. (2023). *Indonesian Journal of Science & Technology Interpretation of Fourier Transform Infrared Spectra (FTIR): A Practical Approach in the Polymer / Plastic Thermal Decomposition*. *8*, 113–126.

Beagan, A. M. (2021). Investigating Methylene Blue Removal from Aqueous Solution by Cysteine-Functionalized Mesoporous Silica. *Journal of Chemistry*, *2021*, 1–12. https://doi.org/10.1155/2021/8839864

Benkhaya, S., Harfi, S. El, & Harfi, A. El. (2022). Classifications , properties and applications of textile dyes : A review Discover the world ' s research Classifications , properties and applications of textile dyes : A review. *Applied Journal of Environmental Engineering*

Science, *3*(3), 2022.

Benkhaya, S., Souad, M., & Harfi, A. El. (2020). A review on classifications , recent synthesis and applications of textile dyes. *Inorganic Chemistry Communications*, *115*(March), 107891. https://doi.org/10.1016/j.inoche.2020.107891

Bery, H. M. El, Saleh, M., Gendy, R. A. El, Saleh, M. R., & Thabet, S. M. (2022). High adsorption capacity of phenol and methylene blue using activated carbon derived from lignocellulosic agriculture wastes. *Scientific Reports*, 1–17. https://doi.org/10.1038/s41598-022-09475-4

Besbes, M., Fakhfakh, N., & Benzina, M. (2009a). Characterization of silica gel prepared by using sol-gel process. *Physics Procedia*, *2*(3), 1087–1095. https://doi.org/10.1016/j.phpro.2009.11.067

Besbes, M., Fakhfakh, N., & Benzina, M. (2009b). Characterization of silica gel prepared by using sol-gel process. *Physics Procedia*, *2*(3), 1087–1095. https://doi.org/10.1016/j.phpro.2009.11.067

Boumediene, M., Benaïssa, H., George, B., Molina, S., & Merlin, A. (2018). Effects of pH and ionic strength on methylene blue removal from synthetic aqueous solutions by sorption onto orange peel and desorption study. *Journal of Materials and Environmental Sciences*, *9*(6), 1700–1711. https://doi.org/10.26872/jmes.2018.9.6.190!http://www.jmaterenvironsci.com

Chan, S. H., & Wisconsin, U. S. A. (1989). *x (Si02) OH-*. *18*(1), 49–56.

Chowdhury, M., Azam, F., & Hasan, M. (2020). Removal of Methylene Blue Using A Low-Cost Tea Waste. *J. Wat. Env. Sci*, *4*, 528–535. http://revues.imist.ma/?journal=jwes

Contractor, R. M., Sleight, A. W., & Today, C. (2006). *119 2.3.4*.

Dąbrowski, A. (2001). Adsorption - From theory to practice. *Advances in Colloid and Interface Science*, *93*(1–3), 135–224. https://doi.org/10.1016/S0001-8686(00)00082-8

Dahliyanti, A., Yunitama, D. A., Rofiqoh, I. M., & Mustapha, M. (2022). Synthesis and

characterization of silica xerogel from corn husk waste as cationic dyes adsorbent. *F1000Research*, *11*, 1–11. https://doi.org/10.12688/f1000research.75979.1

Ekwenna, E. B., Wang, Y., & Roskilly, A. (2023). Bioresource Technology Reports The production of bio-silica from agro-industrial wastes leached and anaerobically digested rice straws. *Bioresource Technology Reports*, *22*(February), 101452. https://doi.org/10.1016/j.biteb.2023.101452

El-didamony, H., El-fadaly, E., Amer, A. A., & Abazeed, I. H. (2019). Synthesis and characterization of low cost nanosilica from sodium silicate solution and their applications in ceramic engobes. *Boletín de La Sociedad Española de Cerámica y Vidrio*, *59*(1), 31–43. https://doi.org/10.1016/j.bsecv.2019.06.004

Engineering, B. (2017). *PRODUCTION AND CHARACTERIZATION OF SILICA GEL FOR TEXTILE WASTEWATER TREATMENT (METHYLENE BLUE DYE) By Temechachew Tigabu*.

Fleury, M., Sissmann, O., Brosse, E., & Chardin, M. (2017). A silicate based process for plugging the near well bore formation. *Energy Procedia*, *114*(November 2016), 4172–4187. https://doi.org/10.1016/j.egypro.2017.03.1558

Gómez, J. M., Galán, J., Rodríguez, A., & Walker, G. M. (2014). Dye adsorption onto mesoporous materials: PH influence, kinetics and equilibrium in buffered and saline media. *Journal of Environmental Management*, *146*, 355–361. https://doi.org/10.1016/j.jenvman.2014.07.041

Gunde, M. K. (2000). Vibrational modes in amorphous silicon dioxide. *Physica B: Condensed Matter*, *292*(3–4), 286–295. https://doi.org/10.1016/S0921-4526(00)00475-0

Han, R., Wang, Y., Han, P., Shi, J., Yang, J., & Lu, Y. (2006). Removal of methylene blue from aqueous solution by chaff in batch mode. *Journal of Hazardous Materials*, *137*(1), 550–557. https://doi.org/10.1016/j.jhazmat.2006.02.029

Hastuti, S., Nuryono, & Kuncaka, A. (2019). Synthesis and characterization of L-Arginine modified silica by sol-gel method prepared rice hull ash. *IOP Conference Series:*

Materials Science and Engineering, *509*(1). https://doi.org/10.1088/1757-899X/509/1/012135

Hessel, C., Allegre, C., Maisseu, M., Charbit, F., & Moulin, P. (2007). Guidelines and legislation for dye house effluents. *Journal of Environmental Management*, *83*(2), 171–180. https://doi.org/10.1016/j.jenvman.2006.02.012

Houas, A., Lachheb, H., Ksibi, M., Elaloui, E., Guillard, C., & Herrmann, J. M. (2001). Photocatalytic degradation pathway of methylene blue in water. *Applied Catalysis B: Environmental*, *31*(2), 145–157. https://doi.org/10.1016/S0926-3373(00)00276-9

Hu, H., & Xu, K. (2019). Physicochemical technologies for HRPs and risk control. In *High-Risk Pollutants in Wastewater*. https://doi.org/10.1016/B978-0-12-816448-8.00008-3

Huang, C., Chang, K., Ou, H., Chiang, Y., & Wang, C. (2011). Microporous and Mesoporous Materials Adsorption of cationic dyes onto mesoporous silica. *Microporous and Mesoporous Materials*, *141*(1–3), 102–109. https://doi.org/10.1016/j.micromeso.2010.11.002

Iakovleva, E., & Sillanpää, M. (2020). Novel sorbents from low-cost materials for water treatment. In *Advanced Water Treatment: Adsorption*. https://doi.org/10.1016/B978-0-12-819216-0.00004-7

Ibrahem, S., & Ibrahem, H. (2013). *Preparation and study properties of xerogel silica using sol-gel method*. *2*(9), 111–116.

Igwegbe, C. A., Mohmmadi, L., Ahmadi, S., Rahdar, A., Khadkhodaiy, D., Dehghani, R., & Rahdar, S. (2019). Modeling of adsorption of Methylene Blue dye on Ho-CaWO4 nanoparticles using Response Surface Methodology (RSM) and Artificial Neural Network (ANN) techniques. *MethodsX*, *6*, 1779–1797. https://doi.org/10.1016/j.mex.2019.07.016

Il'Ves, V. G., Zuev, M. G., & Sokovnin, S. Y. (2015). Properties of Silicon Dioxide Amorphous Nanopowder Produced by Pulsed Electron Beam Evaporation. *Journal of Nanotechnology*, *2015*. https://doi.org/10.1155/2015/417817

Imoisili, P. E., Ukoba, K. O., & Jen, T. C. (2020). Synthesis and characterization of amorphous mesoporous silica from palm kernel shell ash. *Boletin de La Sociedad Espanola de Ceramica y Vidrio*, *59*(4), 159–164. https://doi.org/10.1016/j.bsecv.2019.09.006

Ingrachen-Brahmi, D., Belkacemi, H., & Brahem-Mahtout, L. A. (2020). Adsorption of Methylene Blue on silica gel derived from Algerian siliceous by- product of kaolin. *Journal of Materials and Environmental Science*, *11*(7), 1044–1057.

Jamwal, R., Kumari, S., Sharma, S., Kelly, S., Cannavan, A., & Kumar, D. (2021). Vibrational Spectroscopy Recent trends in the use of FTIR spectroscopy integrated with chemometrics for the detection of edible oil adulteration. *Vibrational Spectroscopy*, *113*(April 2020), 103222. https://doi.org/10.1016/j.vibspec.2021.103222

Jia, Z., Li, Z., Li, S., Li, Y., & Zhu, R. (2016). Adsorption performance and mechanism of methylene blue on chemically activated carbon spheres derived from hydrothermally-prepared poly (vinyl alcohol) microspheres. *Journal of Molecular Liquids*, *220*, 56–62. https://doi.org/10.1016/j.molliq.2016.04.063

Jodeh, S., Amarah, J., Radi, S., Hamed, O., Warad, I., Salghi, R., ... & Alkowni, R. (2015). Removal of Methylene Blue from Industrial Wastewater in Palestine Using Polysiloxane Surface Modified with Bipyrazolic Tripodal Receptor. *Moroccan Journal of Chemistry*, *July 2016*, 140–156.

Kappert, E. J., Bouwmeester, H. J. M., Benes, N. E., & Nijmeijer, A. (2014). Kinetic analysis of the thermal processing of silica and organosilica. *Journal of Physical Chemistry B*, *118*(19), 5270–5277. https://doi.org/10.1021/jp502344k

Kathing, C., & Saini, G. (2022). A Review of Various Treatment Methods for the Removal of Dyes from Textile Effluent. *Recent Progress in Materials*, *04*(04), 1–15. https://doi.org/10.21926/rpm.2204028

Katoueizadeh, E., Rasouli, M., & Zebarjad, S. M. (n.d.). A comprehensive study on the gelation process of silica gels from sodium silicate. *Integrative Medicine Research*, *9*(5), 10157–10165. https://doi.org/10.1016/j.jmrt.2020.07.020

Kecili, R., & Hussain, C. M. (2018). Mechanism of adsorption on nanomaterials. In *Nanomaterials in Chromatography: Current Trends in Chromatographic Research Technology and Techniques*. Elsevier Inc. https://doi.org/10.1016/B978-0-12-812792-6.00004-2

Khan, T. A., Singh, V. V., & Kumar, D. (2004). Removal of some basic dyes from artificial textile wastewater by adsorption on Akash Kinari coal. *Journal of Scientific and Industrial Research*, *63*(4), 355–364.

Koner, S., Saha, B. K., Kumar, R., & Adak, A. (2011). *Adsorption kinetics and mechanism of methyl orange dye on modified silica gel factory waste ADSORPTION KINETICS AND MECHANISM OF METHYL ORANGE DYE ON MODIFIED SILICA GEL FACTORY WASTE*. *June*.

Lailun, Y., Suprapto, S., Subandi, A. P. K., Yuningsih, N. E., & Pertiwi, A. C. (2022). The optimization of silica gel synthesis from chemical bottle waste using response surface methodology. *Arabian Journal of Chemistry*, *15*(12), 104329. https://doi.org/10.1016/j.arabjc.2022.104329

Lazaar, K., Hajjaji, W., Pullar, R. C., Labrincha, J. A., Rocha, F., & Jamoussi, F. (2017). Production of silica gel from Tunisian sands and its adsorptive properties. *Journal of African Earth Sciences*, *130*, 238–251. https://doi.org/10.1016/j.jafrearsci.2017.03.017

Lazaar, K., Pullar, R., Hajjaji, W., Mefteh, S., Medhioub, M., & Jamoussi, F. (2022). Preparation of Silica Gel Obtained from Early Cretaceous Sidi Aich Sands (Central Tunisia) and its Potential to Remove Pollutant Dye Anionic from Wastwaters. *Silicon*, *14*(5), 2351–2362. https://doi.org/10.1007/s12633-021-01251-9

Ledakowicz, S., & Pazdzior, K. (2021). Recent Achievements in Dyes Removal Focused on Advanced. *Molecules (Basel, Switzerland)*, *26*(n. 4), 870.

Liu, S., Yan, J., Cui, L., & Quan, G. (2015). *Removal of Methylene Blue from Aqueous Solution using Porous Biochar Removal of Methylene Blue from Aqueous Solution using Porous Biochar Obtained by KOH Activation of*. *March*. https://doi.org/10.15376/biores.10.2.2836-2849

Liu, Z., Li, W., & Huang, C. (2014). Synthesis of mesoporous silica materials from municipal solid waste incinerator bottom ash. *Waste Management*, *34*(5), 893–900. https://doi.org/10.1016/j.wasman.2014.02.016

Lonappan, L., Rouissi, T., Kumar, R., Brar, S. K., Avalos, A., Verma, M., Surampalli, R. Y., & Valero, J. R. (2016). Adsorption of methylene blue on biochar microparticles derived from different waste materials. *WASTE MANAGEMENT*, 1–8. https://doi.org/10.1016/j.wasman.2016.01.015

Lorber, B., Sauter, C., & Moreno, A. (2009). *Crystal growth of proteins , nucleic acids , and viruses in gels*. *December*. https://doi.org/10.1016/j.pbiomolbio.2009.12.002

Lyu, C., Zhou, X., Lu, X., Zhang, Y., Li, C., Zhou, Q., Sun, Z., & Chen, G. (2021). The Effect of Particle Size on the Interpretation of Pore Structure of Shale by N2Adsorption. *Geofluids*, *2021*. https://doi.org/10.1155/2021/8898142

Minju, N., Nair, B. N., & Savithri, S. (2021). Sodium silicate-derived aerogels: Effect of processing parameters on their applications. *RSC Advances*, *11*(25), 15301–15322. https://doi.org/10.1039/d0ra09793d

Momina, Rafatullah, M., Ismail, S., & Ahmad, A. (2019). Optimization study for the desorption of methylene blue dye from clay based adsorbent coating. *Water (Switzerland)*, *11*(6). https://doi.org/10.3390/w11061304

Mousavi, S. A., Mahmoudi, A., Amiri, S., Darvishi, P., & Noori, E. (2022). Methylene blue removal using grape leaves waste: optimization and modeling. *Applied Water Science*, *12*(5), 1–11. https://doi.org/10.1007/s13201-022-01648-w

Mousavi, S. A., Mehralian, M., Khashij, M., & Parvaneh, S. (2017). Methylene blue removal from aqueous solutions by activated carbon prepared from N. Microphyllum (AC-NM): RSM analysis, isotherms and kinetic studies. *Global Nest Journal*, *19*(4), 697–705. https://doi.org/10.30955/gnj.002422

Mubarak, N. M., Fo, Y. T., & Al-salim, H. S. (2015). *Removal of Methylene Blue and Orange-G from Waste Water Using Magnetic Biochar*. *14*(4), 1–13.

https://doi.org/10.1142/S0219581X1550009X

Northcott, K., Oshima, S., & Perera, J. (2007). Synthesis , characterization and evaluation of mesoporous silicates for adsorption of metal ions. *Advanced Powder Technology*, *18*(6), 751–762. https://doi.org/10.1163/156855207782515012

Oros, G., Forgacs, E., & Cserha, T. (2004). *Removal of synthetic dyes from wastewaters : a review*. *30*, 953–971. https://doi.org/10.1016/j.envint.2004.02.001

Pamukoglu, M. Y., Kirkan, B., & Yoldas, B. (2022). Green synthesis of SiNH2@FeNP nanocomposite using and removal of methylene blue from aqueous solution: experimental design approach. *International Journal of Environmental Analytical Chemistry*, *00*(00), 1–19. https://doi.org/10.1080/03067319.2022.2087516

Park, J., Han, Y., & Kim, H. (2012). *Formation of Mesoporous Materials from Silica Dissolved in Various NaOH Concentrations : Effect of pH and Ionic Strength*. *2012*. https://doi.org/10.1155/2012/528174

Patel, K. (2017). *Preparation and Characterization of Silica Gel from Wheat Straw*. *February 2016*. https://doi.org/10.18178/ijcea.2016.7.5.603

Protection, T. E., United, T., & Industrial, N. (2003). Ambient Environment Standards for. *Esid*, *August*, 6–108.

Radoor, S., Karayil, J., Parameswaranpillai, J., & Siengchin, S. (2020). Adsorption of methylene blue dye from aqueous solution by a novel PVA/CMC/halloysite nanoclay bio composite: Characterization, kinetics, isotherm and antibacterial properties. *Journal of Environmental Health Science and Engineering*, *18*(2), 1311–1327. https://doi.org/10.1007/s40201-020-00549-x

Rahman, S. A., & Foisal, A. B. M. (2016). Dyeing of Cotton Fabric with Basic Dye in Conventional Method and Pretreated Dyeing of Cotton Fabric with Basic Dye in Conventional Method and Pretreated with Cationic Polyacrylamide. *SEU Journal of Science and Engineering*, *10*(2), 76–80.

Rauf, M. A., Meetani, M. A., & Hisaindee, S. (2011). An overview on the photocatalytic

degradation of azo dyes in the presence of TiO2 doped with selective transition metals. *Desalination*, *276*(1–3), 13–27. https://doi.org/10.1016/j.desal.2011.03.071

Ravindra, N. M., & Narayan, J. (1986). Optical properties of amorphous silicon and silicon dioxide. *Journal of Applied Physics*, *60*(3), 1139–1146. https://doi.org/10.1063/1.337358

Ref, T., Intel, P., Refundido, T., Intelectual, P., Consolidated, S., & Act, C. (2015). *SILICON DIOXIDE MICROSTRUCTURES BASED ON MACROPOROUS María Alba Martín Silicon Dioxide Microstructures Based on Macroporous Silicon for Biomedical Applications*.

Rosly, N. Z., Abdullah, A. H., Kamarudin, M. A., Ashari, S. E., & Alang Ahmad, S. A. (2021). Adsorption of methylene blue dye by calix[6]arene-modified lead sulphide (Pbs): Optimisation using response surface methodology. *International Journal of Environmental Research and Public Health*, *18*(2), 1–20. https://doi.org/10.3390/ijerph18020397

Samsami, S., Mohamadi, M., Sarrafzadeh, M. H., Rene, E. R., & Firoozbahr, M. (2020). Recent advances in the treatment of dye-containing wastewater from textile industries: Overview and perspectives. *Process Safety and Environmental Protection*, *143*, 138–163. https://doi.org/10.1016/j.psep.2020.05.034

Sarkar Phyllis, A. K., Tortora, G., & Johnson, I. (2022). Photodegradation. *The Fairchild Books Dictionary of Textiles*. https://doi.org/10.5040/9781501365072.12105

Science, E. (2020). *Synthesis and characterization of silica gel from Lapindo mud Sidoarjo Synthesis and characterization of silica gel from Lapindo mud*. https://doi.org/10.1088/1755-1315/456/1/012007

Sdiri, A. (2014). Synthesis and characterization of silica gel from siliceous sands of southern Tunisia. *Arabian Journal of Chemistry*, *7*(4), 486–493. https://doi.org/10.1016/j.arabjc.2010.11.007

Sharma, K., Sharma, S., Sharma, V., Mishra, P. K., Ekielski, A., Sharma, V., & Kumar, V. (2021). Methylene blue dye adsorption from wastewater using hydroxyapatite/gold

nanocomposite: Kinetic and thermodynamics studies. *Nanomaterials*, *11*(6). https://doi.org/10.3390/nano11061403

SHEKHAWAT, M. S. (2013). Thermo Gravimetric and Differential Thermal Analysis of Clay of Western Rajasthan (India). *International Journal of Modern Physics: Conference Series*, *22*, 458–465. https://doi.org/10.1142/s2010194513010519

Suresh Kumar, P., Korving, L., Keesman, K. J., van Loosdrecht, M. C. M., & Witkamp, G. J. (2019). Effect of pore size distribution and particle size of porous metal oxides on phosphate adsorption capacity and kinetics. *Chemical Engineering Journal*, *358*, 160–169. https://doi.org/10.1016/j.cej.2018.09.202

Taylor, P., & Kushwaha, A. K. (n.d.). *Desalination and Water Treatment Enhanced adsorption of methylene blue on modified silica gel : equilibrium , kinetic , and thermodynamic studies*. *October 2013*, 37–41. https://doi.org/10.1080/19443994.2013.803319

Ui, S., Choi, I., & Choi, S. (2014). *Synthesis of High Surface Area Mesoporous Silica Powder Using*. *2014*.

Vaiano, V., & De Marco, I. (2023). Removal of Azo Dyes from Wastewater through Heterogeneous Photocatalysis and Supercritical Water Oxidation. *Separations*, *10*(4). https://doi.org/10.3390/separations10040230

Wakene, A., Zewge, F., Chebude, Y., & Tesfaye, M. (2021). Phosphate abatement using calcium silicate hydrate synthesized from alum factory solid waste residue. *Separation Science and Technology*, *00*(00), 1–19. https://doi.org/10.1080/01496395.2021.1998125

Wang, X., Cheng, H., Ye, G., Fan, J., Yao, F., Wang, Y., Jiao, Y., Zhu, W., Huang, H., & Ye, D. (2022). Key factors and primary modification methods of activated carbon and their application in adsorption of carbon-based gases: A review. *Chemosphere*, *287*(P2), 131995. https://doi.org/10.1016/j.chemosphere.2021.131995

Xing, Y., Liu, D., & Zhang, L. P. (2010). Enhanced adsorption of Methylene Blue by EDTAD-modified sugarcane bagasse and photocatalytic regeneration of the adsorbent.

Desalination, *259*(1–3), 187–191. https://doi.org/10.1016/j.desal.2010.04.008

Yanti, E. D., & Pratiwi, I. (2018). Correlation between thermal behavior of clays and their chemical and mineralogical composition: A review. *IOP Conference Series: Earth and Environmental Science*, *118*(1). https://doi.org/10.1088/1755-1315/118/1/012078

Yu, L. Y., Huang, Z. X., & Shi, M. X. (2014). Synthesis and characterization of silica by sol-gel method. *Advanced Materials Research*, *1030–1032*(July), 189–192. https://doi.org/10.4028/www.scientific.net/AMR.1030-1032.189

Yuan, N., Cai, H., Liu, T., Huang, Q., & Zhang, X. (2019). Adsorptive removal of methylene blue from aqueous solution using coal fly ash-derived mesoporous silica material. *Adsorption Science and Technology*, *37*(3–4), 333–348. https://doi.org/10.1177/0263617419827438

Yusuff, S. M., Ong, K. K., Yunus, W. M. Z. W., Fitrianto, A., & Ahmad, M. B. (2018). Removal of methylene blue from aqueous solutions using alum Sludge: Sorption optimization by response surface methodology. *Journal of Fundamental and Applied Sciences*, *9*(3S), 532. https://doi.org/10.4314/jfas.v9i3s.41

Ziarani, G. M., Moradi, R., Lashgari, N., & Kruger, H. G. (2018). Introduction and Importance of Synthetic Organic Dyes. *Metal-Free Synthetic Organic Dyes*, 1–7. https://doi.org/10.1016/b978-0-12-815647-6.00001-7

APPENDICES

Appendix A: Sodium silicate solution preparation

SWR

Milling

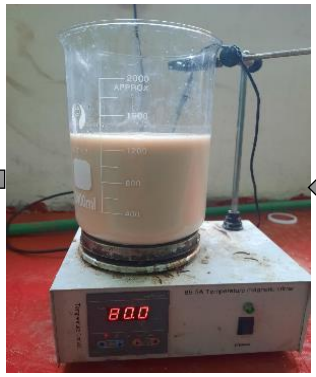

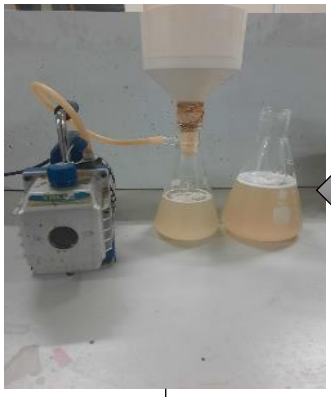

Filtration

Reaction

Sodium silicate solution

Appendix B: Sodium silicate solution preparation

Reaction

sol

Gel

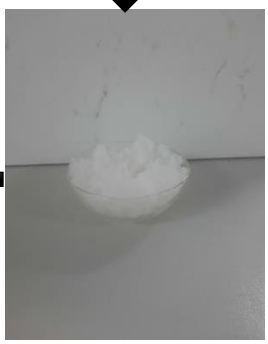

aging

washing

Crushing

Powder silica gel

Appendix C: Appendix Adsorption experiment

MB for calibration curve

Absorbance

UV-vis spectrophotometer

Adsorption experimen

Silica gel before and after adsorption,

Appendix D: calibration curve Methylene blue solution with different concentration

Test	CON.N	ABS
1	0	0
2	2	0.519
3	4	0.793
4	6	1.086
5	8	1.508
6	10	1.846
7	12	2.183
8	14	2.471

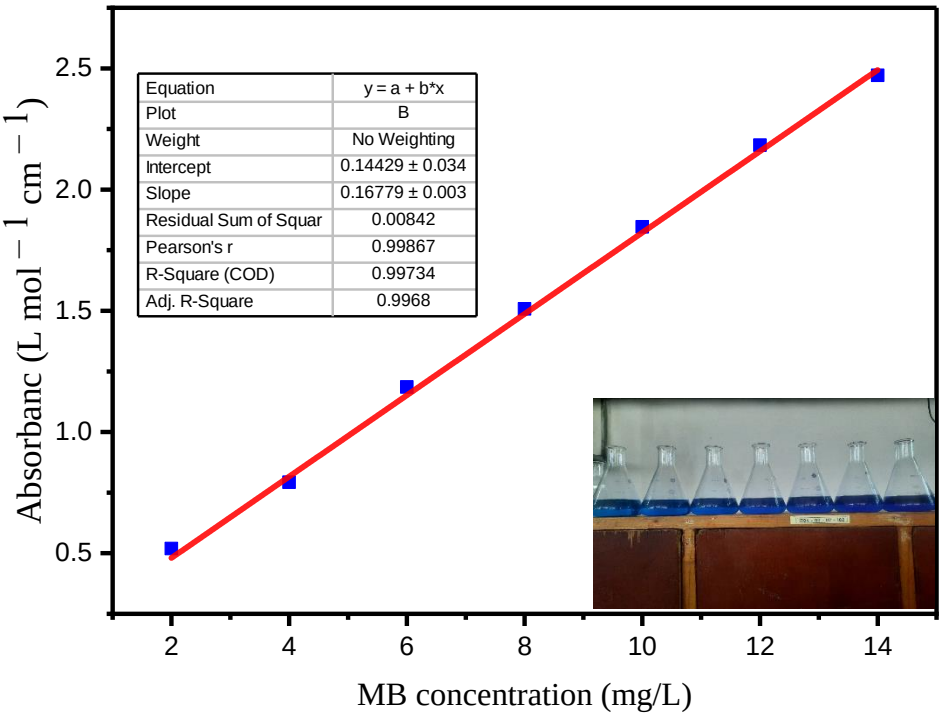

Appendix E: complete silicate analysis of silica Awash melkassa chemical factory solid waste residue

	GEOLOGICAL SURVEY OF ETHIOPIA	Doc.Number: GLD/F5.10.2	Version No: 1
	GEOCHEMICAL LABORATORY DIRECTORATE		Page 1 of 1
Document Title:	Complete Silicate Analysis Report	Effective date:	May, 2017

Issue Date:- 09/02/2022

Customer Name:-Awash Melkassa Chemical Factory

Request No:- GLD/RQ/594/22

Report No:- GLD/RN/130/22

Sample type : Powder

Sample Preparation: - 200 Mesh

Date Submitted:-20/01/2022

Number of Sample:-Five (05)

Analytical Result: In percent (%) Element to be determined Major Oxides & Minor Oxides.

Analytical Method: $LiBO_2$ FUSION, HF attack, GRAVIMETERIC, COLORIMETRIC and AAS.

Collector's code	SiO_2	Al_2O_3	Fe_2O_3	CaO	MgO	Na_2O	K_2O	MnO	P_2O_5	TiO_2	H_2O	LOI
Batch No. -1	54.50	15.79	<0.01	<0.01	0.22	0.18	0.30	<0.01	<0.01	<0.01	6.95	22.90
Batch No. -2	67.80	12.87	<0.01	0.20	0.08	<0.01	0.46	<0.01	<0.01	<0.01	5.16	14.75
Batch No. -3	64.94	15.97	0.34	0.18	0.04	0.36	0.78	<0.01	<0.01	<0.01	4.79	13.58
Batch No. -4	59.52	14.47	<0.01	0.30	0.02	<0.01	0.42	<0.01	<0.01	<0.01	6.61	17.33
Batch No. -7	55.66	15.54	0.40	<0.01	<0.01	0.10	0.44	<0.01	<0.01	<0.01	6.29	21.42

Note: - This result represent only for the sample submitted to the laboratory.

Analysts	Checked By	Approved By	Quality Control
Elisa Fiseha Yirgalem Abraham Lidet Endeshaw	Tizita Zemene	Yohannes Getachew	Gosa Haile

Appendix F: complete silicate analysis of silica gel

	GEOLOGICAL INSTITUTE OF ETHIOPIA	Doc. Number: GLD/F5.10.2	Version No: 1
	Geochemical Laboratory Desk		Page 1of 1
Document Title:-	Complete Silicate Analysis Report	Effective date:	Nov. 2022

Customer Name:- Belete Asmamaw
Sample type :-Silica gel
Sample Preparation: -200 Mesh
Date Submitted:- 24/04/2023
Analytical Result: In percent (%) Element to be determined Major Oxides & Minor Oxides.
Analytical Method: $LiBO_2$ FUSION, HF attack, GRAVIMETERIC, COLORIMETRIC and AAS

Issue Date:-31/05/2023
Request No:- GLD/RQ/1241/23
Report No:- GLD/RN/1867/23
Number of Sample:-One (01)

Collector's code	SiO_2	Al_2O_3	Fe_2O_3	CaO	MgO	Na_2O	K_2O	MnO	P_2O_5	TiO_2	H_2O	LOI	Weight of Sample
SG	86.40	<0.01	<0.01	0.18	0.28	0.74	<0.01	<0.01	0.09	<0.01	8.25	5.29	10.00gm

Note:- This result represent only for the sample submitted to the laboratory.

Analysts	Checked By	Approved By	Quality Control
Haimanot Bayeh Gadisa Wakuma Nigist Fikadu	for Lidet Endeshaw	Yohannes Getachew	Negash Worku

Geochemical Laboratory Desk Page 1

Appendix G: BET test result of silica gel

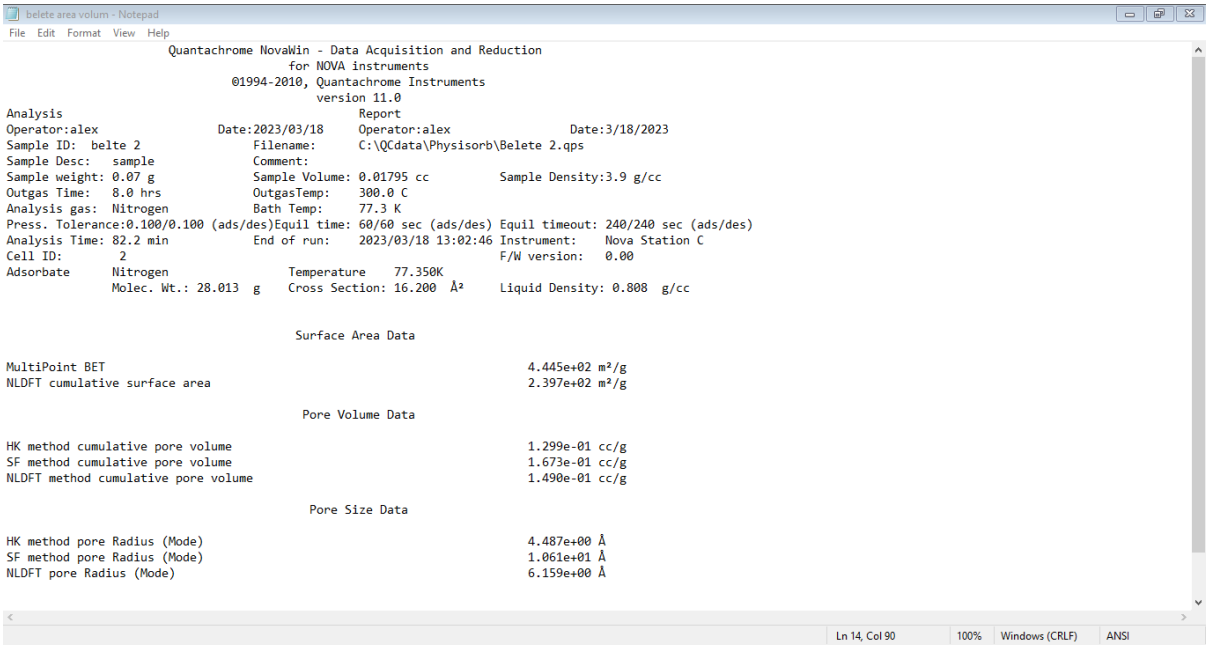

belete area volum - Notepad

File Edit Format View Help

```
                    Quantachrome NovaWin - Data Acquisition and Reduction
                                    for NOVA instruments
                            01994-2010, Quantachrome Instruments
                                    version 11.0
Analysis                                    Report
Operator:alex               Date:2023/03/18     Operator:alex               Date:3/18/2023
Sample ID:  belte 2             Filename:       C:\QCdata\Physisorb\Belete 2.qps
Sample Desc:   sample           Comment:
Sample weight: 0.07 g           Sample Volume: 0.01795 cc       Sample Density:3.9 g/cc
Outgas Time:   8.0 hrs          OutgasTemp:    300.0 C
Analysis gas:  Nitrogen         Bath Temp:     77.3 K
Press. Tolerance:0.100/0.100 (ads/des)Equil time: 60/60 sec (ads/des) Equil timeout: 240/240 sec (ads/des)
Analysis Time: 82.2 min         End of run:    2023/03/18 13:02:46 Instrument:    Nova Station C
Cell ID:       2                                                   F/W version:   0.00
Adsorbate      Nitrogen             Temperature    77.350K
               Molec. Wt.: 28.013  g    Cross Section: 16.200  Å²     Liquid Density: 0.808  g/cc


                                    Surface Area Data

MultiPoint BET                                                  4.445e+02 m²/g
NLDFT cumulative surface area                                   2.397e+02 m²/g

                                    Pore Volume Data

HK method cumulative pore volume                                1.299e-01 cc/g
SF method cumulative pore volume                                1.673e-01 cc/g
NLDFT method cumulative pore volume                             1.490e-01 cc/g

                                    Pore Size Data

HK method pore Radius (Mode)                                    4.487e+00 Å
SF method pore Radius (Mode)                                    1.061e+01 Å
NLDFT pore Radius (Mode)                                        6.159e+00 Å
```

Ln 14, Col 90 | 100% | Windows (CRLF) | ANSI

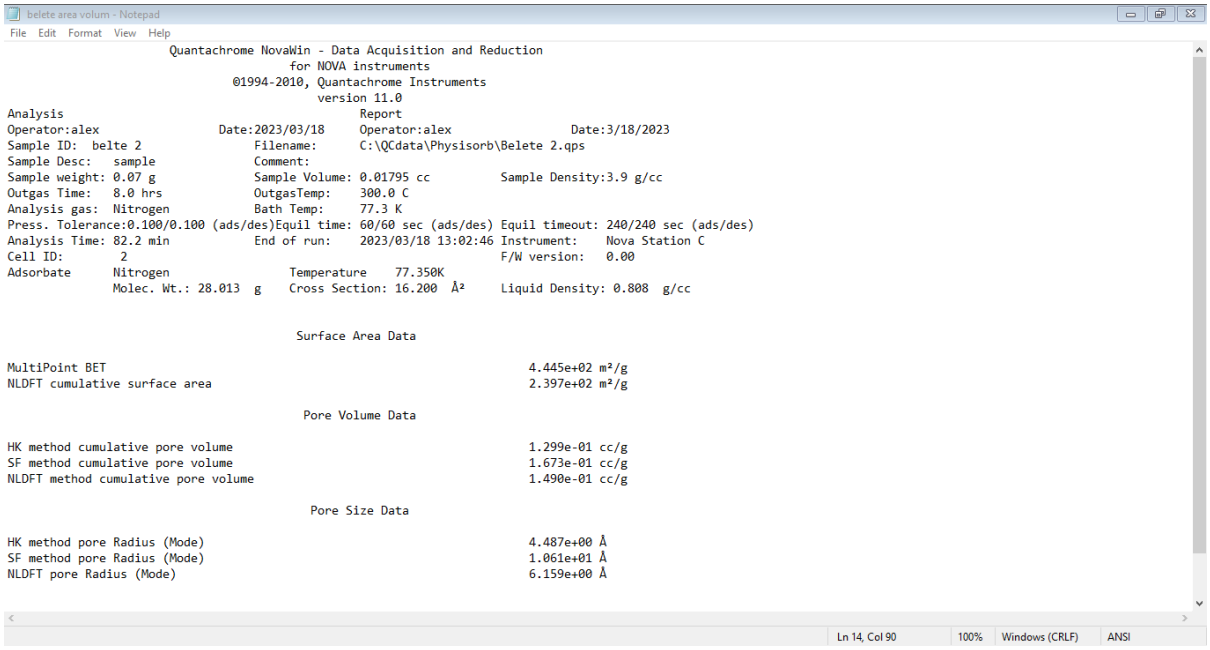

belete area volum - Notepad

File Edit Format View Help

```
                    Quantachrome NovaWin - Data Acquisition and Reduction
                                    for NOVA instruments
                            01994-2010, Quantachrome Instruments
                                    version 11.0
Analysis                                    Report
Operator:alex               Date:2023/03/18     Operator:alex               Date:3/18/2023
Sample ID:  belte 2             Filename:       C:\QCdata\Physisorb\Belete 2.qps
Sample Desc:   sample           Comment:
Sample weight: 0.07 g           Sample Volume: 0.01795 cc       Sample Density:3.9 g/cc
Outgas Time:   8.0 hrs          OutgasTemp:    300.0 C
Analysis gas:  Nitrogen         Bath Temp:     77.3 K
Press. Tolerance:0.100/0.100 (ads/des)Equil time: 60/60 sec (ads/des) Equil timeout: 240/240 sec (ads/des)
Analysis Time: 82.2 min         End of run:    2023/03/18 13:02:46 Instrument:    Nova Station C
Cell ID:       2                                                   F/W version:   0.00
Adsorbate      Nitrogen             Temperature    77.350K
               Molec. Wt.: 28.013  g    Cross Section: 16.200  Å²     Liquid Density: 0.808  g/cc


                                    Surface Area Data

MultiPoint BET                                                  4.445e+02 m²/g
NLDFT cumulative surface area                                   2.397e+02 m²/g

                                    Pore Volume Data

HK method cumulative pore volume                                1.299e-01 cc/g
SF method cumulative pore volume                                1.673e-01 cc/g
NLDFT method cumulative pore volume                             1.490e-01 cc/g

                                    Pore Size Data

HK method pore Radius (Mode)                                    4.487e+00 Å
SF method pore Radius (Mode)                                    1.061e+01 Å
NLDFT pore Radius (Mode)                                        6.159e+00 Å
```

Ln 14, Col 90 | 100% | Windows (CRLF) | ANSI

Appendix H: Pseudo first and second order kinetics and constant values

Run	Time (min.)	Co (mg/L)	Ct (mg/L)	Qt (mg/L)	Qe – Qt (mg/L)	ln(Qe - Qt)	t/Qt (g.min/mg)	$t^{1/2}$
0	0	0	0	0	0	0	0	0
1	15	15	2.099	43.03	6.15	1.8164	0.348	3.873
2	30	15	1.776	44.08	5.10	1.6292	0.680	5.477
3	45	15	1.239	45.87	3.31	1.1969	0.981	6.7
4	60	15	0.888	47.04	2.14	0.7608	1.2755	7.746
5	75	15	0.599	48.03	1.15	0.1397	1.561	8.66
6	90	15	0.506	48.31	0.87	-0.1392	1.862	9.487
7	150	15	0.248	49.17	0.006	-5.1159	3.660	12.247
8	210	15	0.245	49.18				14.49

Pseudo first order kinetics

Intercept	slope (k1)	q_e cal (mg/g)	K_1	R^2
3.0785	-0.04295	21.727	-0.043	0.958

Pseudo second order kinetics

Intercept	slope	q_e cal (mg/g)	q_{e2}	K_2	R^2
0.439	0.0199	50.125	2512.5	0.006	0.999

Appendix I: Limit values for discharge to in land water

Parameter	Limit values
Temperature	40^{o}C
BOD5 at 20^{o}C	6-9
Total nitrogen (as N)	50 mg/L
COD (mg O_2/l)	40 mg/L
Total phosphorous (as P)	150 mg/L
Suspended solids	10 mg/L
Total ammonia (as N)	30 mg/L
Oil, fats and grease	20mg/L
Phenols	1mg/L
Mercury (as Hg)	0.001mg/L
Nickel (as Ni)	2mg/L
Cobalt (as Co)	1mg/L
Lead (as Pb)	0.5mg/L
Antimony (as Sb)	2 mg/L
Tin (as Sn)	5mg/L
Chromium (as Cr VI)	0.1mg/L
Chromium (as total Cr)	1mg/L
Arsenic (as As)	0.25mg/L
Cadmium (as Cd)	1mg/L
Zinc (as Zn)	5mg/L
Copper (as Cu)	2mg/L
Mineral oils (Interceptors)	20mg/L
Benzene, toluene and xylene (combined)	1mg/L
Mineral oils (Biological Treatment)	5mg/L
Organochlorine pesticides (as Cl)	0.03mg/L
Organophosphorous pesticides (as P)	0.003mg/L
Adsorbable organic halogen compounds(AOX)	5mg/L
Sulfides (as S)	2mg/L

Source: Environmental protection authority (EPA) 2004

Equipment used for characterization of solid waste residue and silica gel

AAS

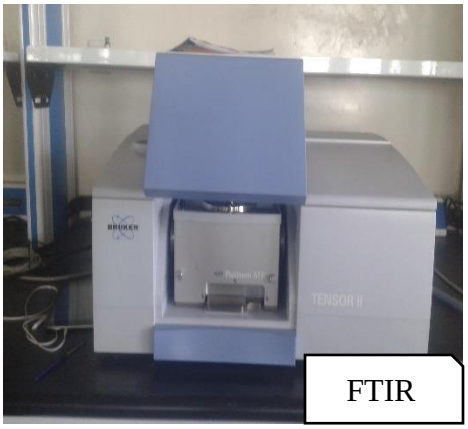

FTIR

BET

XRD

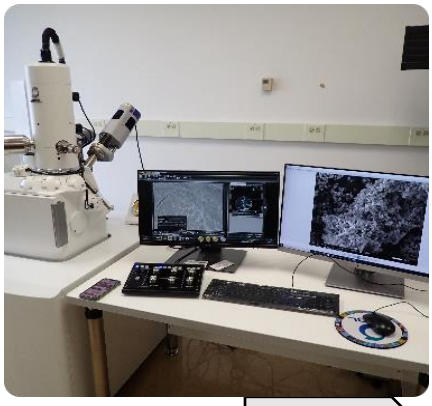

SEM

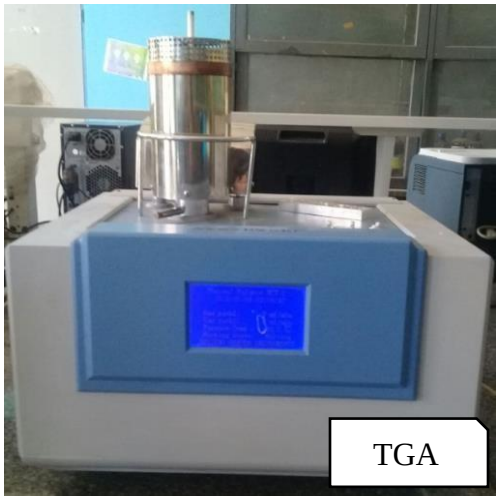

TGA

Solid waste Residue of Aluminum sulfate plant in Awash Melkassa Chemical Factory